ANALYTICAL AND EXPERIMENTAL INVESTIGATION OF A FLUSH MOMENT END-PLATE CONNECTION WITH SIX BOLTS AT THE TENSION FLANGE

by

Douglas Edward Bond

Thesis Submitted to the Faculty of
Virginia Polytechnic Institute and State University
in partial fulfillment of the requirements for the degree of

MASTER OF SCIENCE

in

Civil Engineering

Approved

T. M. Murray, Chairman

W. S. Easterling

R. M. Barker

September 1989

Blacksburg, Virginia

ANALYTICAL AND EXPERIMENTAL INVESTIGATION OF A FLUSH MOMENT END-PLATE CONNECTION WITH SIX BOLTS AT THE TENSION FLANGE

By

Douglas Edward Bond

Committee Chairman: Thomas M. Murray
Civil Engineering

(ABSTRACT)

An analytical and experimental investigation was conducted to study the six bolt flush moment end-plate connection configuration which is used in steel frame construction. The limit states of plate yielding and bolt fracture were analyzed using yield-line theory to predict end-plate thicknesses and a split-tee analogy to develop a method to predict bolt forces. Five experimental tests were conducted on four configurations within a matrix of geometric parameters. The predicted ultimate moment showed good correlation to the yield moment obtained from the experimental deflection plots. The experimental bolt forces correlated well with the predicted bolt forces when plotted versus the applied moment. Additionally, an equation to model the moment-rotation relationship was developed from a regression analysis to determine the construction type suitable for a given connection configuration. Finally, a method of designing the six-bolt flush end-plate configuration is presented and an example given.

ACKNOWLEDGEMENTS

The author is sincerely grateful for the guidance, experience, and understanding given to the author by his advisor, Dr. Thomas M. Murray, throughout the work involved in completing this thesis. The author is also indebted to Dr. Richard Barker and Dr. W. Samuel Easterling for serving on the thesis committee. Additionally, the author extends his appreciation to the students of the Structural Division for their help during the experiments.

This thesis is dedicated to the author's parents, and , for their love and support during the author's education.

TABLE OF CONTENTS

	Page
Acknowledgements	ii
List of Figures	v
List of Tables	vi
CHAPTER	
I Introduction	1
1.1 Background	1
1.2 Literature Review	4
1.3 Scope of Research	6
II Analytical Study	10
2.1 Yield-Line Theory	10
2.1.1 General	10
2.1.2 Application to Flush End-Plates	13
2.2 Bolt Force Predictions	18
2.3 Moment-Rotation Relationships	28
III Experimental Investigation	35
3.1 Test Setup	35
3.2 Test Specimens	38
3.3 Testing Procedure	40
3.4 Test Results	41
3.4.1 Introduction	41
3.4.2 End-Plate Limit State	43
3.4.3 Bolt Force Limit State	48
3.4.4 Moment Rotation Comparison	51
IV Summary, Design Recommendations and Example	58
4.1 Summary	58
4.2 Design Recommendations	59
4.3 Design Example	62
References	69
Appendix A Nomenclature	71
Appendix B MRF-7/8-3/8-28 Test Results	75
Appendix C MRF-1-1/2-28 Test Results	83
Appendix D MRF-3/4-3/8-36 Test Results	91
Appendix E MRF-7/8-1/2-36 Test Results	99

TABLE OF CONTENTS (CONTINUED)

Appendix F MRF-7/8-1/2-36B Test Results 107

Appendix G Coupon and Tensile Test Results 115

VITA 118

ABSTRACT vi

LIST OF FIGURES

Figure		Page
1.1	Typical Uses of End-Plate Connections	2
1.2	Typical End-Plate Configurations	3
1.3	Six-Bolt Flush End-Plate Configuration	5
1.4	Six-Bolt Flush End-Plate Geometry	8
2.1	Yield-line Mechanisms for the Six-Bolt Flush End-Plate	14
2.2	Photograph of Test Specimen Yield-Line Pattern.....	17
2.3	Kennedy Method Split-Tee Model	19
2.4	Kennedy Method Split-Tee Behavior	20
2.5	Idealization of the End-Plate at the Beam Tension Flange Showing Contribution of Prying Forces to Bottom and Top Bolts	22
2.6	Location of Prying Force Acting on the Middle Bolt	27
2.7	Idealized M-u curves for Typical Connections	30
2.8	Typical Moment versus Rotation Curve with Beam Line and Dividing Regions	33
3.1	Test Setup Longitudinal Elevation	36
3.2	Test Setup Traverse Section	37
3.3	Location of Test Specimen Instrumentation	39
3.4	Determination of Experimental Yield Moment	45
3.5	Predicted Rotation versus Actual Rotation	56
3.6	Moment versus Predicted and Actual Rotation	57
4.1	Flowchart to Determine End-Plate Thickness	60
4.2	Flowchart to Determine Bolt Force	61

LIST OF TABLES

Table		Page
1.1	Limits of Tested Geometric Parameters	9
3.1	End-Plate Limit State Based on Centerline Deflection	46
3.2	End-Plate Limit State Based on End-Plate Separation	47
3.3	Bolt force Limit State Results	49

CHAPTER 1

INTRODUCTION

1.1 Background

Bolted moment end-plate connections are often used in steel frame construction and are commonly used by metal building manufacturers for beam-to-beam, or "splice plate connections", Figure 1.1 (a), or in beam-to-column connections, Figure 1.1 (b). Moment end-plate connections consist of a steel plate welded to the end of a steel beam with holes punched for rows of pre-tensioned high strength bolts.

The metal building industry has sought to develop the use of moment end-plate connections because they are economically fabricated and possess excellent strength characteristics. Also, since end-plate connections are welded in the shop and bolted in the field, the erection process is relatively quick. The main disadvantage of end-plate connections is that the required squareness of both the columns and the end-plate attached to the beam can cause erection difficulties.

There are two classifications of end-plates, extended and flush. Extended end-plates, shown in Figure 1.2 (a), extend beyond the flanges to allow a row of bolts beyond the flange. Flush end-plates, shown in Figure 1.2 (b) are flush with the flanges and all bolt rows are between the flanges. Extended end-plates are typically more resistant to rotation than flush end-plates and are used for heavier design loads in

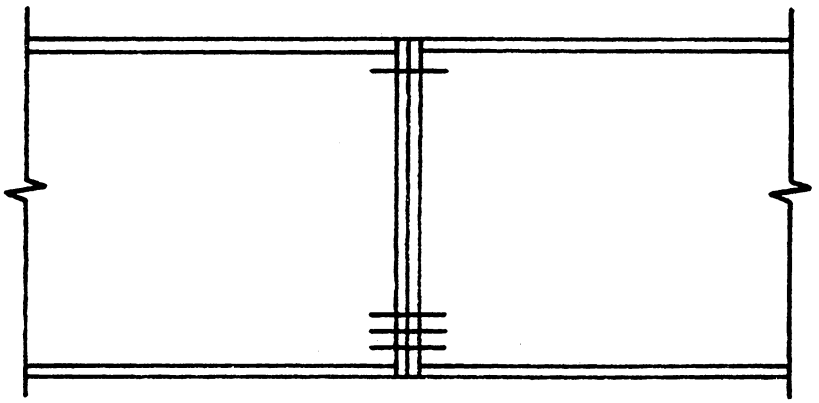

(a) Splice-Plate Connection

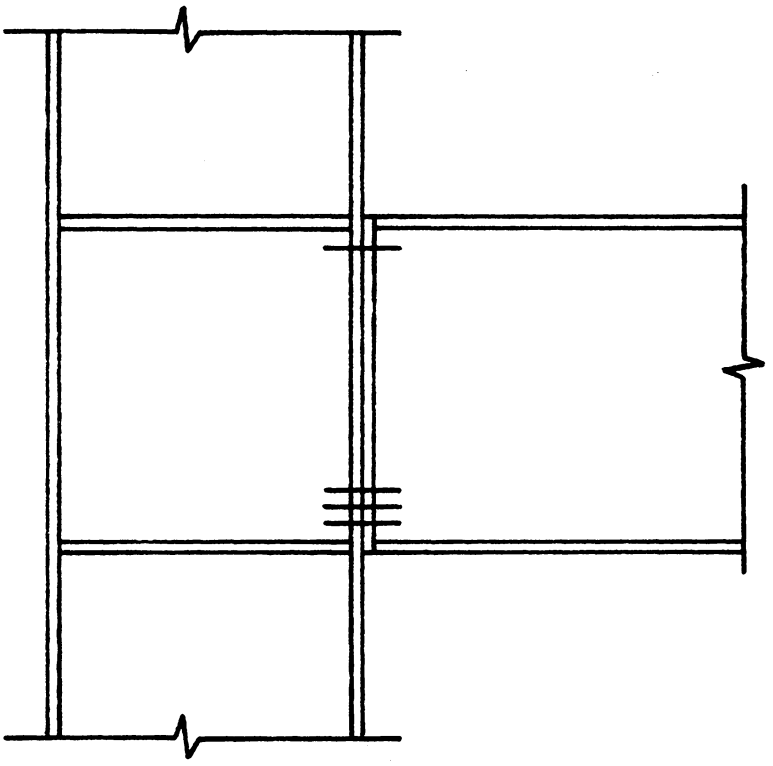

(b) Beam-to-Column Connection

Fig. 1.1 Typical Uses of End-Plate Connections

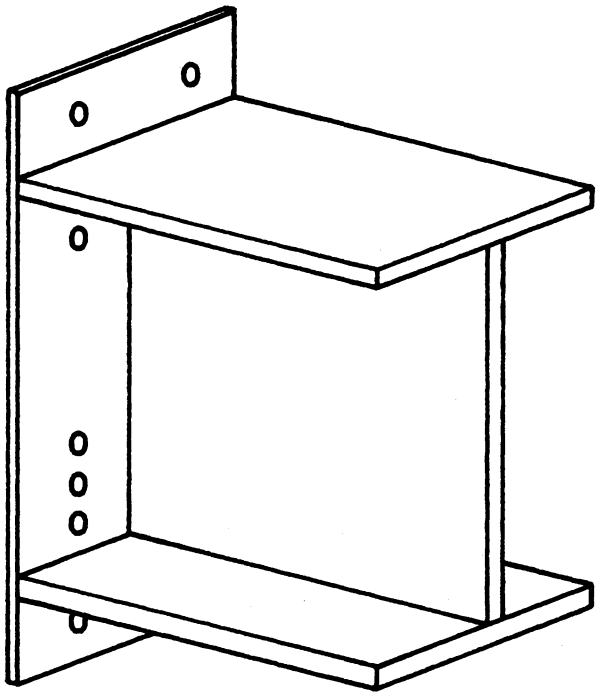

(a) Typical Extended End–Plate Configuration

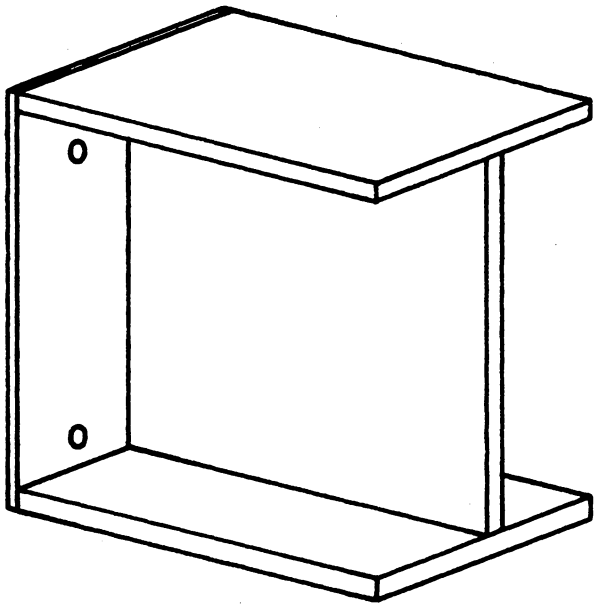

(b) Typical Flush End–Plate Configuration

Fig. 1.2 End–Plate Configurations

splice-plate or beam-column connections. Flush end-plates usually are designed for smaller loadings as found at inflection points in gable frames (Murray 1988).

Two limit states control the design of end-plates: plate yielding and bolt fracture. Also, the rotational resistance of the end-plate connection will determine its suitability for a specific application. Many design procedures exist for determining end-plate thicknesses and bolt diameters for various end-plate configurations. However, to the writer's knowledge, no design procedures exist for the six-bolt flush moment end-plate connection shown in Figure 1.3. The purpose of this study was to develop design procedures for this configuration.

1.2 Literature Review

Early end-plate design methods were developed using statics and assumptions to account for prying forces. These methods resulted in over conservatively large diameter bolts and thick end-plates. In the 1970's, methods based on yield-line theory were developed to predict end-plate capacity. A review of these methods was presented by Murray [1988] and is not repeated here.

Bolt force predictions using the tee-stub analogy were also studied. An extensive review of the developments of this method was presented by Srouji [1983]. A method developed by Kennedy, Vinnakota, and Sherbourne [1981] to predict bolt forces based on a split-tee analogy was used by Srouji [1983] for studying four types of end-plate configurations. Bolt forces were predicted using equations accounting

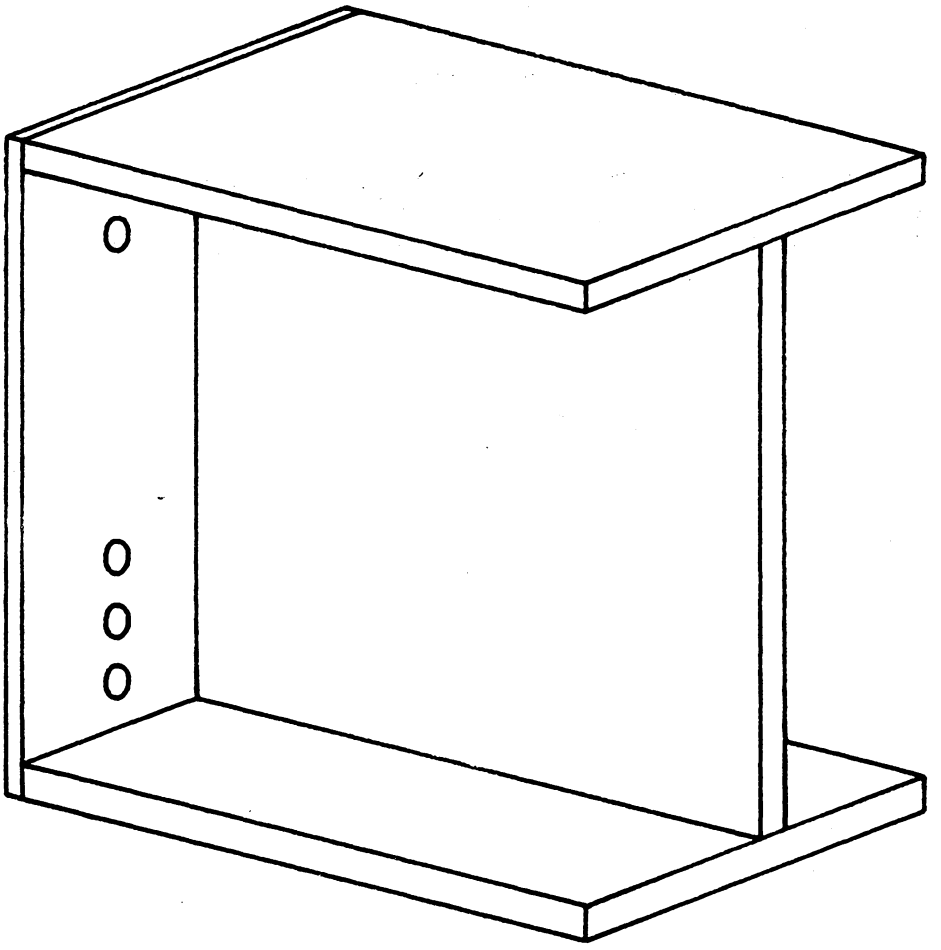

Fig. 1.3 Six Bolt Flush End–Plate Configuration

for prying forces. The equations were verified by experimental results. Srouji also used a yield-line analysis to predict the ultimate end-plate capacity. He considered many types of yield mechanisms consisting of both curved and straight yield lines. Yield-line analyses and bolt force predictions based on the method developed by Kennedy [1981] were recommended by Srouji for end-plate design and for further study on other end-plate configurations.

A unification of design procedures was presented by Hendrick [1985]. Design methods based on yield-line analysis and a modified Kennedy method of predicting bolt forces were experimentally verified for four end-plate configurations. A comparison of the stiffness, or the resistance to rotation, of the configurations was made based on experimental results.

Two extended multi-row end-plate configurations were analyzed using the design methods suggested by Srouji and Hendrick and verified with experimental tests by Morrisson [1986]. Based on previous results, these methods were adopted for analyzing the six-bolt, flush moment end-plate configuration studied here.

1.3 Scope of Research

The purpose of this study was to develop a method of design for the six-bolt flush end-plate connection. The design procedures will include:

1. End-plate thickness determination given end-plate and beam geometry, and material yield stress; a strength criterion.

2. Prediction of bolt forces given end-plate and beam geometry, and bolt type; a bolt force criterion.
3. Determination of moment curvature characteristics to determine the construction type for which the connection is suitable; a stiffness criterion.

The study was completed using yield-line theory to determine end-plate thicknesses and the Kennedy [1981] method to predict bolt forces. Five full-scale tests were conducted using four different end-plate geometries. The geometric properties used to define the six-bolt flush end-plate, shown in Figure 1.4 were varied within the limits shown in Table 1.1 to develop the experimental test matrix. Nomenclature is summarized in Appendix A.

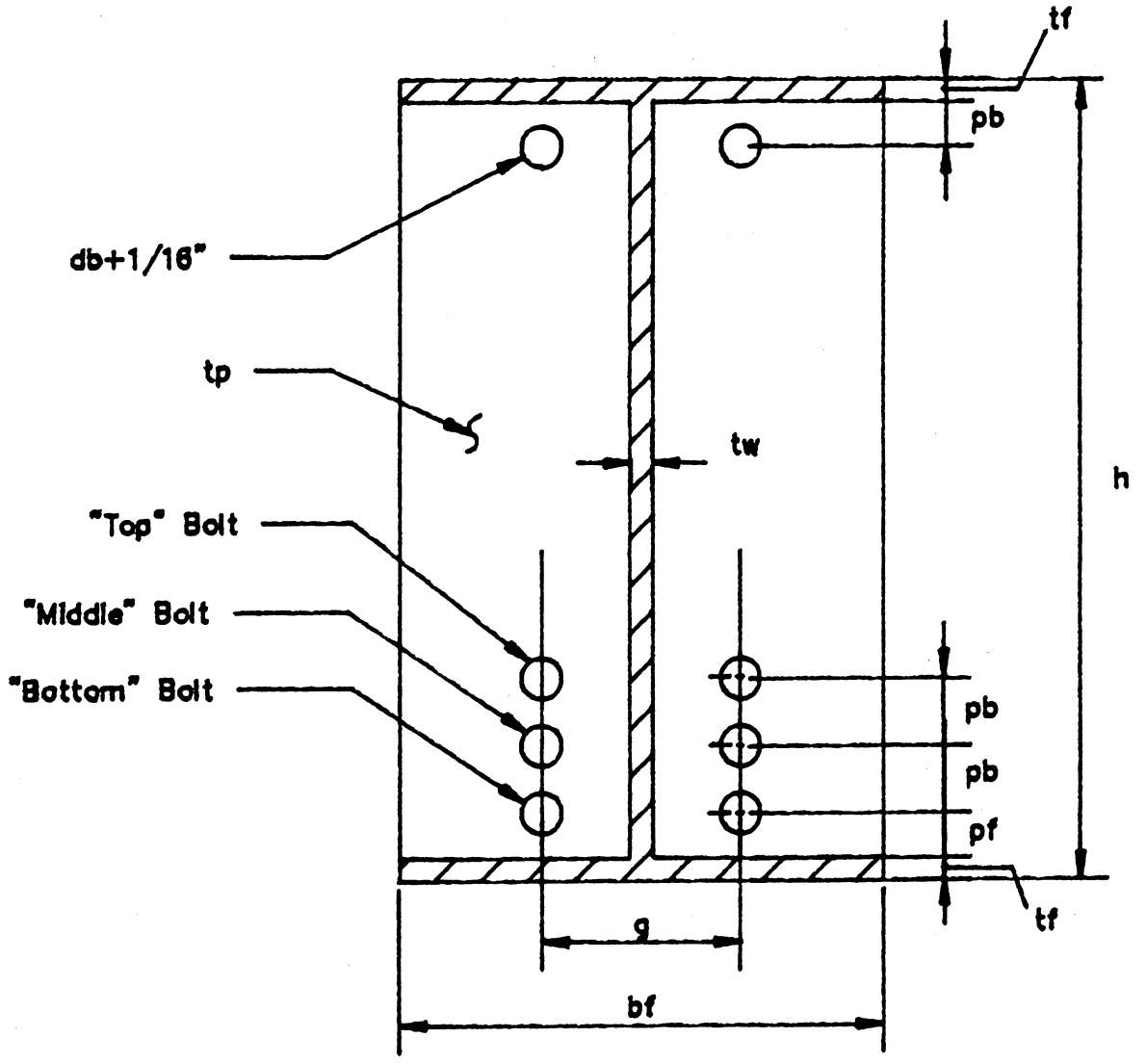

Fig. 1.4 Six Bolt Flush End-Plate Geometry

Table 1.1

Limits of Tested Geometric Parameters

Parameter	Low (in.)	High (in.)
d_b	0.750	1.000
p_f	1.500	2.000
p_b	2.500	2.500
g	3.000	4.000
h	28.00	36.00
b_f	6.000	10.00
t_w	0.313	0.313
t_f	0.375	0.375
t_p	0.375	0.500

CHAPTER II

ANALYTICAL STUDY

2.1 Yield-Line Theory

2.1.1 General

Yield-line theory, originally developed to analyze concrete slabs, can be applied to many problems which would be difficult to solve using elastic methods. A yield line is a continuous plastic hinge formed along a straight or curved line. A failure mechanism forms in the slab when the yield lines form a kinetically valid collapse mechanism. Thus, yield line theory is analogous to plastic design theory. Because elastic deformations are negligible compared to plastic deformations, yield lines divide the slab into rigid plane regions. This allows the deformed shape of the slab to be geometrically defined.

In determining the location of a yield line, the following guidelines have been established [Srouji 1983]:

1. Axes of rotation generally lie along lines of support.
2. Yield lines pass through the intersections of axes of rotation of adjacent plate segments.
3. Along a yield line, the bending moment is assumed to be constant and equal to the plastic moment of the plate.

Yield-line mechanisms can be analyzed using two methods: equilibrium and virtual work. The method of virtual work is more suitable for end-plate applications because it is easier to analyze the geometry of the deformed plate. In this method, the external work done by the applied load acting through an arbitrary deflection is set equal to the internal work done as the plate deforms into rigid segments which rotate at the yield line to cause a virtual deflection. A failure mechanism consists of a specific pattern of yield lines. This yield-line pattern has a corresponding loading required to cause the yield-line formation. Other mechanisms consisting of different yield-line patterns may form under smaller applied loads. Hence, the controlling pattern of yield lines is the one which requires the smallest applied load, or conversely, the one which requires the largest plastic moment. Thus, yield-line theory is an upper bound procedure and the governing mechanism is where the smallest applied load is the least upper bound.

To determine the least upper bound, all possible failure mechanisms are determined. By equating the internal and external work, a relationship is established between the applied load and the ultimate moment capacity. This equation is then solved for the unknown load or the end-plate ultimate moment capacity. By comparing the values obtained from each of the possible mechanisms, the controlling yield-line mechanism is that with the largest required plastic moment capacity or the smallest failure load.

The internal energy stored in a yield-line mechanism is the sum of the internal energies stored in each yield-line forming the mechanism. The internal energy stored in a given yield line is equal to the normal moment on the yield line, where the moment in rector notation lies along the yield line, multiplied by the normal rotation of the yield line, with respect to the rigid plane segment.

Thus, the energy stored, w, in the nth yield line of length L_n is [Srouji 1983]:

$$w = \int_{L_n} m_p \theta_n ds \tag{2.1}$$

where m_p is the plastic moment capacity, θ_n is the relative rotation of line n, and d_s is the elemental length of line n. The internal energy stored by a yield-line mechanism, W, is [Srouji 1983]:

$$W = \sum_{n=1}^{N} \int_{L_n} m_p \theta_n ds$$

$$W = \sum_{n=1}^{N} m_p \theta_n Ln \tag{2.2}$$

where N is the number of yield lines in the mechanism. For complex yield-line patterns, the expressions for the relative rotation are difficult to obtain; therefore, it is more efficient to resolve the slopes of the rigid segments into x- and y- directions. This results in:

$$W = \sum_{n=1}^{N} (m_{px}\theta_{nx}L_x + m_{py}\theta_{nx}L_y) \qquad (2.3)$$

where m_{px} and mpy are the x- and y- components of the normal moment capacity per unit length, L_x and L_y are the x- and y- components of the yield line length, and θ_{nx} and θ_{ny} are the x- and y- components of the relative normal rotation of yield line n. The θ_{nx} and θ_{ny} values are calculated by first drawing straight lines parallel to the x- and y-axis in the two segments intersecting at the yield-line. Then their relative rotation is calculated by selecting straight lines with known displacements at the end [Srouji 1983].

The external energy is calculated by the applied load, Mu, acting through the rotation 1/h, assuming small deflections occur. By equating the external and internal work, the ultimate moment capacity can be determined given end-plate geometry and thickness. Conversely, the end-plate thickness can be determined given the applied load and the end-plate geometry.

2.1.2 Application to Flush End-Plates

Many yield-line patterns are possible for the six-bolt flush end-plate geometry defined in Figure 1.2. The two controlling yield-line mechanisms for the six-bolt configuration are shown in Figure 2.1. These patterns were determined from a study of possible yield-line patterns. One of the two mechanisms will control the yield-line

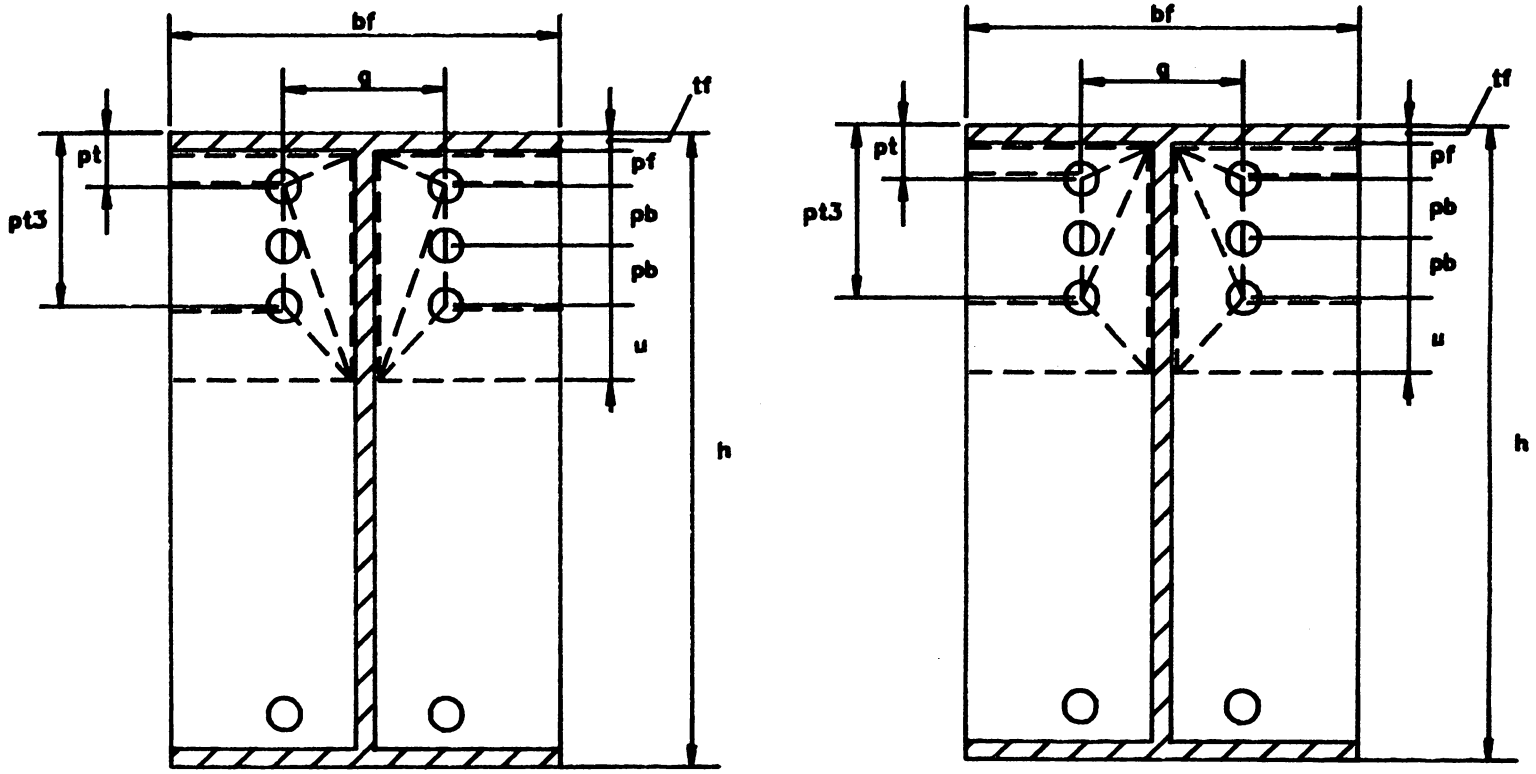

(a) Mechanism I

(b) Mechanism II

Fig. 2.1 Yield–Line Mechanisms for the Six–Bolt Flush End–Plate

analysis based on the variable geometric parameters of a specific end-plate. These mechanisms differ in the location of a yield line near the beam tension flange. For Mechanism 1, Figure 2.1 (a), the yield-line begins at the first bolt from the inside of the beam tension flange and ends at the face of the beam web a distance u below the third bolt from the inside of the beam tension flange. This pattern is symmetrical about the beam web. From Mechanism 2, Figure 2.1 (b), the distinguishing yield-line begins at the intersection of the inside face of the beam flange and the face of the beam web and ends at the third bolt from the inside of the beam tension flange. This pattern is also symmetrical about the beam web.

The dimension u for either Mechanism 1 or Mechanism 2 is initially unknown but can be determined by differentiating the internal work expression for either mechanism with respect to u and equating to zero. The resulting expression for u in Mechanism 1 is:

$$u = (1/2)\sqrt{b_{fg}(h-pt_3)/(h-Pt)} \quad \text{Mechanism 1} \tag{2.4}$$

The resulting expression for u in Mechanism 2 is:

$$u = (1/2)\sqrt{b_{fg}} \quad \text{Mechanism 2} \tag{2.5}$$

The equations for Mechanism 1 and Mechanism 2 can be written in terms of the ultimate moment capacity of the end-plate M_u, or when rearranged, for the required end-plate thickness, t_p.

For Mechanism 1:

$$M_u = 4m_p \{(h-p_t)((b_f/2p_f)+(2p_f+4p_b+2u)/g) + (h-p_{t3})b_f/(2u)\} \quad (2.6)$$

where m_p is the plastic moment of the plate, $f_{py}t_p^2$, and

$$t_p = \left[\frac{M_u/f_{py}}{(h-p_t)(b_f/(2_{pf}) + (2p_f+4p_b+2u)/g)+(h-p_{t3})b_f/(2u)}\right]^{1/2} \quad (2.7)$$

For Mechanism 2:

$$M_u = 4m_p \{g/2+(2p_f(p_f+2p_b))/g + (h-p_t)(b_f/(2_{pf})+2(p_f+2p_b)/g) + (h-p_{t3})(b_f/(2u)+2u/g)\} \quad (2.8)$$

and

$$t_p = \left[\frac{M_u/f_{py}}{g/2+(p_f+h-p_t)(2p_f+4p_b)/g+b_f/2((h-p_t)/p_f + (h-p_{t3})/u)+(h-p_{t3})2u/g}\right]^{1/2} \quad (2.9)$$

A photograph of an observed yield-line pattern is shown in Figure 2.2. The yield-line pattern is indicated by the flaking of "white wash" from the test specimen.

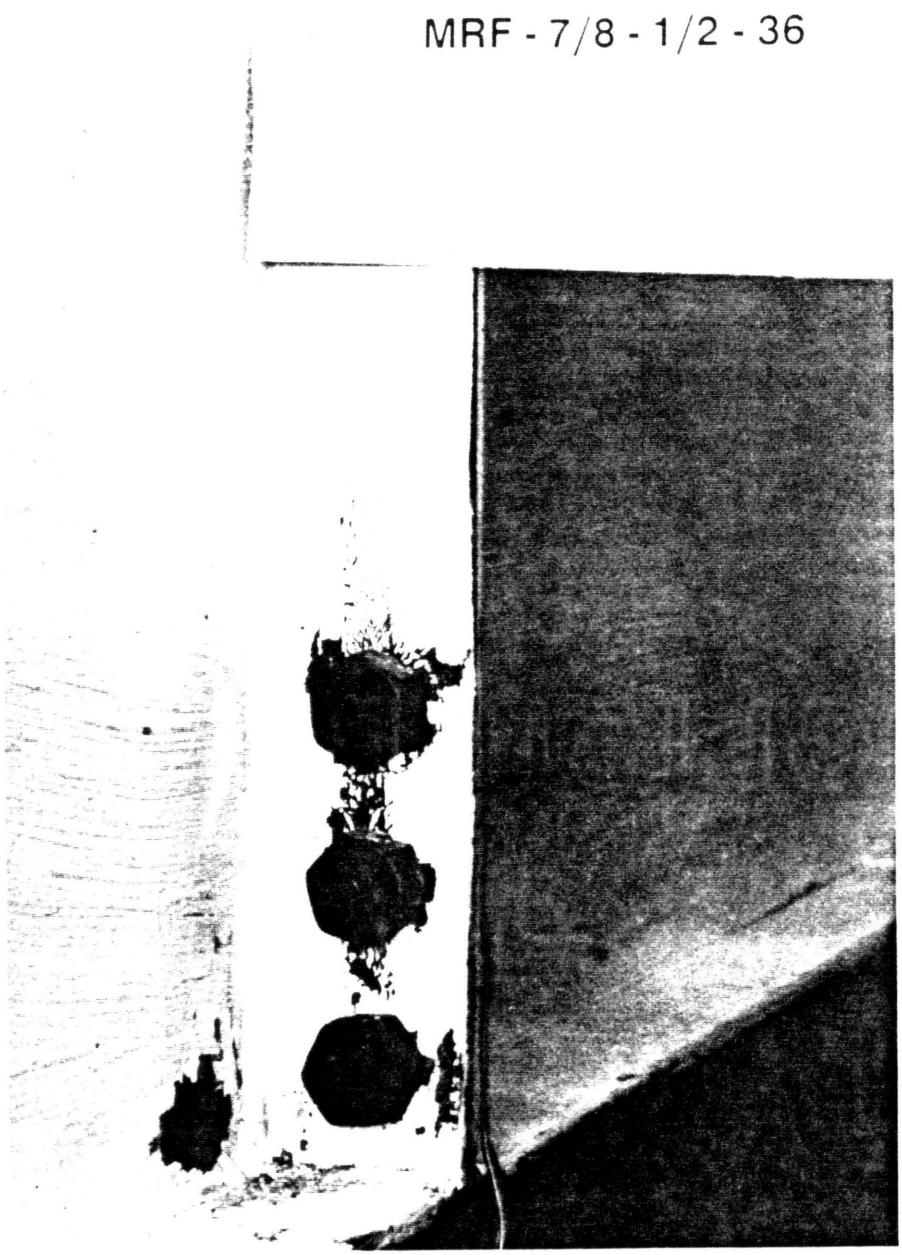

Figure 2.2 Photograph of Test Specimen Yield–Line Pattern

2.2 Bolt Force Predictions

Yield-line analysis procedures do not predict bolt forces if prying forces are considered. Since experimental results indicate that prying action is present in end-plate connections, a method suggested by Kennedy [1981] was used to predict bolt forces.

The Kennedy method is based on the split-tee analogy, Figure 2.3, and three assumed stages of end-plate behavior. The first stage, referred to as "thick", is defined by the absence of plastic hinges in the end-plate. At this stage, the prying forces are assumed to be zero, Figure 2.4(a). The upper limit of this stage occurs when a plastic hinge forms in the plate at the beam flange, Figure 2.4(b). At this point, the plate is considered to be in the "intermediate" stage and the magnitudes of the prying forces acting on the bolts are between zero and a maximum value. As the load increases, another plastic hinge forms at the centerline of the bolt, Figure 2.4(c). At this point, the plate is in the third stage and is considered "thin". In this stage, the prying force is constant at its maximum value. The distance "a" between the point of prying force application and the centerline of the bolt was determined by Hendrick [1985] for other flush end-plate configurations as a function of t_p/d_b:

$$a = 3.682\ (t_p/d) - 0.085 \qquad (2.10)$$

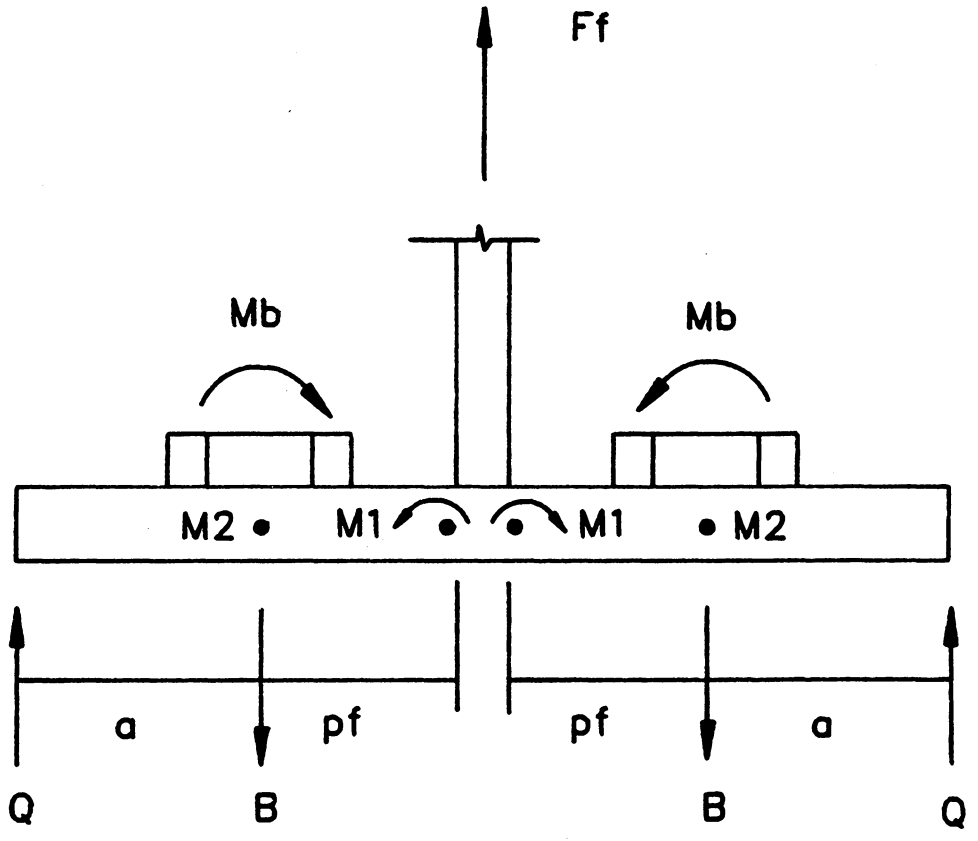

Fig. 2.3 Kennedy Method Split Tee Model

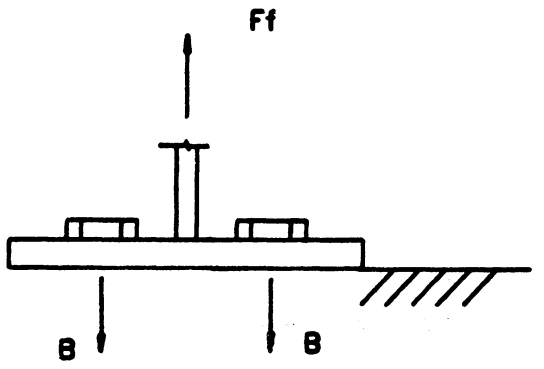

(a) Thick Plate Behavior / First Stage

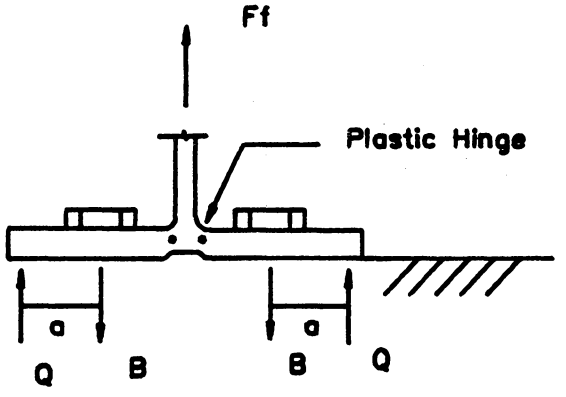

(b) Intermediate Plate Behavior / Second Stage

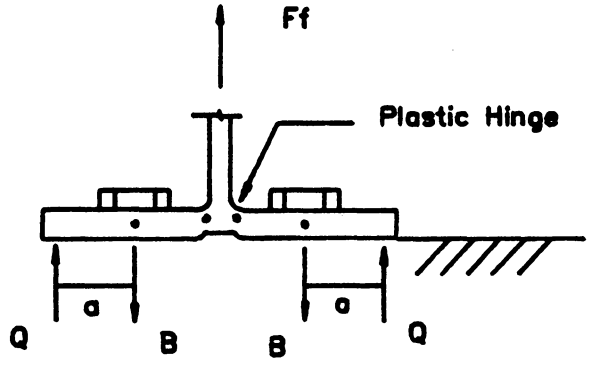

(c) Thin Plate Behavior / Third Stage

Fig. 2.4 Kennedy Method Split–Tee Behavior

However, this value of "a" did not correspond well with the experimental data from the five six-bolt flush end-plate tests. Suggestions have been made which relate "a" to t_p [Kennedy 1981]. From these, a value of $a=t_p$ was found to correspond well with the experimental results and is therefore used herein.

The Kennedy [1981] method of predicting bolt forces must be modified for application to the six-bolt flush end-plate connection. Three factors: α_1, α_2, and α_3 are introduced to proportion the amount of tension flange force each tension bolt receives. The factors were empirically developed to satisfy:

$$\alpha_1 + \alpha_2 + \alpha_3 \geq 1.0 \tag{2.11}$$

For the six-bolt flush end-plate configuration, the sum of the factors proportioning the tension flange force to the bolts was measured experimentally to be greater than unity. After significant plastic deformation occurred in the end-plate under loading, the prying forces acting on the bolts were found to be larger than those predicted by the modified Kennedy method. Hence, the factors α_1, α_2, and α_3 were developed directly from experimental data to correlate with the bolt force predictions.

The bottom and top bolts, as defined in Figure 1.3, receive prying forces as shown in Figure 2.5. Due to the shape of the deformed plate, no prying force in the middle bolt along the bolt line is believed to occur. To determine the magnitude of the prying forces acting on the

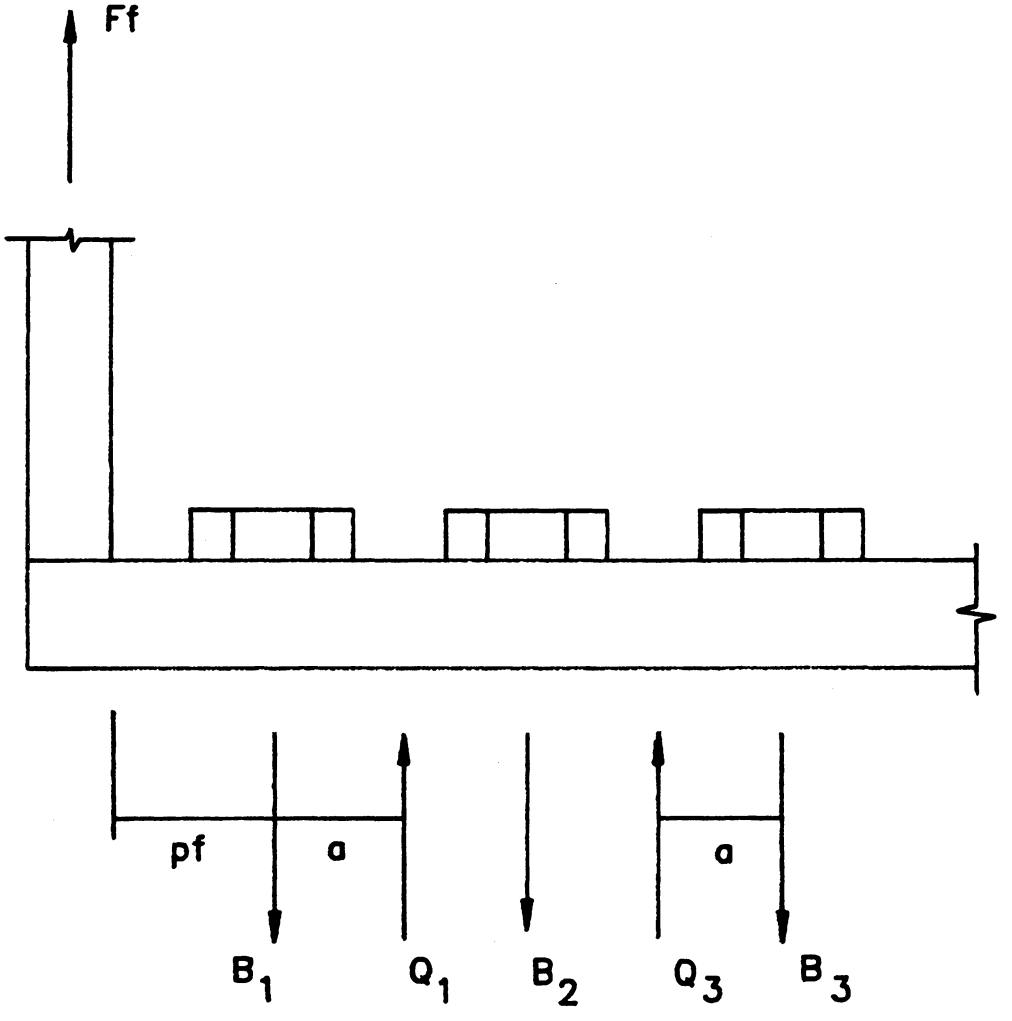

Fig. 2.5 Idealization of the End–Plate at the Beam Tension Flange Showing Contribution of Prying Forces to Bottom and Top Bolts

bottom and top bolts, one must first determine the stage of end-plate behavior. The stage of end-plate behavior is established by comparing the appropriate portion on the tension flange force, either $\alpha_1 F_f$ or $\alpha_3 F_f$ with the flange force at the thick plate limit F_1, and if necessary, the flange force at the thin plate limit F_{11}. At the thick plate limit, F_1, is [Morrisson 1986]:

$$F_1 = \frac{b_f t_p^2 f_{py}}{4p_f\sqrt{1+(3t_p^2/16p_f)}} \tag{2.12}$$

At the thin plate limit, F_{11}, is: [Morrisson 1986]

$$F_{11} = t_p^2 f_{py} \frac{[0.85(b_f/2)+0.80W']+[\pi d_b^3 F_{yb}/8]}{2p_f} \tag{2.13}$$

For the bottom bolt B_1, if the appropriate flange force, $\alpha_1 F_f$, is less than the flange force at the thick plate limit, F_1, the end-plate is considered in the "thick" stage and there is no prying force assumed to act on the bolt. Therefore, the force in B_1 is:

$$B_1 = \alpha_1 F_f/2 \quad \text{when} \quad \alpha_1 F_f < F_1 \tag{2.14}$$

If the inner flange force, $\alpha_1 F_f$, is greater than or equal to the flange force at the thick plate limit, F_1, and less than or equal to the flange force at the thick plate limit, F_{11}, the end-plate behavior is

"intermediate" and the prying force magnitude is between zero and its maximum value. The prying force Q per bottom bolt for this case is [Morrisson 1986]:

$$Q_1 = \frac{\alpha_2 F_f p_f}{2a} - \frac{\pi d_b^3 F_y b}{32a} - \frac{b_f t_p^2}{8a}\sqrt{F_{py} - 3(\alpha_1 F_f / t_p B_f)^2} \qquad (2.15)$$

Thus, for intermediate end-plate behavior, the bolt force B_1 is equal to the inner flange force, $\alpha_1 F_f$, divided by the number of bolts, 2, plus the prying force, Q_1:

$$B_1 = \alpha_1 F_f/2 + Q_1 \quad \text{when} \quad F_1 \le \alpha_2 F_f \le F_{11} \qquad (2.16)$$

When the inner flange force, $\alpha_1 F_f$, is greater than the flange force at the thin plate limit, F_{11}, the end-plate behavior is thin and the prying force is at a maximum, Q_{1max}, and is [Morrisson 1986]:

$$Q_{1max} = \frac{w' t_p^2}{4a}\sqrt{f_{py}^2 - 3(F'/w' t_p)^2} \qquad (2.17)$$

where F' in the term Q_{1max} is the lesser of:

$$F_{limit} = F_{11}/2 \qquad (2.18)$$

or

$$F_{1max} = \alpha_1 F_f/2 \qquad (2.19)$$

The Q_{1max} term is actually the plastic moment capacity of the plate accounting for shear deformations divided by the distance to the location of the prying force from the centerline of the bolt, a. Therefore, the bottom bolt force, B_1, is the proportioned inner flange force per bolt, plus the prying force, Q_{1max}:

$$B_1 = \alpha_1 F_f/2 + Q_{1max} \quad \text{when} \quad \alpha_1 F_f > F_{11} \tag{2.20}$$

The explanation of the top bolt force, B_3, parallels that for the bottom bolt force, B_1, but is given for completeness:

$$B_3 = \alpha_3 F_f/2 \quad \text{when} \quad \alpha_3 F_f/2 < F_1 \tag{2.21}$$

$$Q_3 = \frac{\alpha_3 F_f p_f}{2a} - \frac{\pi d_b^3 F_y b}{32a} - \frac{b_f t_p^2}{8a} \sqrt{F_{py}^2 - 3(\alpha_3 F_f/b_f t_p)^2} \tag{2.22}$$

$$B_3 = \alpha_3 F_f/2 \quad \text{when} \quad F_1 \leq \alpha_3 F_f \leq F_{11} \tag{2.23}$$

$$Q_{3max} = \frac{w_p' t^2}{4a} \sqrt{F_{py}^2 - 3(F'/w' t_p)^2} \tag{2.24}$$

$$F^1 = \text{minimum} \begin{cases} F_{limit} = F_{11}/2 \\ F_{3max} = \alpha_3 F_f/2 \end{cases} \tag{2.25}$$

$$B_3 = \alpha_3 F_f/2 + Q_{3max} \quad \text{when} \quad \alpha_3 F_f > F_{11} \tag{2.26}$$

Note that when the quantities under the radicals in Equations 2.15, 2.17, 2.22, and 2.24 are negative, the end-plate will fail locally in shear before prying forces can be developed. Thus the connection is not adequate for the applied load.

The explanation of the middle bolt force is similar to the top and bottom bolts. The main difference is the location of the prying force acting on the middle bolt, which is caused by the beam web pulling the end-plate as the connection rotates when load is applied, Figure 2.6. The bottom and top bolts receive no prying forces in this manner because there is no plate contact at the point in question, due to the formation of a yield-line across the width of the end-plate. The Kennedy method can be modified to predict the prying force the middle bolt receives. The b_f term becomes $2p_b$, the w' term becomes w'', or $2p_b$ less the width of a bolt hole, and p_f becomes p_f', the distance from the outside of the web to the center or the middle bolt. Thus, the middle bolt force, B_2, is:

$$B_2 = \alpha_2 F_f/2 \quad \text{when} \quad \alpha_2 F_f < F_1 \tag{2.27}$$

where

$$F_1 = \frac{p_b t_p^2 f_{py}}{2p_f' \sqrt{1+(3t_p^2/16)}} \tag{2.28}$$

$$Q_2 = \frac{\alpha_2 F_f p_f'}{2a} - \frac{\pi d_b^3 F_{yb}}{32a} - \frac{p_b t_p^2}{8a} \sqrt{F_{py}^2 - 3(\alpha_2 F_f/2p_b t_p)^2} \tag{2.29}$$

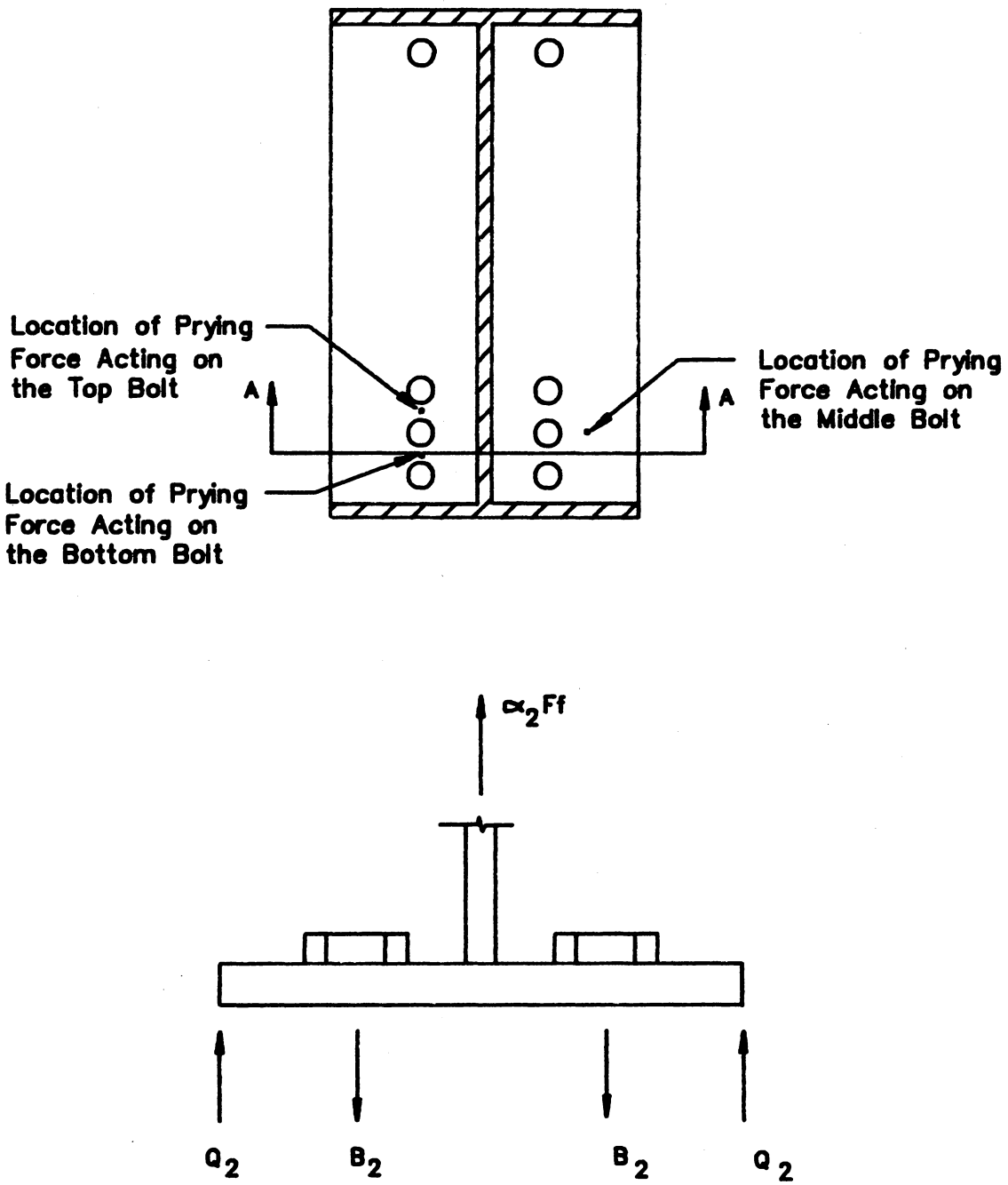

Fig. 2.6 Location of Prying Force Acting on the Middle Bolt

$$B_2 = \alpha_2 F_f/2 + Q_2 \qquad \text{when} \qquad F_1 \leq \alpha_2 F_f \leq F_{11} \tag{2.30}$$

where

$$F' = \frac{t_p^2 f_{py}[0.85(p_b)+0.8W'']+[\pi d_b^3 F_{yb}/8]}{2p_f'} \tag{2.31}$$

$$Q_{2max} = \frac{W'' t_p^2}{4a} \sqrt{f_{py}^2 - 3(F'/w'' t_p)^2} \tag{2.32}$$

$$F' = \text{minimum} \begin{cases} F_{limit} = F_{11}/2 \\ F_{2max} = \alpha_2 F_f/2 \end{cases} \tag{2.33}$$

$$B_2 = \alpha_2 F_f/2 + Q_{2max} \qquad \text{when } \alpha_2 F_f > F_{11} \tag{2.34}$$

A negative value under the radical in Equations 2.29 or 2.32 indicates the connection will fail locally in shear and is not adequate for the applied load.

2.3 Moment-Rotation Relationships

The relationship between the applied moment and subsequent rotation of a connection is needed to distinguish the degree of stiffness which can be assumed for the connection in designing the members to be connected. A plot of the applied moment, M, versus the rotation, ϕ, for a connection can be used to analyze the rotation characteristics of a connection. Plots of applied moment versus

rotation are shown in Figure 2.7. A line along the ordinate represents a fixed end boundary condition since no rotation occurs. Similarly, a line along the abscissa represents a simply supported boundary condition since there is no resistance to rotation. The moment-rotation curves for actual connections lie in the region between the perfect boundary conditions, as in Figure 2.7. The slope of a moment-rotation curve for an actual connection is an indication of the degree of the connection's stiffness. A steeper slope indicates greater connection stiffness.

Connection stiffness is classified into three types of construction defined by the AISC [1989] specification: Type I, Type II, and Type III. Rigid framing, or Type I construction, are those connections which have sufficient rigidity to fully resist rotation at joints. Simple framing, or Type II construction, are those connections that are free to rotate under gravity load, that have beams connected for shear resistance only, and have both the connection and the connected members able to adequately resist wind moments. Finally, Type III construction, or semi-rigid framing, are those connections which have a known moment capacity as a function of rotation between Type I and Type II construction. Idealized M-ϕ curves for all three types of construction are shown in Figure 2.7.

Typically, the moment rotational characteristics of an end-plate connection are dependant on the end-plate geometry in a given configuration. Hence, a general design recommendation classifying an end-plate connection configuration as suitable for all possible end-plate geometries cannot be made. Therefore, the moment versus rotation

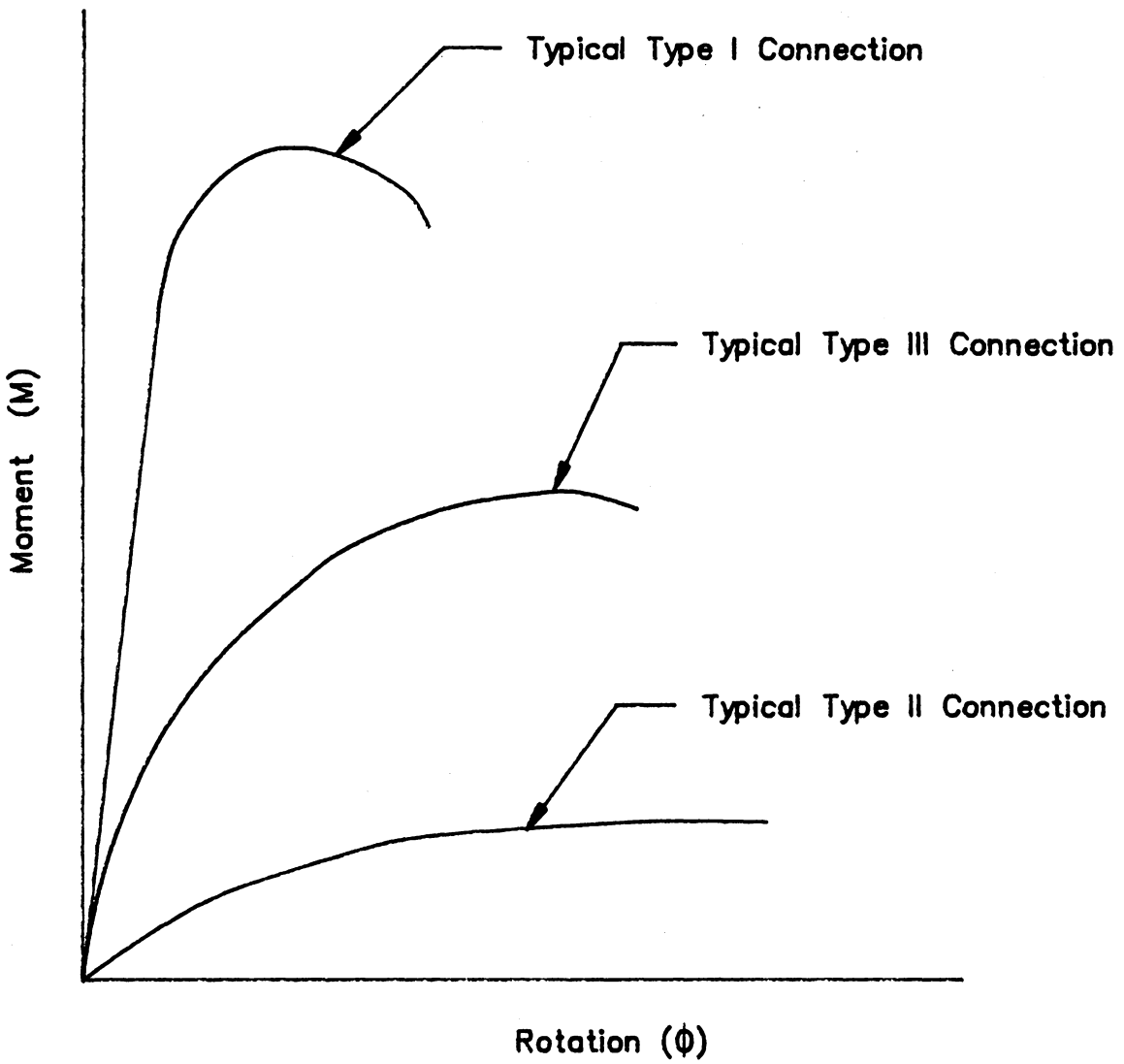

Fig. 2.7 Idealized M–ϕ curves for Typical Connections

characteristics of a connection configuration based on end-plate geometry must be known for the designer to classify which type of construction the connection is suitable for in design. Once the rotation of a connection is determined as a function of applied moment, the relation can be used to determine if a specific connection and applied load will meet the rotation criteria which are assumed for the connection in design. Conversely, a specific configuration and rotation criteria can be used to determine the maximum load which can be applied to a connection within the rotation criteria. Also, the moment-rotation relation can be used to study the characteristics of a connection after yielding.

To determine an expression for end-plate rotation as a function of moment, a regression analysis was performed on the experimental data and is presented in Section 3.4.4. Since the behavior of the end-plate during deformation is complex, a multiplicate regression model was used instead of a linear one. Many independent geometrical parameters, including those suggested by Abomaali [1984] were included in the analysis. The best combination of parameters to fit the data used to obtain the final regression model of rotation expressed as a function of the applied moment, is given in Section 3.4.4.

Once the rotation of an end-plate configuration is calculated from the applied moment, the construction type suitable for the end-plate can be determined based on a specific system of connection classification. Salmon and Johnson [1980] suggested guidelines for a system of classification to correlate moment-rotation curves with the AISC types

of construction. A Type I connection should resist an end-moment greater than 90% of the fixed end moment and rotate less than or equal to 10% of the end rotation for a simple span. A Type II connection should resist an end moment equal to or less than 20% of the fixed end moment and rotate at least 80% of the simple span end rotation. A Type III connection has a rotational resistance between the limits of Type I and Type II connections.

The end rotation for a simple span, ϕ_S, under any loading is:

$$\phi_S = M_F L/2EI \tag{2.35}$$

where M_F is the yield moment of the beam, $S_x F_y$. With I/S=h/2, Equation 2.35 becomes:

$$\phi_S = \frac{F_y L}{Eh} \tag{2.36}$$

A beam line can be constructed using an ordinate of M_F representing a perfectly rigid connection and an abscissa determined from Equation 2.36 representing a connection without rotational constraint. Once the abscissa is known, the value $0.1\phi_S$ can be calculated and a line drawn from the origin to the point where a vertical line drawn through $0.1\phi_S$ intersects the beam line. This line divides the rotation resistance into Type I and Type III regions as illustrated in Figure 2.8. Similarly, a dividing line can be found to separate the Type II and Type III regions. A typical connection, as plotted in Figure 2.8, will satisfy the criteria for a Type I connection

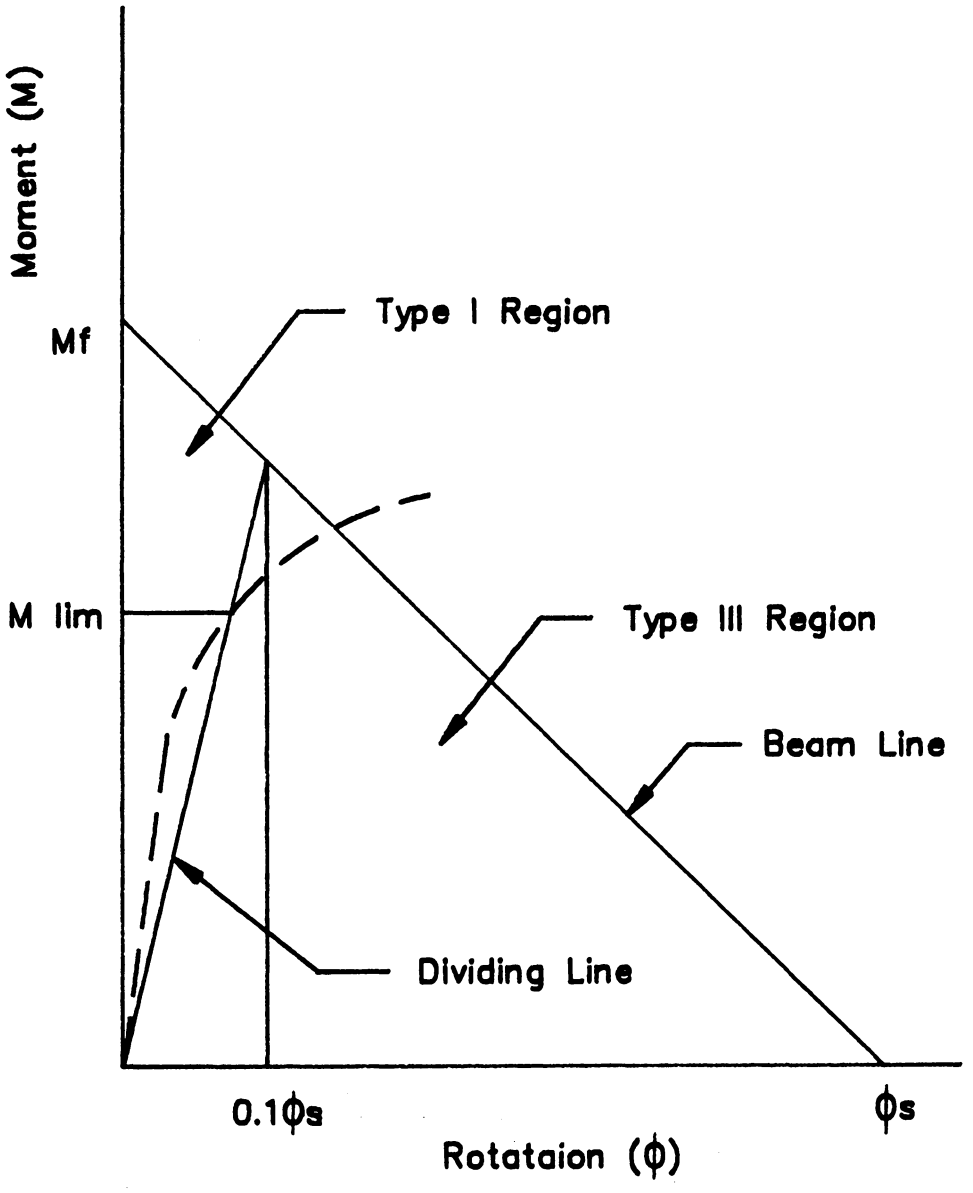

Fig. 2.8 Typical Moment versus Rotation Curve With Beam Line and Dividing Regions

until its plot crosses the dividing line or beam line, at which point a limiting moment, M_{LIM}, can be determined. At loads higher than M_{LIM}, the connection becomes suitable for Type III construction.

Using the guidelines suggested by Salmon and Johnson [1980], the equation of the dividing line can be determined as:

$$M = \frac{9M_F u}{u_s} \tag{2.37}$$

where M is the applied moment and u is the limiting connection rotation for Type I construction. By incorporating Equation 2.36 into 2.37, Equation 2.38 is determined as

$$M_d = \frac{9M_F Ehu}{F_y L} \tag{2.38}$$

where M_d is the moment on the dividing line for a given rotation. Hence, the rotation of an end-plate for a given applied moment for the six-bolt flush end-plate can be determined from the regression Equation developed in Section 3.4.4 and substituted into Equation 2.38 to determine if the connection is suitable for Type I construction. If M_d is less than or equal to the applied moment, M, the connection is suitable for Type I construction. Thus, Equation 2.38 can be used in conjunction with the regression equation developed in Section 3.4.4 to determine the suitability of a given six-bolt flush moment end-plate for Type I construction.

CHAPTER III

EXPERIMENTAL INVESTIGATION

3.1 Test Setup

The five experimental tests were setup as shown in Figure 3.1 where the end-plates are welded to two beam segments and tested in a splice plate connection under loading which produced a constant moment across the connection. A hydraulic ram was used to apply load to the specimen through a load cell, which measured the load magnitude, and a spreader beam which transferred the load to the test beams, as shown in Figures 3.1 and 3.2. The test beams and spreader beam were laterally braced at the lateral brace locations shown in Figure 3.1 such that only lateral forces were resisted.

Test setup instrumentation consisted of a load cell, a wire displacement transducer, two gaged calipers, and three instrumented bolts. Test data was collected and stored on a PC-based data acquisition system.

The load cell was used to measure the applied load from the hydraulic ram to the test specimen. A wire transducer, connected to the splice-plate connection, measured the midspan vertical deflection. Two gaged calipers were used to measure end-plate separation on each side of the test specimen. The end-plate separation was measured on both sides of the beam at the intersection of the beam tension flange and beam web

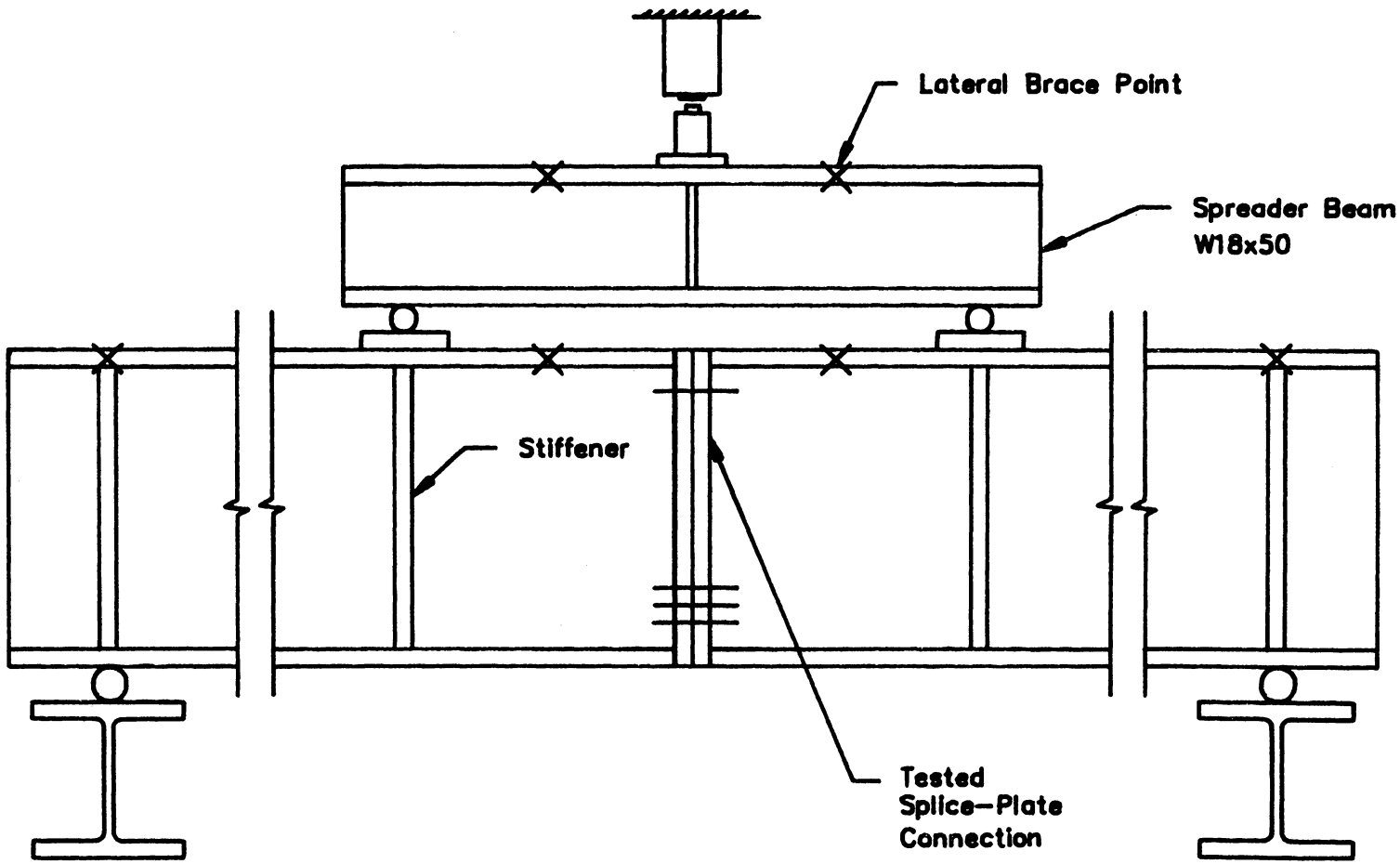

Fig. 3.1 Test Setup Longitudinal Elevation

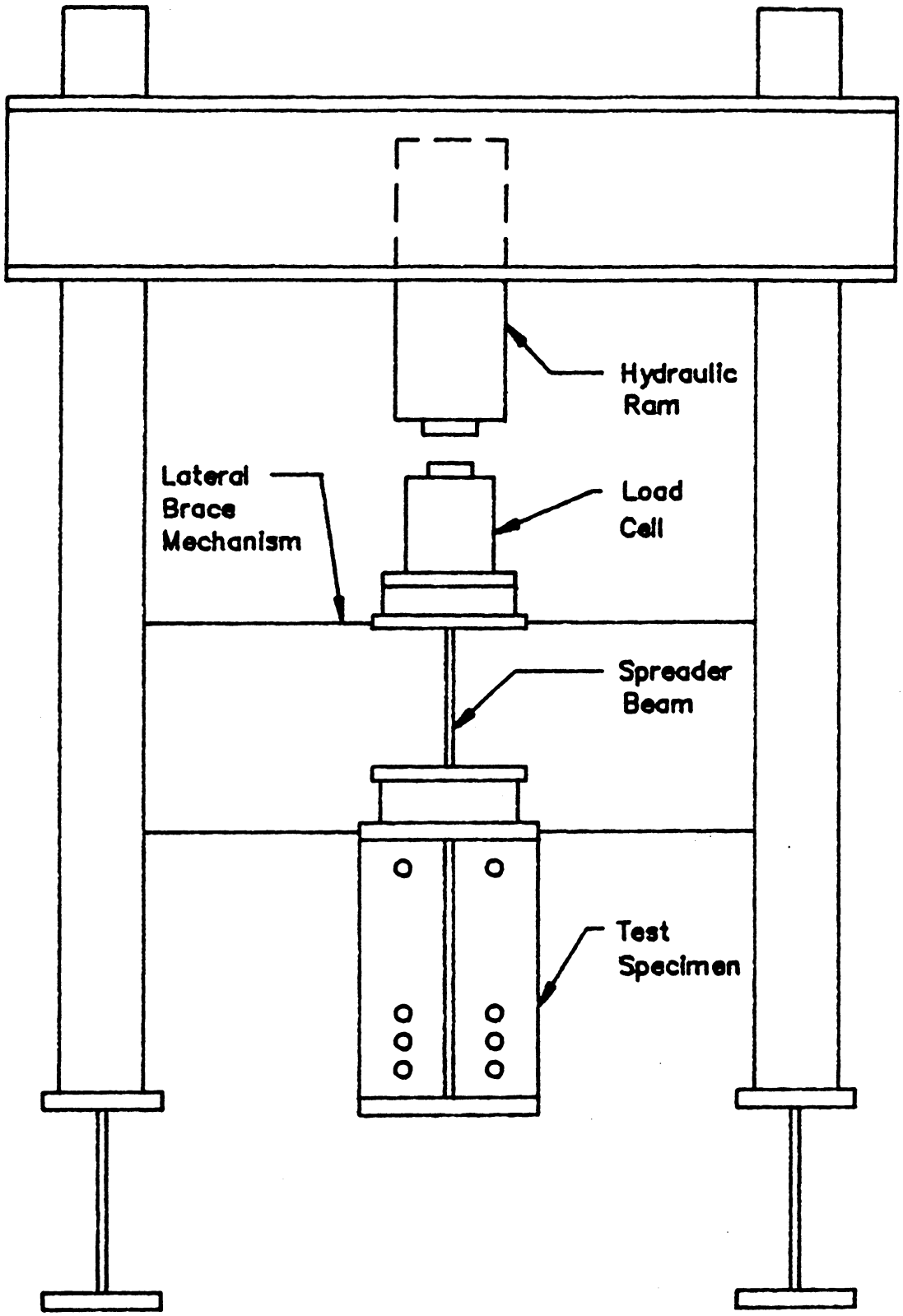

Fig. 3.2 Test Setup Traverse Section

as indicated in Figure 3.3. Bolt forces were measured by instrumented bolts at one of each of the three bolt locations as shown in Figure 3.3. Since the end-plate is symmetric, the bolt forces are distributed symmetrically and only one bolt per row needed instrumentation.

Bolts are instrumented by first drilling a 2mm diameter hole through the bolt head into the unthreaded portion of the bolt shank. A special type of strain gage, a "bolt gage", is then glued in the hole with a low viscosity epoxy. The bolt gage is positioned between the bolt head and threaded portion of the bolt shank. The effective tension area in the unthreaded portion of the bolt shank is greater than the effective area in the threaded portion of the shank. The instrumented bolts were then loaded to 90% of their proof load using a universal testing machine to obtain a calibration factor used to calculate bolt force from bolt strain.

3.2 Test Specimens

Five tests were performed for the eight-bolt flush end-plate connection. All five test specimens were fabricated using A572 Gr50 steel and all bolts were A325 type. The test matrix was based on the limits shown in Table 1.1. A convention for labeling each test was adopted to enable quick recognition of the parameters used in the test. The convention has the form:

Configuration - d_b - t_p - h

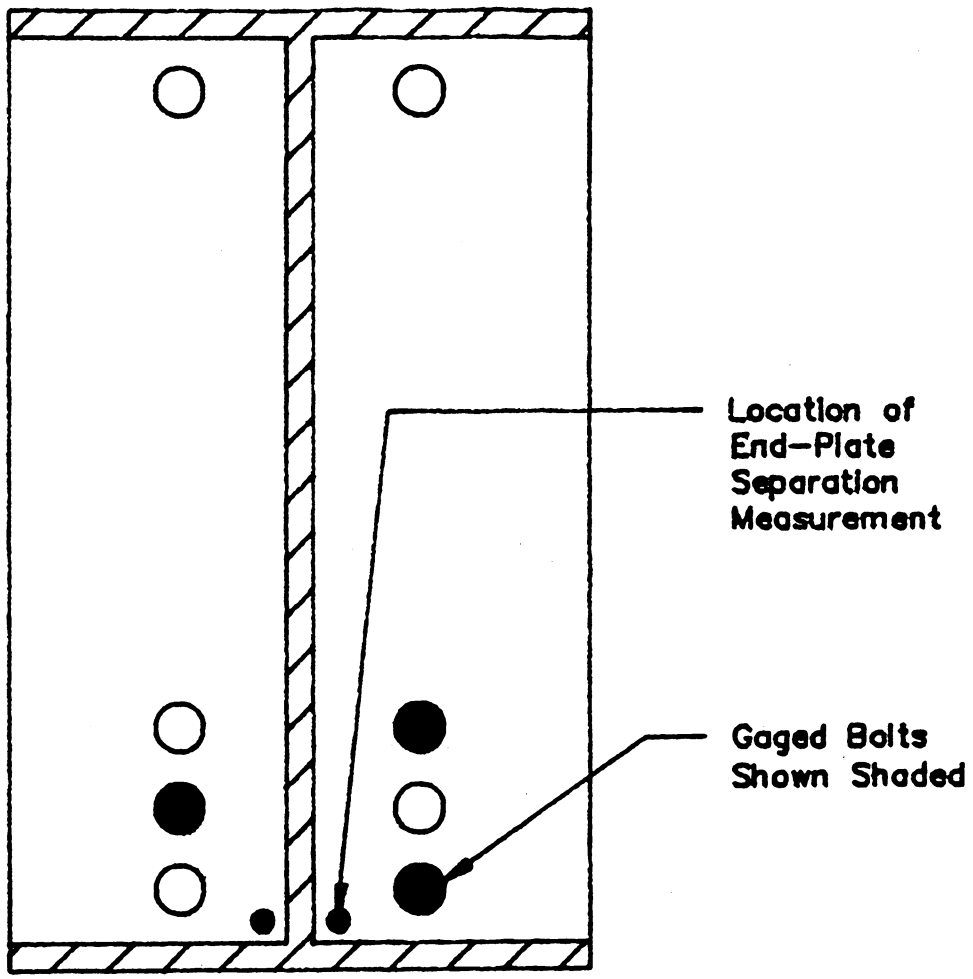

Fig. 3.3 Location of Test Specimen Instrumentation

where the configuration is MRF, or Multi-Row Flush end-plate, d_b is the diameter of the bolts used, t_p is the end-plate thickness, and h is the depth of the beam. The measured parameters for each specimen are included in an appropriate appendix. All specimens except MRF-7/8-1/2-36B were fabricated by Varco-Pruden Buildings, AMCA International. Test specimen MRF-7/8-1/2-36B was field welded at V P I and S U using end-plates obtained from Varco Pruden.

3.3 Testing Procedure

After placing the test beams in the test frame, the high strength bolts were installed and pretensioned to 70% of their proof load [AISC 1989]. The three instrumented bolts were pretensioned by a direct reading of the bolt force, while the uninstrumented bolts were pretensioned to the same degree of tightness by feel. Washers were not used on either the nut or bolt head side. Since the bolts were tightened in a random sequence, adjacent bolts sometimes became loose and were again tightened to the pretension level.

The connection was initially loaded to approximately 20% of the predicted capacity and then unloaded. Load was then applied in five kip increments until one of the following definitions of end-plate, bolt or beam failure occurred. Beam failure occurs when a yield plateau is reached on the applied load versus centerline deflection plot. End-plate failure occurs when a yield plateau is reached on the applied load versus centerline deflection plot, or the applied load versus end-plate separation plot. Bolt failure occurs when one of the bolts reaches its

proof load which is twice the AISC [1989] allowable tension capacity. Usually, the connection was loaded past the point of bolt proof load until the bolt strain increased rapidly with a small increase in load so that the behavior of the other bolts could be observed.

3.4 Test Results

3.4.1 Introduction

Detailed results for each of the five six-bolt flush end-plate tests are presented in Appendices B through F. Each appendix contains the data for a single test and consists of the following: a Test Synopsis sheet, measured dimensions, calculation of predicted end-plate and bolt failure, and six plots.

The Test Synopsis sheet summarizes all beam, end-plate and bolt data including the design dimensions. Additionally, predicted and experimental failure values are given.

The second sheet contains figures showing all the measured dimensions for each end-plate and the measured weld sizes.

The third and fourth sheets contain calculations of the predicted failure moments for the end-plate and the bolts, respectively. These values are calculated for the end-plate which controlled the analysis using the measured dimensions. The yield-line analysis and bolt force predictions were modified to include each of the two end-plates compromising a test in the analysis.

The fifth sheet contains two plots: applied moment versus centerline deflection and applied moment versus end-plate separation, respectively. The moment versus centerline deflection plot contains one curve of the experimental results, one curve showing the yield-line moment prediction, and another curve of the theoretical centerline deflection. The theoretical deflection is determined assuming linear elastic material properties for a simply supported beam with two equally spaced concentrated loads:

$$\delta_{theo} = \frac{P_{RAM}\, b}{48EI}(3L^2 - 4b^2) \qquad (3.1)$$

where b is the distance from one of the loads to the closest support. The applied moment versus end-plate separation plot has two curves. One shows the experimentally measured end-plate separation at the intersection of the beam web and tension flange and the other is the ultimate moment prediction from the yield-line analysis shown on the third sheet.

The sixth sheet contains two plots. The first plot of applied moment versus rotation is developed by first solving the following equation for ϕ:

$$\delta_{test} = \delta_{theo} + \phi L/2 \qquad (3.2)$$

where ϕ_{test} is the experimentally measured centerline deflection and ϕ_{theo} is the theoretical centerline deflection, Equation 3.1. Small

deflections are assumed in developing Equation 3.2. The second plot showing the bottom bolt force (defined in Figure 1.4), B_1, versus moment contains two curves: the experimental test results and the predicted values from the modified Kennedy method equal to or less than the bolt proof load.

The last sheet contains two plots: the force in the middle bolt, B_2, versus moment, and the force in the top bolt, B_3, versus moment respectively. Both plots have one curve showing the experimental test results and another showing the bolt force prediction equal to or less than the proof load. Since the bolts were calibrated within the elastic range, the bolt forces are only valid within the elastic range.

Bolt force predictions and end-plate analyses were calculated using measured strengths of the end-plate and bolt materials found in Appendix G. The tensile tests for the end-plate material were conducted by the author using a universal testing machine. The bolt tests were performed by Pittsburgh Testing Laboratories and used the ASTM F-606 test method.

3.4.2 End-Plate Limit State

The limit state of end-plate yielding is characterized by the formation of plastic hinges in the end-plate followed by large plastic deformation of the connection. The end-plate ultimate moment, M_{yp}, for each specimen was predicted using yield-line theory, measured dimensions, and the measured ultimate material yield stress. Calculations for the predicted ultimate moment for each specimen are

given in the appropriate Appendix. The experimental yield moment, M_y, for each test specimen, was determined from the plot of moment versus centerline deflectionby dividing the experimental curve into two linear segments which intersect at the yield moment as in Figure 3.4. When a curve is non-linear throughout, many yield points can be determined and the best approximation is found by trial and error.

Predicted and experimental results for the end-plate limit state are summarized in Table 3.1. The applied-to-predicted moment ratios, M_y/M_{yp}, for the tests ranged from 0.90 (unconservative) to 1.10 (conservative). These results suggest that the yield-line mechanisms for the six-bolt flush end-plate presented in Chapter II adequately predict the load at which yielding will occur.

Experimental moment capacities were determined from the moment versus end-plate separation plots using the same method as the one using the centerline deflection plots. These results are summarized in Table 3.2 The experimental moment capacity determined from the moment versus end-plate separation plots, M_{ye}, closely resembles those from the moment versus centerline deflection plots. The experimental yield moment is given for both sides of the beam, M_{ye1}, and M_{ye2}. The applied-to-predicted moment ratios, M_{ye}/M_{yp} ranged from 0.87 (unconservative) to 1.17 (conservative). The results from the end-plate separation plots also indicate that the yield-line mechanisms adequately predict the yield moment.

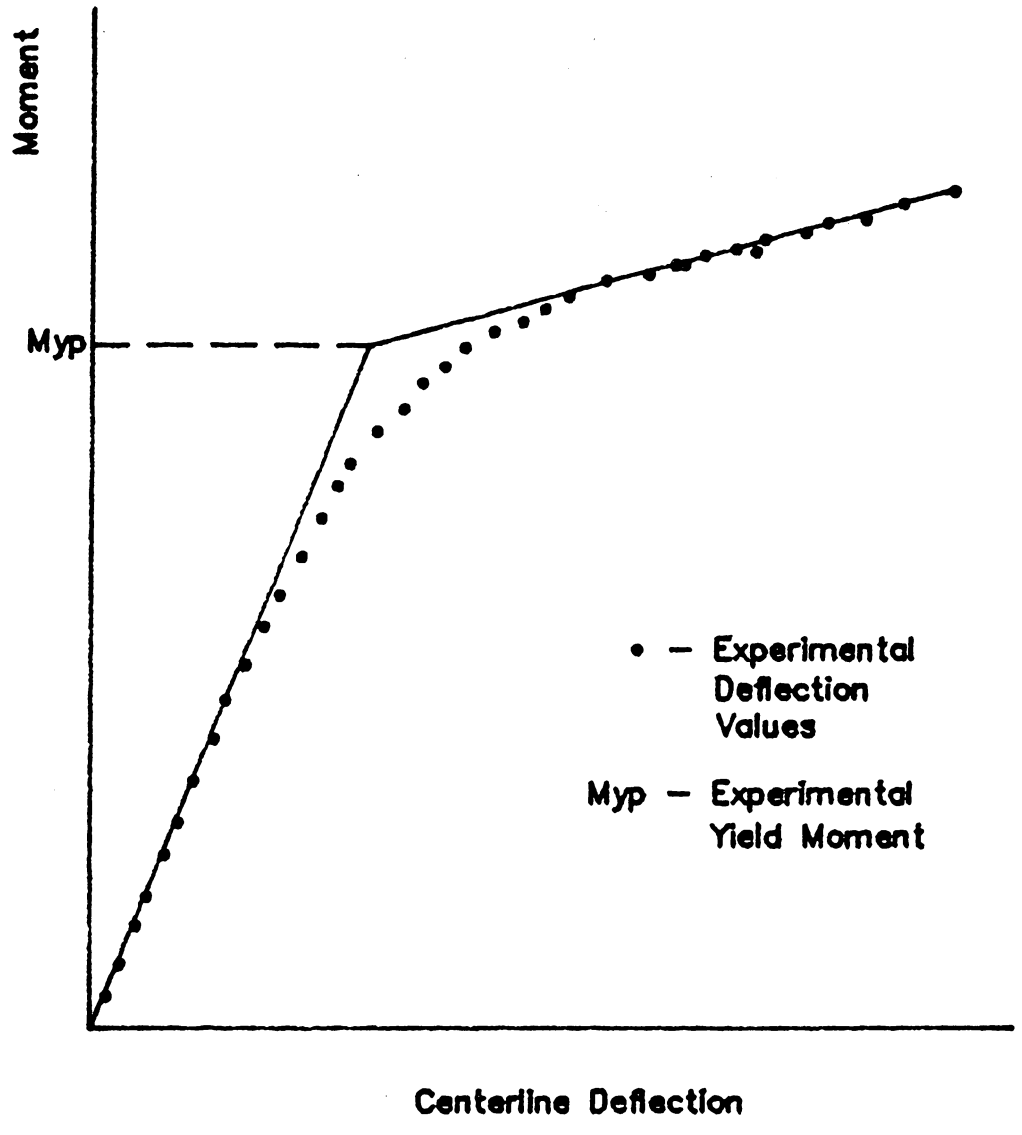

Fig. 3.4 Determination of Experimental Yield Moment

Table 3.1

End-Plate Limit State Based on Centerline Deflection

Test Specimen	M_{yp}[1] (ft-kip)	M_y[2] (ft-kip)	$\frac{M_y}{M_{yp}}$	M_{max} (ft-kip)
MRF-7/8-3/8-28	173.9	192	1.10	365
MRF-1-1/2-28	309.2	277	0.90	399
MRF-3/4-3/8-36	210.6	224	1.07	365
MRF-7/8-1/2-36	361.2	344	0.95	459
MRF-7/8-1/2-36B	357.2	347	0.97	379

[1] M_{yp} = predicted end-plate ultimate moment from yield-line analysis.

[2] M_y = experimental determined end-plate yield moment.

[3] M_{max} = maximum experimentally applied moment to specimen.

Table 3.2

End-Plate Limit State Based on End-Plate Separation

Test Specimen	M_{yp}[1] (ft-kip)	M_{ye1}[2] (ft-kip)	M_{ye2}[3] (ft-kip)	$\frac{M_{ye1}}{M_{yp}}$	$\frac{M_{ye2}}{M_{yp}}$	M_{max}[4] (ft-kip)
MRF-7/8-3/8-28	173.9	204	192	1.17	1.10	365
MRF-1-1/2-28	309.2	268	276	6.87	0.89	399
MRF-3/4-3/8-36	210.6	218	228	1.04	1.08	365
MRF-7/8-1/2-36	361.2	383	371	1.06	1.02	459
MRF-7/8-1/2-36B	357.3	330	335	0.92	0.93	379

[1] M_{yp} = predicted end-plate ultimate moment from yield-line analysis.

[2] M_{ye1} = experimental determined end-plate yield moment, north side.

[3] M_{ye2} = experimental determined end-plate yield moment, south side.

[4] M_{max} = maximum experimentally applied moment to specimen.

All specimens except MRF-7/8-1/2-36B were loaded to at least 20% beyond the experimental and predicted yield points, indicating a significant reserve capacity. Test MRF-7/8-1/2-36B was ended because of a local shear failure in the weld between the end-plate and the beam near the tension flange.

3.4.3 Bolt Force Limit State

The applied and predicted moments at which the bolt proof load is reached in the bolt closest to the tension flange are summarized in Table 3.3. The bolt proof load is defined as twice the allowable AISC [1989] tension capacity. The proof load values are shown on the bolt force versus moment plots in the appendices. The applied moment, M_u, was calculated from the bolt force plots from the location where the experimental bolt force line crosses the line representing the bolt proof load. The predicted moment values at the bolt proof loads were calculated using the measured dimensions and measured yield stresses found in the appendices.

The values α_1, α_2, and α_3 used to proportion the tension flange force were determined from the experimental plots of bolt force versus moment by trial and error to best fit the data. They are:

$$\alpha_1 = 0.55 \tag{3.3}$$

$$\alpha_2 = 0.40 \tag{3.4}$$

$$\alpha_3 = 0.45 \tag{3.5}$$

Table 3.3

Bolt Force Limit State Results

Test Specimen	Applied Moment at Proof Load M_u			Predicted Moment at Proof Load M_{ub}			$\frac{\text{Applied}}{\text{Predicted}}$ or $\frac{M_u}{M_{ub}}$		
	B_1 (ft-kips)	B_2 (ft-kips)	B_3 (ft-kips)	B_1 (ft-kips)	B_2 (ft-kips)	B_3 (ft-kips)	B_1	B_2	B_3
MRF-7/8-3/8-28	275.8	N.R.	317.1	268.8	430.7	328.6	1.02	--	0.97
MRF-1-1/2-28	328.2	N.R.	395.0	321.8	543.9	393.3	1.02	--	1.00
MRF-3/4-3/8-36	293.2	N.R.	299.3	280.9	295.0	343.3	1.04	--	0.87
MRF-7/8-1/2-36	358.8	384.5	N.R.	414.1	454.6	506.2	0.86	0.85	--
MRF-7/8-1/2-36B	363.6	N.R.	N.R.	412.0	445.0	503.6	0.88	--	--

N.R. - not reached

Thus

$$\alpha_1 + \alpha_2 + \alpha_3 = 1.40 > 1.0 \qquad (3.6)$$

The amount of tension flange force distributed to each of the bolts by the α factors is actually larger than what actually occurs because the actual prying forces acting on the bolts, particularly on the two rows farthest from the tension flange, are larger than those predicted by the Kennedy method. This is probably due to significant deformation of the end-plate as loading continues beyond first yield.

On the plots of bolt force versus moment in the appendices, the bolts remain at their pretension load along a relatively straight line until forces due to the tension flange force or prying action load the bolts above their pretension load along a curved line beyond the proof load. The predicted bolt force line is based on the "thin" stage of plate behavior discussed in Chapter II.

In all five tests, the bottom bolt B_1 (defined in Figure 1.4), reached the bolt proof load before the middle and top bolts, B_2, and B_3, respectively. The applied-to-predicted moment ratios for the bottom bolt, B_1, ranged from 0.86 (unconservative) to 1.0415 (conservative). After the proof load was reached, the force in the bolt was observed to increase rapidly at smaller increments of load indicating the yield plateau had been reached.

In three of the five tests, the top bolt, B_3, reached its proof load before the middle bolt B_2. The applied-to-predicted moment ratios for the top bolt ranged from 0.87 (unconservative) to 1.00 (conservative).

The middle bolt was not expected to reach its proof load before the top bolt in Test MRF-7/8-1/2-36. Results from previous testing of an eight-bolt multiple row extended end-plate connection [Morrison 1985] indicated that no prying forces act at the middle bolt. However, due to the manner in which the six-bolt flush end-plate configuration deforms, some prying forces act on the middle bolt. These prying forces are caused by the beam web pulling the end-plate as the connection rotates, as shown in Figure 2.6. Thus, test MRF-7/8-1/2-36B was conducted to verify that the middle bolt, B_2, does reach its proof load before the top bolt, B_3. The applied-to-predicted moment ratio for Test MRF-7/8-1/2-36B was not obtained for the middle bolt, B_2, due to a shear failure in the weld between the end-plate and the beam tension flange which occurred just before the middle bolt reached its proof load. By extrapolating the experimental curve, an applied-to-predicted moment ratio of 0.86 was determined.

Based on the experimentally results shown in Table 3.3 and the correlation of the experimental bolt force curves to the prediction curves in the appendices, the modified Kennedy method of predicting bolt forces adequately predicts the bolt forces in the six-bolt flush end-plate connection.

3.4.4 Moment Rotation Relationships

The experimentally determined moment versus rotation plots are given in the appendices. A general design recommendation of connection

type for the six-bolt end-plate configuration could not be made because of a wide variation in observed rotation characteristics for the five tests. This variation is caused by the different end-plate geometric parameters affecting the moment-rotation characteristics of the tests. Therefore, a relationship of moment versus rotation was determined in a regression analysis based on the experimental results.

The regression analysis was conducted by first determining all the geometric independent variables which might effect the rotation characteristics of the six-bolt configuration. These were determined from a parametric study on end-plate configurations [Abomaali 1984] to be: t_p = thickness of the end-plate; p_f = distance from the inside of the beam tension flange to the first row of tension bolts; d_b = bolt diameter; g = bolt gage distance, or the distance between vertical bolt rows; b_f = width of the end-plate; h = height of the end-plate. The independent variable representing force was to be the experimentally applied moment.

The geometric parameters were then non-dimensionalized with respect to the end-plate width, b_f. Thus, five independent geometric variables were developed as follows [Abomaali 1984]:

$$\pi_1 = t_p/b_f, \text{ the plate thickness parameter} \tag{3.7}$$

$$\pi_2 = p_f/b_f, \text{ the bolt pitch parameter} \tag{3.8}$$

$$\pi_3 = d_b/b_f, \text{ the bolt diameter parameter,} \tag{3.9}$$

$$\pi_4 = g/b_f, \text{ the bolt gage parameter, and} \tag{3.10}$$

$$\pi_5 = h/b_f, \text{ the plate height parameter} \tag{3.11}$$

A parameter suggested by Abomaali [1984] to represent bending stiffness of the end-plate is given as:

$$\pi_6 = p_f^3/b_p t_p^3 \tag{3.12}$$

and has a unit of $(\text{length})^{-1}$. The independent parameter representing applied force is given as:

$$\pi_7 = M_p/M_y \tag{3.13}$$

where M is the applied moment and M_{yp} is the yield moment of the end-plate predicted by yield-line theory as presented in Chapter II. The dependent variable in the regression analysis was taken to be the rotation of the connection:

$$\pi_r = \phi \tag{3.14}$$

The limits and values used in the regression analysis were taken directly from the experimental data.

A regression equation was developed for the dependant parameter π_r as a function of the independent parameters π_1-π_8. A linear regression model is shown as [Abomaali 1984]

$$\pi_r = C_0+C_1\pi 1+C_2\pi_2+\ldots+C_7\pi_7+C_{12}\pi_1\pi_2+C_{23}\pi_2\pi_3+\ldots \tag{3.15}$$

where C_0, C_1, etc. are unknown coefficients. Since the deformation behavior is very complex, a multiplicate regression model was used instead of the linear model. The multiplicate model is given as [Abomaali 1984]

$$\pi_r = C_0\pi_1^{\Gamma 1}\pi_2^{\Gamma 2}\pi_3^{\Gamma 3}\pi_4^{\Gamma 4}\pi_5^{\Gamma 5}\pi_6^{\Gamma 6}\pi_7^{\Gamma 7} \tag{3.16}$$

or

$$\ln(\pi_r) = \ln(C_0)+C_1\ln(\pi_1)+C_2\ln(\pi_2)+C_3\ln(\pi_3) +C_4\ln(\pi_4)+C_5\ln(\pi_5)+C_6\ln(\pi_6)+C_7\ln(\pi_7) \tag{3.17}$$

A regression equation was developed using Equation (3.18) and the method of least squares.

The computer program, SAS, was used to determine how much of an effect each of the parameters had on the dependant variable and which combination of parameters gave the best results. An evaluation of a combination of parameters was based on the value of the coefficient of multiple determination, R^2, for every possible combination of parameters. The R^2 value gives the proportion of the total variation about the mean of the regression. Therefore, the R^2 value can be used to measure the effectiveness a combination of parameters has in representing the actual data. A value of R^2 close to unity indicates an adequate correlation between the predicted and experimental values.

By comparing the R^2 values for the combinations of parameters, the π_3 and π_6 parameters were found not to significantly affect the rotation characteristics significantly. The following equation was developed as the equation which best fit the experimental data:

$$\phi = (2.857\text{x}10^{-5})(t_p/b_f)^{-8.564}(p_f/b_f)^{-0.510} \quad (3.18)$$
$$(g/b_f)^{18.401}(h/b_f)^{-4.738}(M/M_{yp})^{2.838}$$

The R^2 value for the regression analysis was 0.939. Figure 3.5 compares the predicted values with the experimental values of rotation. The line with a slope of unity indicates a perfect fit. The two other lines depict the 25% error limits. Figure 3.6 shows the correlation between the experimentally measured rotation curve and the predicted rotation curve on a plot of applied moment versus rotation.

The regression equation adequately predicts the moment-rotation relationship as shown in Figures 3.5 and 3.6. The regressopm equation can be used to predict the connection rotation given the geometric parameters and loading, so that the connection type can be classified for design as discussed in Section 2.3.

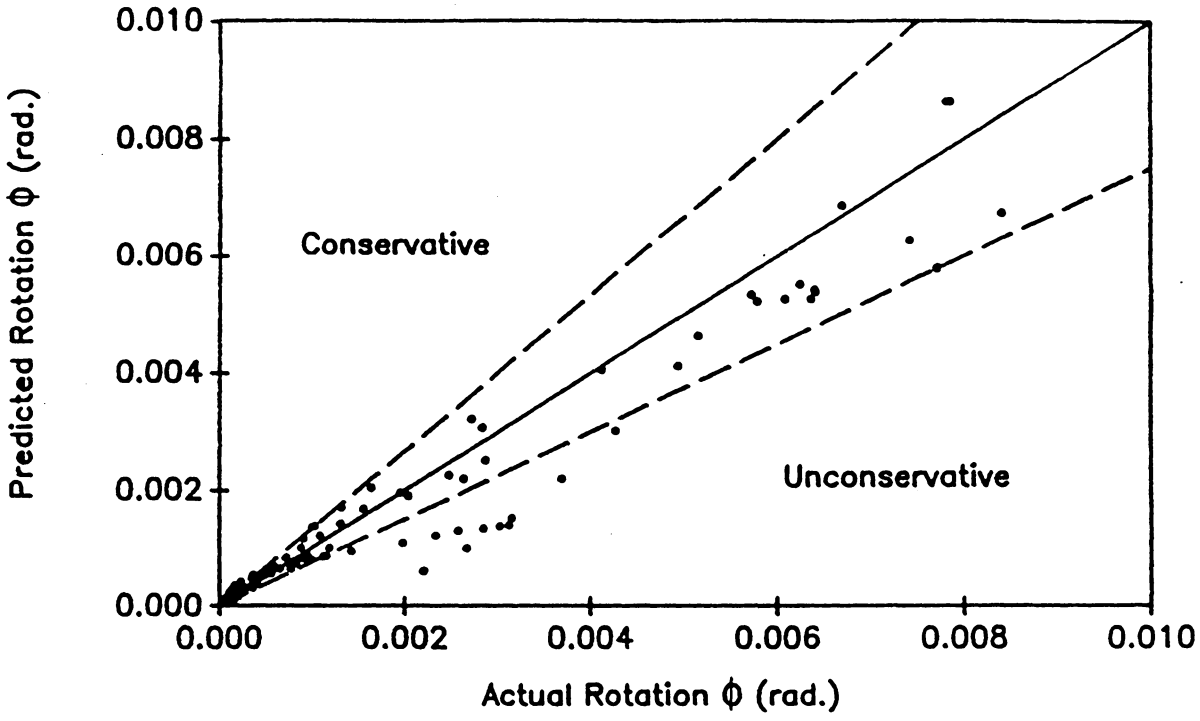

Fig. 3.5 Predicted Rotation versus Actual Rotation

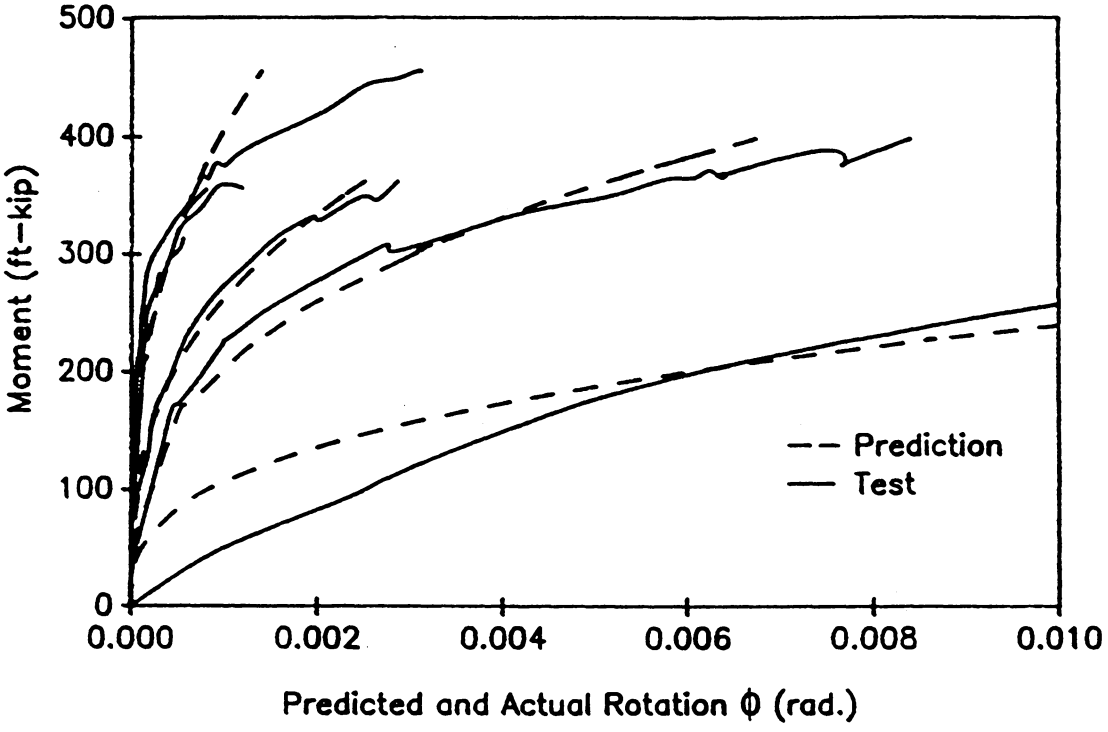

Fig. 3.6 Moment versus Predicted and Actual Rotation

CHAPTER IV

SUMMARY, DESIGN RECOMMENDATIONS AND EXAMPLE

4.1 Summary

A six-bolt flush end-plate configuration was experimentally tested to verify analytical procedures which predict maximum loads for the limit states of end-plate strength and bolt forces. Five specimens representing four different configurations were tested within the limits of Table 1.1. In all five tests, the end-plate yielded before bolt failure. The bottom bolt, B_1, reached its proof load before the middle and top bolts, B_2 and B_3 respectively, in all five tests. The applied-to-predicted moment ratios for the end-plate limit state were from 0.87 (unconservative) to 1.17 (conservative). The applied-to-predicted moment ratios for the bolt force limit state for the bottom bolt were from 0.86 (unconservative) to 1.04 (unconservative). The end-plate capacity was predicted using yield-line theory and the bolt force prediction based on a modified Kennedy method. The moment-rotation relationship for the six-bolt flush end-plate configuration was modeled using the experimental data to develop a regression equation which relates connection rotation, u, as a function of the applied moment, M. The regression equation can be used to determine if a given end-plate configuration can be used as a Type I connection for a given loading.

4.2 Design Recommendations

Predictions of end-plate thickness from yield-line theory and of bolt forces from a modified Kennedy method were adequately verified by experimental testing. A moment-rotation relationship was developed from the experimental data. Based on these methods, the following design procedure is recommended.

1. Compute the factored beam end-moment:

$$M_u = M_w/0.6 \tag{4.1}$$

2. Establish trial values of the end-plate geometry:

h, b_f, g, p_f, p_b, and t_f

3. Use the flow chart in Figure 4.1 to determine the required end-plate thickness using the known yield stress, f_{py}.

4. Select a trial bolt diameter and compute the bolt force using Figure 4.2

5. Determine the required bolt diameter from:

$$d_b = !\overline{2B_1/pF_a} \tag{4.2}$$

where Fa is the allowable stress for the bolt material.

6. Use the regression equation to determine if the connection rotation meets the design requirements

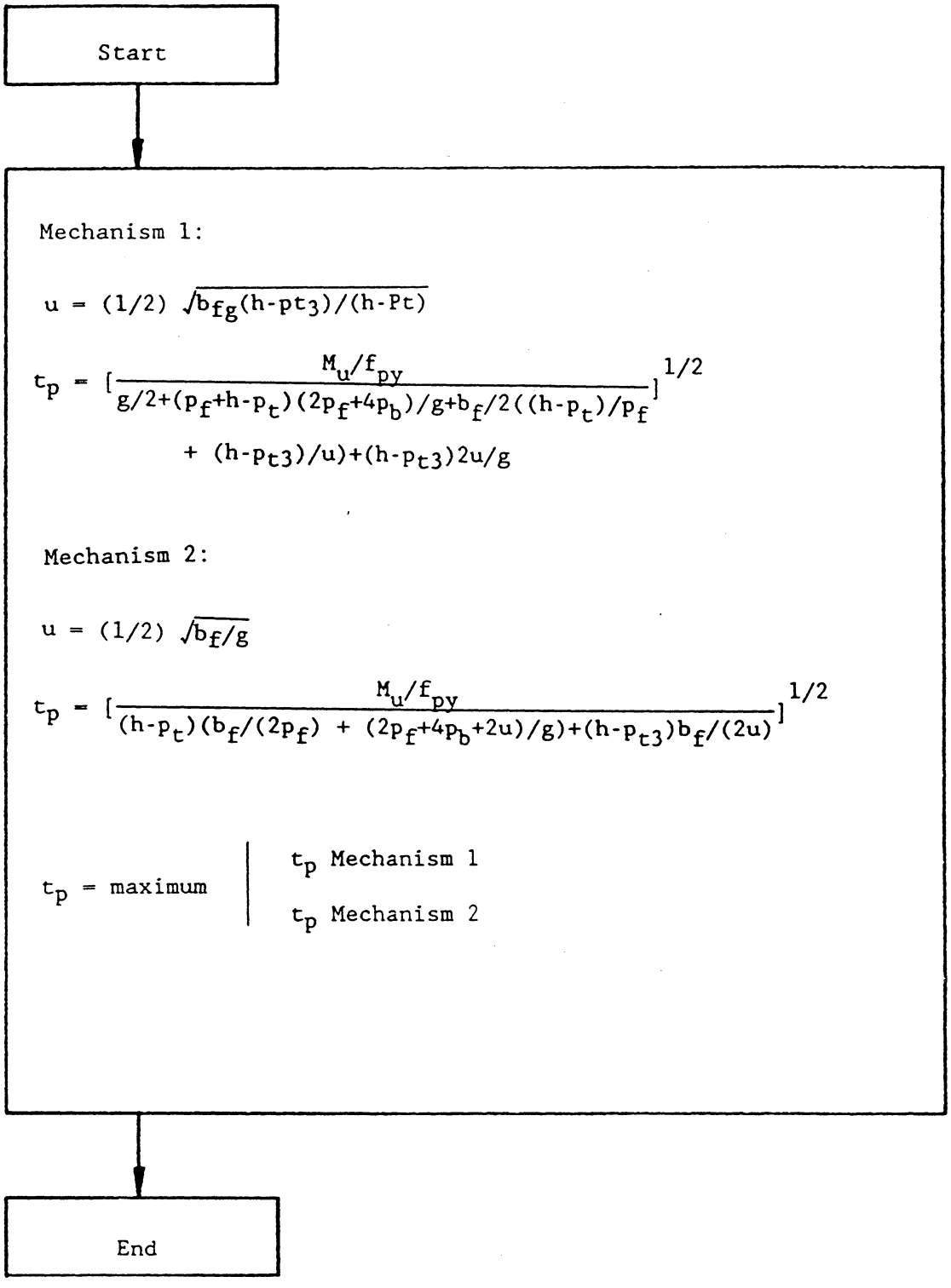

Fig. 4.1 Flowchart to Determine End-Plate Thickness

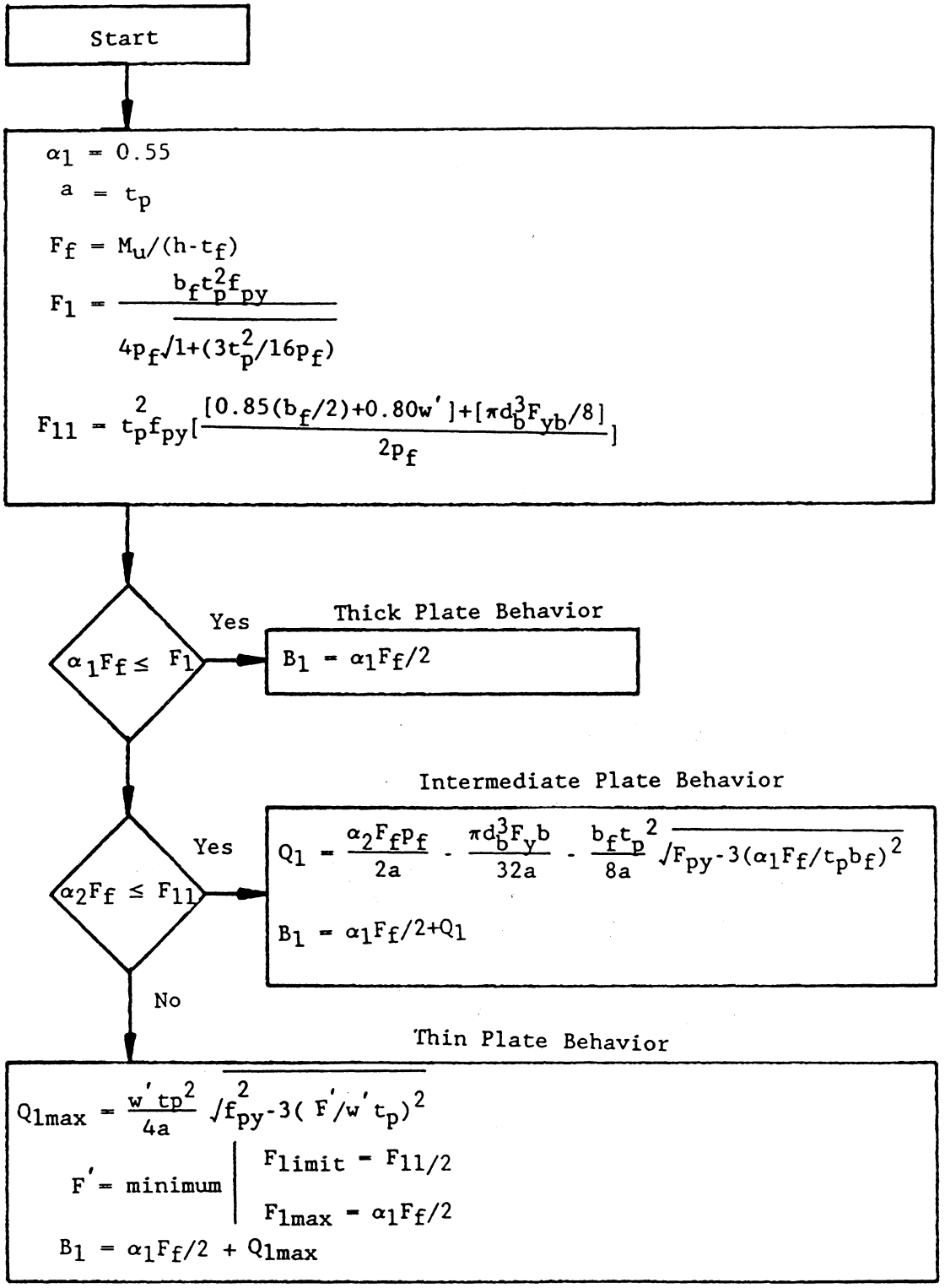

Fig. 4.2 Flowchart to Determine Bolt Force

For Type I Construction:

$$u = (2.857x10^{-5})(t_p/b_f)^{-8.564}(p_f/b_f)^{-0.510} \quad (3.19)$$

$$(g/b_f)^{18.401}(h/b_f)^{-4.738}(M/M_{yp})^{2.838}$$

$$M_d = \frac{9M_F Ehu}{F_y L} \quad (2.38)$$

and

$$M_u > M_d$$

The AISC specification [1989] specifies the allowable tensile stress for A325 type bolts as 44 ksi. This includes a factor of safety of 2.0 which is reflected in Equation 4.1.

4.3 Design Example

Determine the required end-plate thickness and bolt diameter for a six-bolt flush moment end-plate, given the following parameters:

Working Moment: M_w = 200 ft-kips

Beam Data:

Length	L	10 ft
Depth	d	28 in
Section modulus	S_x	192 in^3

Flange width	b_f	10 in
Flange thickness	t_f	3/8 in
Web thickness	t_w	5/16 in
A572 Gr 50	F_y	50 ksi

End-Plate Data:

Gage	g	4 in
Pitch	p_f	2 in
Pitch between bolts	p_b	2-1/2 in
A572 Gr 50	f_{py}	50 ksi

Bolt Data:

A325 type	F_a	44 ksi

Step 1. Determine M_u

$$M_u = M_w/0.6 = 200/0.6 = 333.3 \text{ ft-kips}$$

Step 2. Establish trial values of end-plate geometry

Step 3. Determine t_p from Figure 4.1

Mechanism I

$$p_t = p_f + t_f = 2 + 3/8 = 2.375$$

$$p_{t3} = p_t + 2p_b = 2.375 + 2(2.5) = 7.375$$

$$u = 1/2 \sqrt{b_f g(h-p_{t3})/(h-p_t)}$$

$$u = 1/2 \sqrt{10(4)(28-7.375)/(28-2.375)} = 2.84 \text{ in}$$

$$t_p = \left[\frac{M_u/f_{py}}{(h-p_t)(b_f/(2p_f) + (2p_f+4p_b+2u)/g)+(h-p_{t3})b_f/(2u)}\right]^{1/2}$$

$$t_p = \left[\frac{333.3\ /50}{(28-2.375)(10/(2(2))+(2(2)+4(2.5)+2(2.84)/4)}\right]^{1/2}$$

$$+(28-7.375)10/(2(2.84))$$

$$= .495 \text{ in}$$

Mechanism II

$$u = 1/2\ \sqrt{b_{fg}}$$

$$u = 1/2\ \sqrt{10(4)} = 3.16 \text{ in}$$

$$t_p = \left[\frac{M_u/f_{py}}{g/2+(p_f+h-p_t)(2p_f+4p_b)/g+b_f/2((h-p_t)/p_f}\right]^{1/2}$$

$$+ (h-p_{t3})/u)+(h-p_{t3})2u/g$$

$$t_p = \left[\frac{333.3/50}{4/2+(2+28-2.375)(2(2)+4(2.5))/4+10/2((28-2.375)/2}\right]^{1/2}$$

$$+ (28-7.375)/3.16)+(28-7.375)2(3.16)/4$$

$$= 0.588 \text{ in}$$

$$t_p = \left| \begin{array}{l} t_p \text{ Mechanism I} \\ t_p \text{ Mechanism II} \end{array} \right.$$

$$t_p = \begin{matrix} \circ \\ \circ \\ \circ \end{matrix} \begin{matrix} 0.495 \\ \\ 0.588 \end{matrix} = 0.588 \text{ in} \quad \text{Try } t_p = 5/8 \text{ in}$$

Step 4. Select a trial bolt diameter of 1.00 in. and determine the bolt force from Figure 4.2

$$w' = b_f/2 - [d_b + 1/16]$$

$$w' = 10/2 - [1 + 1/16] = 3.94 \text{ in}$$

Determine the flange force F_f

$$F_f = M_u/(h-t_f)$$

$$= 333.3(12)/(28-0.375)$$

$$= 144.5 \text{ kips}$$

Determine the flange force at the thick plate limit

$$F_1 = \frac{b_f t_p^2 f_{py}}{4p_f\left[1+(3t_p^2/16p_f)\right]}$$

$$F_1 = \frac{10(0.625)^2(50)}{4(2)\left[1+(3(0.625)^2/16(2))\right]}$$

$$= 24.2 \text{ kips}$$

$$F_{11} = t_p^2 f_{py}\left[\frac{[0.85(b_f/2)+0.80w']+[\pi d_b^3 F_{yb}/8]}{2p_f}\right]$$

$$F_{11} = 0.625^2(50)\left[\frac{[0.85(10/2)+0.80(3.94)]+[\pi(1.0)^3(88)/8]}{2(2)}\right]$$

$$= 44.8 \text{ kips}$$

Determine the amount of flange force distributed to the bottom bolt, B_1

$\alpha_1 F_f = 79.6$ kips

Since $\alpha_1 F_f = 17.9$ kips $> F_{11} = 44.8$ kips the end-plate behavior is thin

Determine the maximum amount of prying force

$$F' = \text{minimum}\left|\begin{array}{l} F_{11} = 44.8 \text{ kips} \\ \alpha_1 F_f = 79.6 \text{ kips} \end{array}\right. = 44.8 \text{ kips}$$

$$Q_{1max} = \frac{w' t_p^2}{4a}\sqrt{f_{py}^2 - 3(F^1/w' t_p)^2}$$

$$Q_{1max} = \frac{3.94(0.625)^2}{4(0.625)} \sqrt{50^2 - 3(44.8/3.94(0.625)^2}$$

$$= 23.8 \text{ kips}$$

$$B_1 = \alpha_1 F_f/2 + Q_1$$

$$= 0.55(144.8)/2 + 23.8 = 63.6 \text{ kips}$$

Step 5. Determine required bolt diameter

$$d_b = \sqrt{2B_1/\pi F_a}$$

$$d_b = \sqrt{2(63.6)/\pi(44)}$$

$$= 0.959 \text{ in}$$

Step 6. Determine connection suitability for Type I construction.

Determine yield moment given 9/16" plate thickness

$$M_y = 4m_p[g/2+(2p_f(p_f+2p_b))/g+(h-p_t(b_f/(2u)+2(p_f+2p_b)/g)$$

$$+(h-p_{t3})(b_f/(2u)+2u/g]$$

$$M_y = \frac{4(50)(g/16)^2}{4} [4/2+2(2)(2+2(2.5))/4+(28-2.375)(10/2(1.25)$$

$$+2(2+2(2.5))/y+(28-7.375)(10/2(1.25)+2(1.25)/4]$$

$$= 391.0 \text{ ft-kips}$$

Determine connection rotation

$$\phi = (2.857\text{x}10^{-5})(t_p/b_f)^{-8.564}(p_f/b_f)^{-0.510}$$

$$(g/b_f)^{18.401}(h/b_f)^{-4.738}(M/M_y)^{2.838}$$

$$\phi = (2.857\text{x}10^{-5})(0.05625)^{-8.564}(0.200)^{-0.510}$$

$$(0.400)^{18.401}(4.67)^{-4.738}(333.3/391.0)^{2.838}$$

$$= 0.000072 \text{ radians}$$

$$M_d = \frac{9(132\text{x}50)(29000)(28)(0.000072327)}{50(10\text{x}12)(12)}$$

$$= 48.5 \text{ ft-kips}$$

$M_u = 333.3$ ft-kips $> M_d = 48.5$ ft-kips

Thus, the connection is suitable for Type I construction.

Summary

For the given loading, end-plate geometry, and material, use t_p = 9/16 in. and d_b = 1.00 in.

REFERENCES

1. Abolmaali, A., Kukreti, A., and Murray, T. (1984). "Finite Element Analysis of Two Tension Bolt Flush End-Plate Connections", Fears Structural Engineering Laboratory Report No. FSEL/MBMA 84-01, submitted to the Metal Building Manufacturers Association and to the American Institute of Steel Construction.

2. AISC (1986), Load and Resistance Factor Design Specification for Structural Steel for Buildings, American Institute of Steel Construction, Chicago, Ill.

3. AISC (1989), Manual of Steel Construction, Ninth Edition, American Institute of Steel Construction, Chicago, Ill.

4. Hendrick, D., Kukreti, A., and Murray, T. (1985), "Unification of Flush End-Plate Design Procedures", Fears Structural Engineering Laboratory Report No. FSEL/MBMA 85-01, submitted to the Metal Building Manufacturers Association.

5. Kennedy, N. A., Vinnakota, S., and A. N. Sherbourne (1981), "The Split-Tee Analogy in Bolted Splices and Beam Column Connections", Proceedings of the International Conference on Joints in Structural Steelwork, John Wiley and Sons, New York-Toronto, pp. 2.138-2.157.

6. Morrison, S., Astaneh-Asl, A., and Murray, T. (1986). "Analytical and Experimental Investigation of the Extended Stiffened Moment End-Plate Connection with Four Bolts at the Tension Flange", Fears Structural Engineering Laboratory Report No. FSEL/MBMA 85-05, submitted to the Metal Building Manufacturers Association and to the American Institute of Steel Construction.

7. Morrison, S., Astaneh-Asl, A., and Murray, T., (1985), "Analytical and Experimental Investigation of the Multiple Row Extended Moment End-Plate Connection with Eight Bolts at the Tension Flange", Fears Structural Engineering Laboratory Report No. FSEL/MBMA 86-01, submitted to the Metal Building Manufacturers Association and to the American Institute of Steel Construction.

8. Murray T. (1988), "Recent Developments for the Design of Moment End-Plate Connections", Journal of Constructional Steel Research, Elsevier Science Publishers Ltd, England, pp. 133-161.

9. Salmon, C. G. and Johnson, V. E., (1980), Steel Structures, Design and Behavior, 2nd Edition Harper and Row, New York, pp. 729-735.

10. SAS Institute Inc. (1985), SAS User's Guide: Statistics, Version 5 Edition, Cary, NC: SAS Institute Inc.

11. Srouji, R., Kukreti, A., and Murray, T. (1983), "Yield-Line Analysis of End-Plate Connections with Bolt Force Predictions", Fears Structural Engineering Laboratory, Report No. FSEL/MBMA 83-05, submitted to the Metal Building Manufacturers Association.

APPENDIX A

NOMENCLATURE

NOMENCLATURE

a	=	distance from the bolt centerline to the point of prying force application
α_i	=	factor to proportion amount of tension flange force each tension bolt receives
B_i	=	bolt force for bolt i
b	=	distance from a support to the point of load application
b_f	=	width of end-plate and beam flanges
d_b	=	nominal diameter of bolt
δ_{test}	=	experimentally measured deflection
δ_{theo}	=	theoretical deflection calculated by statics
F_1	=	flange force at thick plate limit
F'	=	the minimum of F11/2 or aiFf/2
F_{11}	=	flange force at the thin plate limit
F_a	=	allowable stress for bolt material
F_f	=	flange force
F_{yb}	=	the yield stress of the bolt material
f_{py}	=	yield stress of end-plate material
g	=	gage distance, the distance between vertical bolt rows
h	=	height of the end-plate and beam
L	=	length of the test setup
L_x	=	x component of yield line length
L_y	=	y component of yield line length
M_{max}	=	maximum moment applied to test specimen
M_u	=	ultimate moment
M_{ub}	=	predicted moment when bolts reach their proof load from bolt force predictions

M_w = working moment established from design loads

M_y = yield moment

M_{yei} = experimental moment capacities for end-plate based on end-plate separation test data for North and South sides of the test beam

M_{yp} = predicted yield moment of end-plates from yield-line theory

m_p = plastic moment capacity of the end-plate

P_f^1 = the distance from the outside of the web to the center of the middle bolt

P_{ram} = load applied by the hydraulic ram

p_b = distance between bolt rows

p_f = distance between inside of the tension flange to the centerline of bolts closest to the tension flange

π_i = independent parameter used in parametric study

π_r = dependant parameter representing the experimentally measured rotation used in the parametric study

p_t = distance from outside of tension flange to the centerline of bolt closest to the tension flange

p_{t3} = distance from the outside of the tension flange to the centerline of the bolt farthest from the tension flange

Q_i = prying force for bolt i

Q_{max} = maximum prying force per bolt

t_f = plastic moment capacity

t_p = thickness of end-plate

t_w = web thickness

ϕ = rotation of the end-plate

u = distance from the tension bolt farthest from the tension flange to a theoretical yield line perpendicular to the web

ϕ_n = relative rotation of line n

W = energy stored in yield-line mechanism

w = energy stored in yield line

w' = the width of the end-plate per bolt less the width of the bolt holes

w'' = twice the distance between bolt rows less the width of a bolt hole

APPENDIX B

MRF-7/8-3/8-28 TEST RESULTS

TEST SYNOPSIS

PROJECT: Varco Pruden Six-Bolt Flush End-plate

TEST: MRF-7/8-3/8-28

TEST DATE: 6/20/89

BEAM DESIGN DATA:

Depth	h	(in.)	28
Flange width	bf	(in.)	10
Web thickness	tw	(in.)	5/16
Flange thickness	tf	(in.)	3/8
Moment of Inertia	I	(in.)	1853

END-PLATE DESIGN DATA:

Plate thickness	tp	(in.)	3/8
Pitch between bolt rows	pb	(in.)	2-1/2
Pitch to bolt from flange	pf	(in.)	1-1/2
Gage	g	(in.)	3-1/2
Steel yield stress	Fpy	(ksi)	50

BOLT DATA:

Type			A325
Diameter	db	(in.)	7/8
Pretension Force	Tb	(kip)	38

ANALYSIS:

Yield-line moment	Myp	(ft-kip)	173.9
Moment at bolt proof	Myb	(ft-kip)	268.8

TEST:

Moment at bolt failure	(ft-kip)	275.8
Maximum applied moment	(ft-kip)	365
Maximum centerline deflection	(in.)	2.25
Maximum end-plate separation	(in.)	0.75

DISCUSSION: End-plates were slightly warped

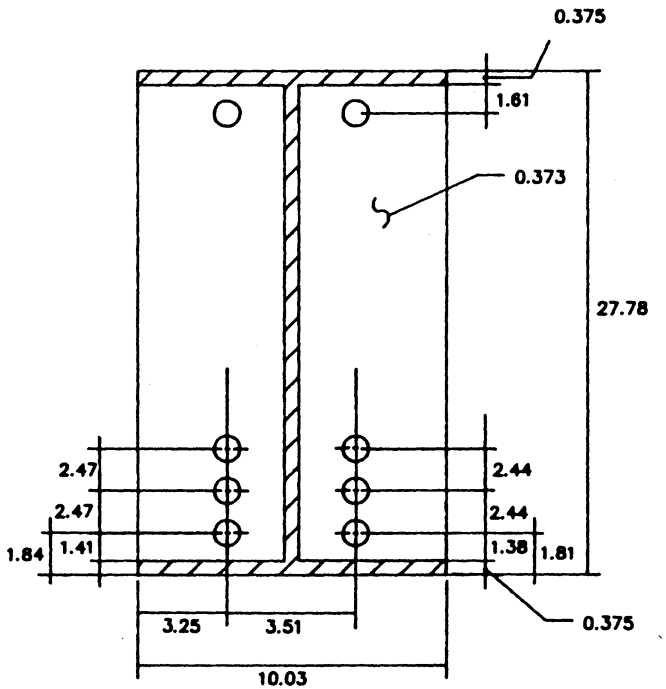

(a) Measured Dimensions End–Plate A

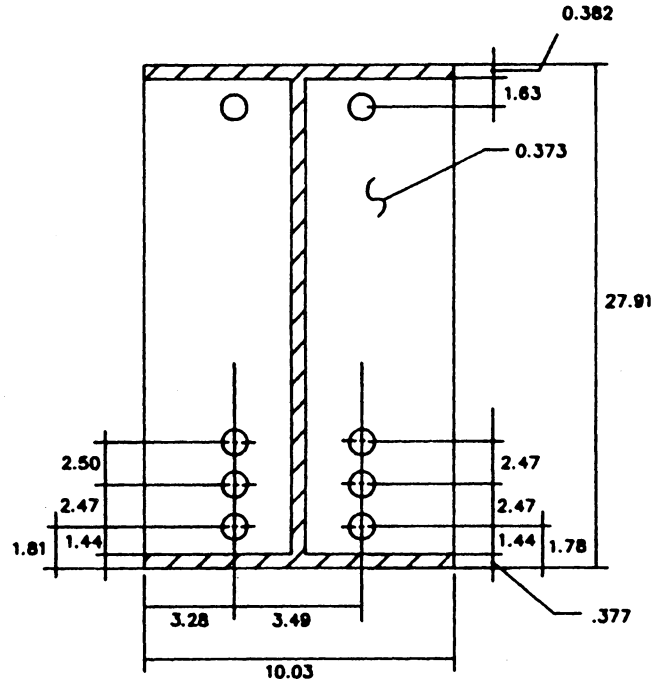

(b) Measured Dimensions End–Plate B

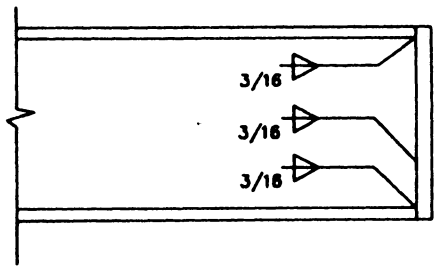

(c) Measured Weld Sizes for End–Plate

Fig. A.1 Measured Dimensions for TEST MRF–7/8–3/8–28

End-Plate Yield Moment

Test MRF-7/8-3/8-28

End-Plate B Controls

Mechanism I

$$u_1 = 1/2((27.91-6.78)(10.03)(3.49)/(27.91-1.81))^{1/2}$$

$$= 2.66 \text{ in.}$$

$$u_2 = 1/2((27.91-6.72)(10.03)(3.49)/(27.91-1.81))^{1/2}$$

$$= 2.66 \text{ in.}$$

$$M_u = 56.5(0.373)^2/2((27.91-1.81)(10.03/2(1.44)$$
$$+2(1.44+2.47+2.50+2.66)/3.49$$
$$+(27.91-6.78)(10.03/2(1.44)+(27.91-1.78)$$
$$(10.03/2(1.44)+2(1.44+2.47+2.47+2.66)/3.49$$
$$+(27.91-6.72)(10.03/2(1.44))/12$$

$$= 174.5 \text{ ft-kips}$$

Mechanism II

$$u = 1/2(10.03(3.49))^{1/2} = 2.96 \text{ in.}$$

$$M_u = 56.5(0.373)^2(3.49+2(1.44)(1.44+2.47+2.50)$$
$$+(27.91-1.81)(10.03/2(1.44$$
$$+2(1.44+2.47+2.50))/3.49+(27.91-6.78)$$
$$(10.03/(2(2.96)+2(2.96)/3.49)$$
$$+2(1.44)(1.44+2.47+2.47)$$
$$+(27.91-1.78)(10.03/2(1.44+2(1.44+2.47+2.47)/3.49$$
$$+(27.91-6.72)(10.03/(2(2.96)+2(2.96)/3.49))$$

$$= 173.9 \text{ ft-kips (controls)}$$

Moment at Bolt Proof Load (Bottom Bolt)

Test MRF-7/8-3/8-28

Plate A controls

$$w' = 10.03/2-(0.875+1/16) = 4.08 \text{ in.}$$

$$F_{11L} = \frac{0.373\text{^}2(56.5)[0.85(10.03/2)+0.8(4.08)]+3.14(0.875)\text{^}385.0/8}{4(1.41)}$$

$$F_{11L} = 14.5 \text{ kips}$$

$$F_{11R} = F_{11L}(1.41)/1.38 = 14.8 \text{ kips}$$

$$Qmax_L = \frac{4.08(0.373)\text{^}2}{4(0.373)}(56.5\text{^}2-3(14.5/((0.373)4.08)1/2$$

$$Qmax_L = 20.6 \text{ kips}$$

$$Qmax_R = \frac{4.08(0.373)\text{^}2}{4(0.373)}(56.5\text{^}2-3(14.8/((0.373)4.08)1/2$$

$$Qmax_R = 20.5 \text{ kips}$$

$$Mu = .0833(27.78-(0.375+0.375)/2)(2(52.9-20.6-20.5))/0.55$$

$$Mu = 268.8 \text{ ft-kips}$$

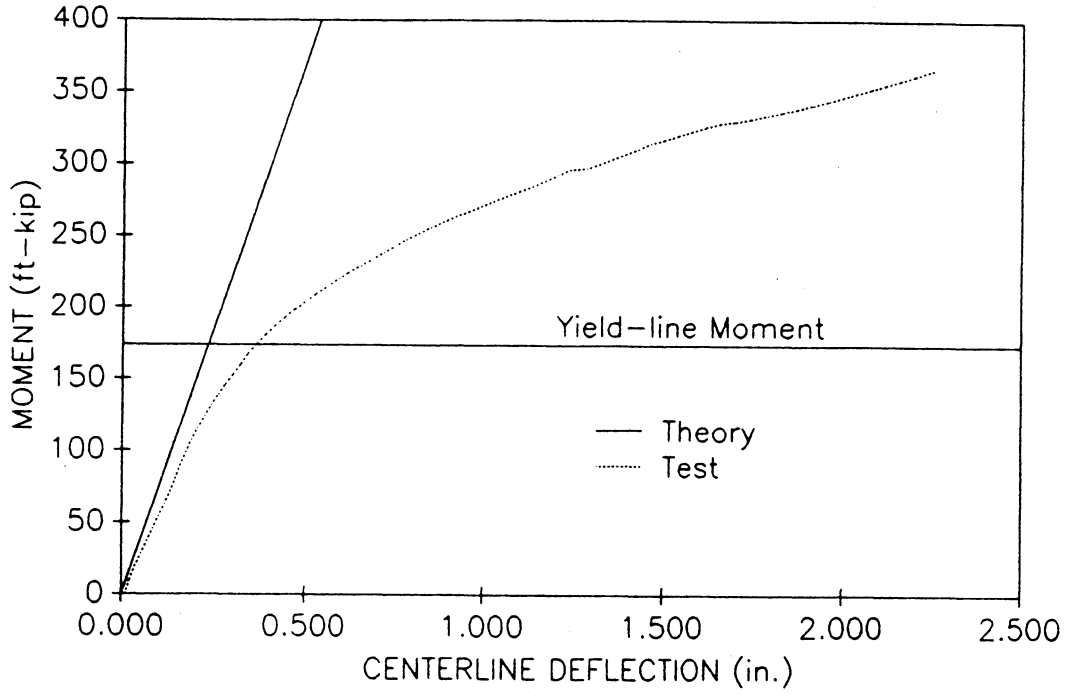

Fig. B.2 Moment versus Centerline Deflection
Test MRF-7/8-3/8-28

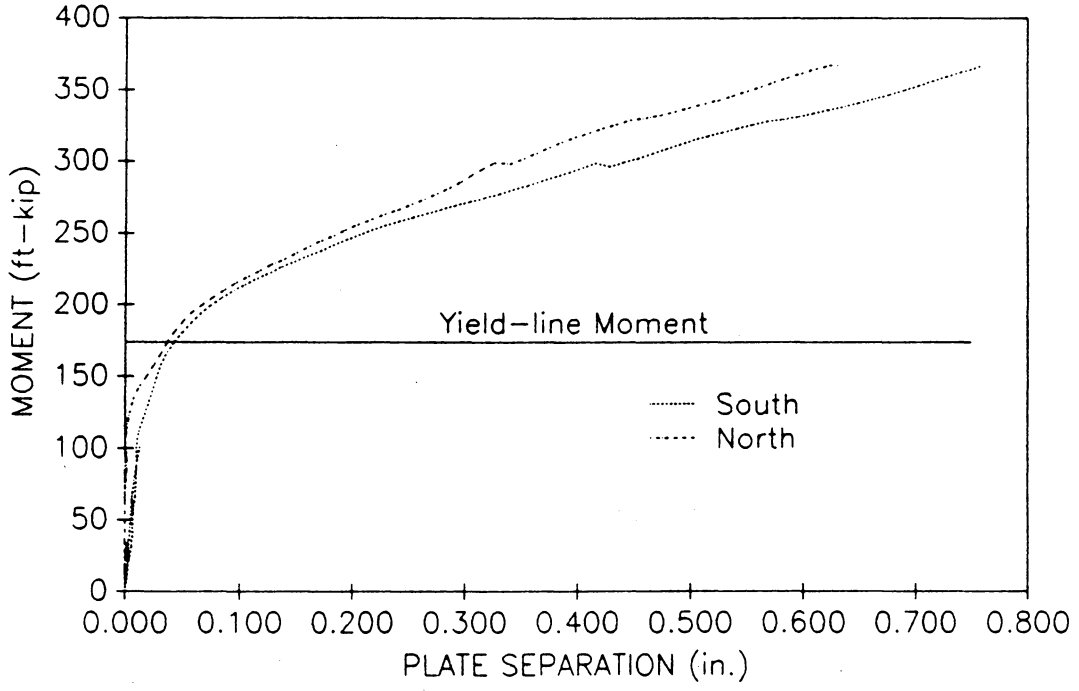

Fig. B.3 Moment versus Plate Separation
Test MRF-7/8-3/8-28

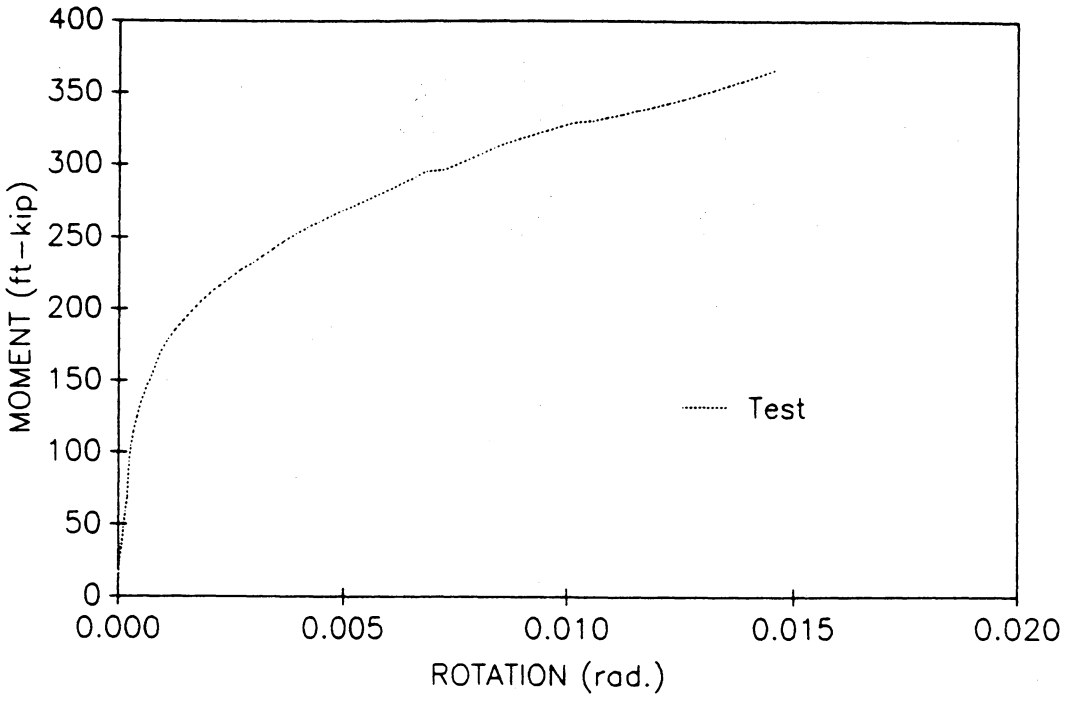

Fig. B.4 Moment versus Rotation
Test MRF-7/8-3/8-28

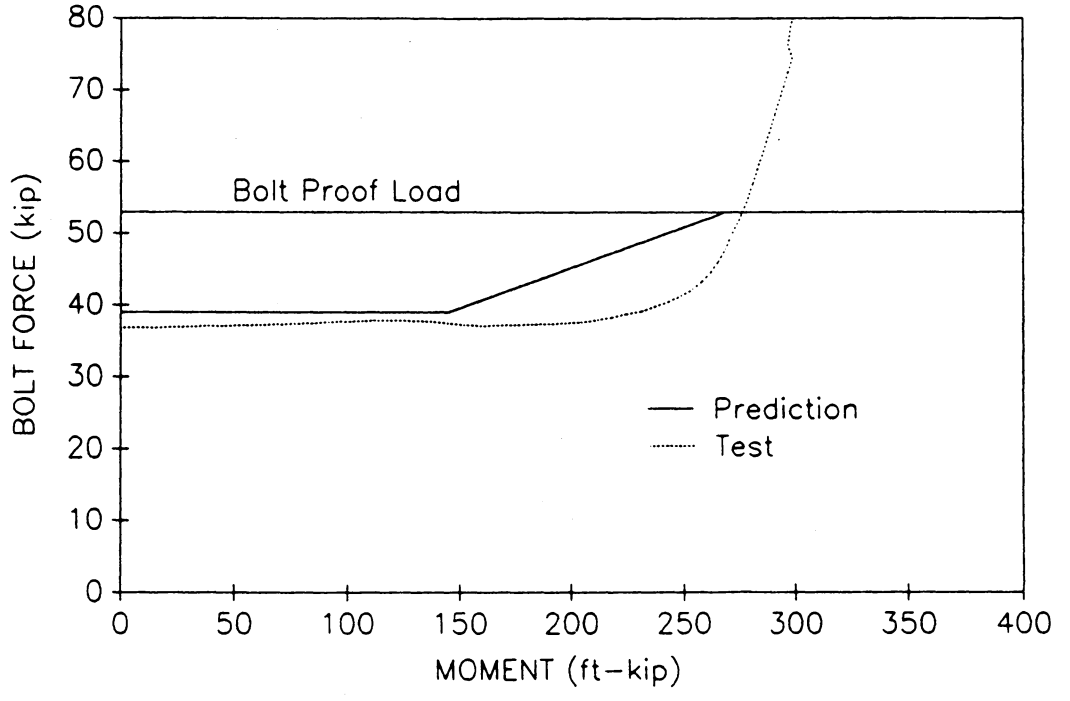

Fig. B.5 Bottom Bolt Force versus Moment
Test MRF-7/8-3/8-28

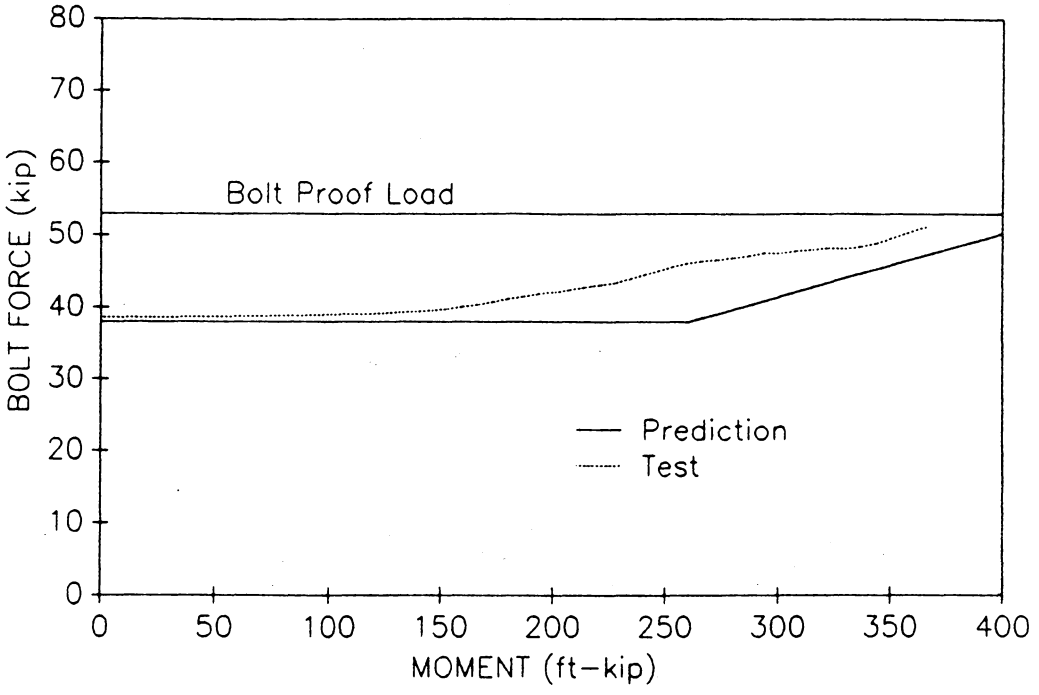

Fig. B.6 Middle Bolt Force versus Moment
Test MRF-7/8-1/2-28

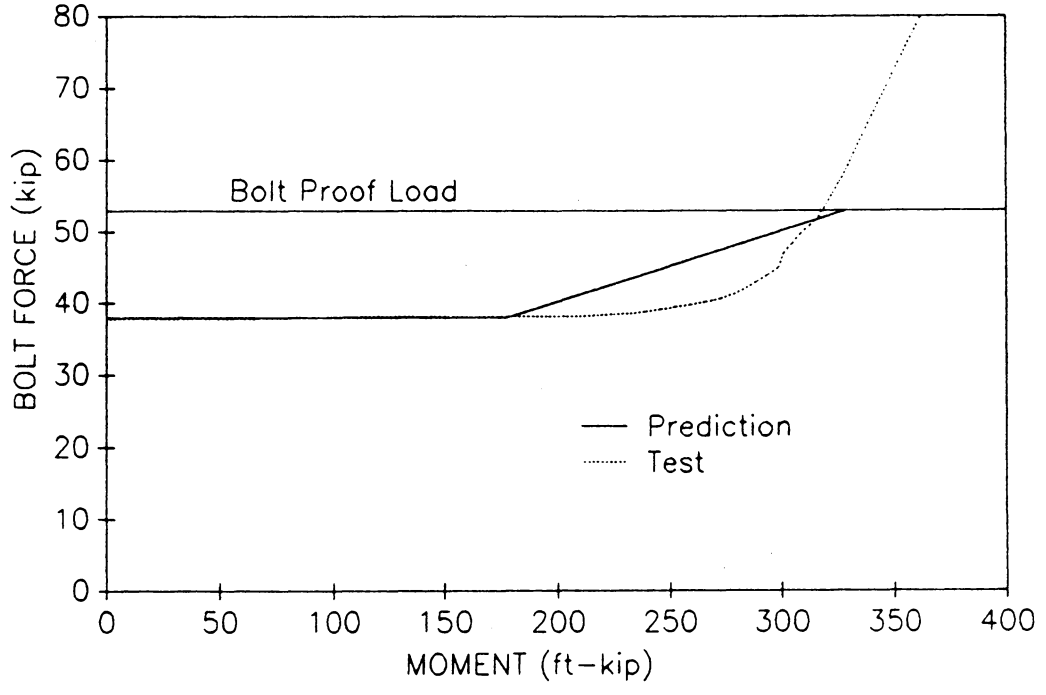

Fig. B.7 Top Bolt Force versus Moment
Test MRF-7/8-3/8-28

APPENDIX C

MRF-1-1/2-28 TEST RESULTS

TEST SYNOPSIS

PROJECT: Varco Pruden Six-Bolt Flush End-Plate

TEST: MRF-1-1/2-28

TEST DATE: 6/16/89

BEAM DESIGN DATA:

Depth	h	(in.)	28
Flange width	bf	(in.)	10
Web thickness	tw	(in.)	5/16
Flange thickness	tf	(in.)	3/8
Moment of Inertia	I	(in.)	1853

END-PLATE DESIGN DATA:

Plate thickness	tp	(in.)	1/2
Pitch between bolt rows	pb	(in.)	2-1/2
Pitch to bolt from flange	pf	(in.)	2
Gage	g	(in.)	4
Steel yield stress	Fpy	(ksi)	50

BOLT DATA:

Type			A325
Diameter	db	(in.)	1.0
Pretension Force	Tb	(kip)	51

ANALYSIS:

Yield-line moment	Myp	(ft-kip)	309.2
Moment at bolt proof	Myb	(ft-kip)	321.8

TEST:

Moment at bolt failure	(ft-kip)	328.2
Maximum applied moment	(ft-kip)	399
Maximum centerline deflection	(in.)	1.58
Maximum end-plate separation	(in.)	0.28

DISCUSSION: End-plates were slightly warped

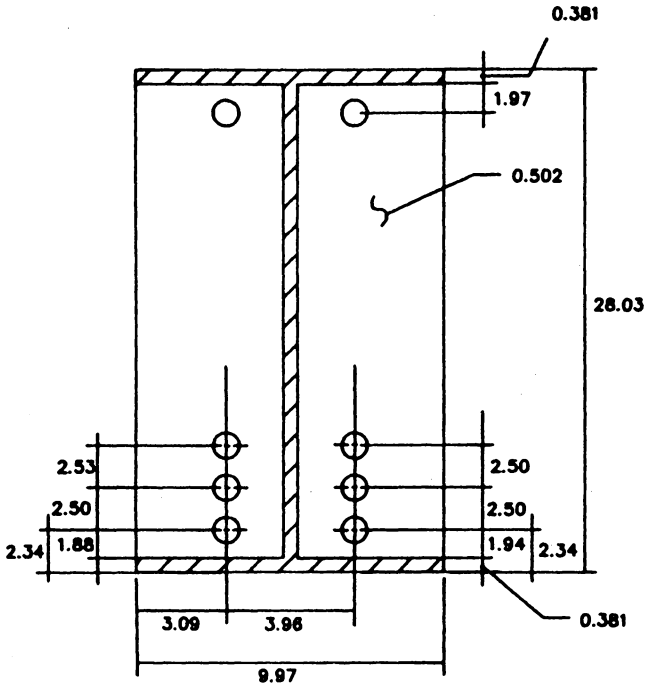

(a) Measured Dimensions End–Plate A

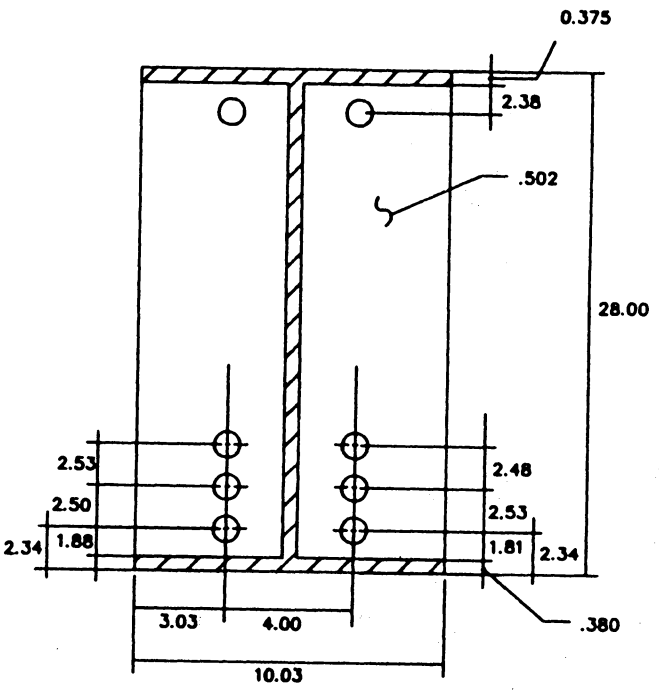

(b) Measured Dimensions End–Plate B

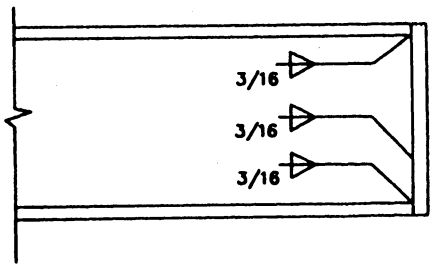

(c) Measured Weld Sizes for End–Plate

Fig. B.1 Measured Dimensions for TEST MRF–1–1/2–28

End-Plate Yield Moment

Test MRF-1-1/2-28

End-Plate B Controls

Mechanism I

$$u_1 = 1/2((28.00-7.32)(10.03)(4.00)/(28.00-2.34))^{1/2}$$

$$= 2.84 \text{ in.}$$

$$u_2 = 1/2((28.00-7.35)(10.03)(4.00)/(28.00-2.34))^{1/2}$$

$$= 2.84 \text{ in.}$$

$$M_u = 64.0(0.502)^2/2((28.00-2.34)(10.03/2(1.88)$$
$$+2(1.88+2.50+2.48+2.84)/4.00$$
$$+(28.00-7.32)(10.03/2(1.88)+(28.00-2.34)$$
$$(10.03/2(1.81)+2(1.81+2.53+2.48+2.84)/4.00$$
$$+(28.00-7.35)(10.03/2(1.81))/12$$

$$= 309.2 \text{ ft-kips (controls)}$$

Mechanism II

$$u = 1/2(10.03(4.00))^{1/2} = 3.17 \text{ in.}$$

$$M_u = 64.0(0.502)^2(4.00+2(1.88)(1.88+2.50+2.48)$$
$$+(28.00-2.34)(10.03/2(1.88$$
$$+2(1.88+2.50+2.48))/4.00+(28.00-7.32)$$
$$(10.03/(2(3.17)+2(3.17)/4.00)$$
$$+2(1.81)(1.81+2.53+2.48)$$
$$+(28.00-2.34)(10.03/2(1.81+2(1.81+2.53+2.48)/4.00$$
$$+(28.00-7.35)(10.03/(2(3.17)+2(3.17)/4.00))$$

$$= 310.8 \text{ ft-kips}$$

Moment at Bolt Proof Load (Bottom Bolt)

Test MRF-1-1/2-28

Plate A controls

$$w' = 9.97/2-(1.0+1/16) = 3.95 \text{ in.}$$

$$F_{11L} = \frac{0.502\text{^}2(64.0)[0.85(9.97/2)+0.8(3.95)]+3.14(1.0)\text{^}385.0/8}{4(1.88)}$$

$$F_{11L} = 20.4 \text{ kips}$$

$$F_{11R} = F_{11L}(1.88)/1.94 = 21.2 \text{ kips}$$

$$Qmax_L = \frac{3.95(0.502)\text{^}2}{4(0.502)}(64.0\text{^}2-3(20.4/((0.502)3.95)1/2$$

$$Qmax_L = 30.5 \text{ kips}$$

$$Qmax_R = \frac{3.95(0.502)\text{^}2}{4(0.502)}(64.0\text{^}2-3(21.2/((0.502)3.95)1/2$$

$$Qmax_R = 30.4 \text{ kips}$$

$$Mu = .0833(27.81-(0.381+0.381)/2)(2(69.2-30.5-30.4))/0.55$$

$$Mu = 321.8 \text{ ft-kips}$$

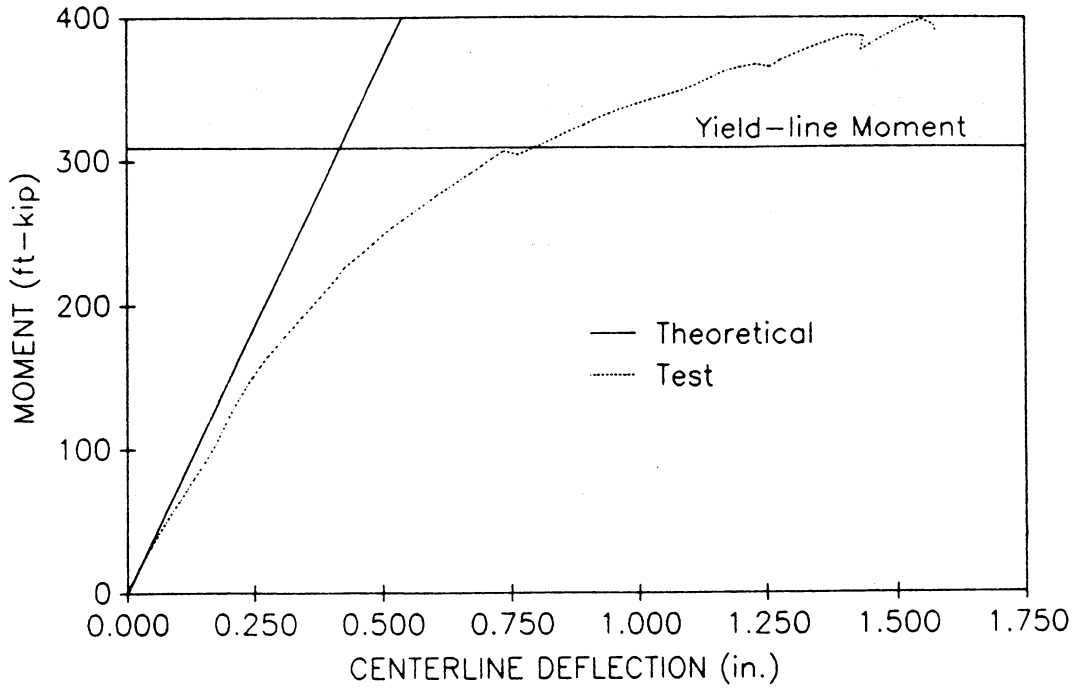

Fig. C.2 Moment versus Centerline Deflection
Test MRF-1-1/2-28

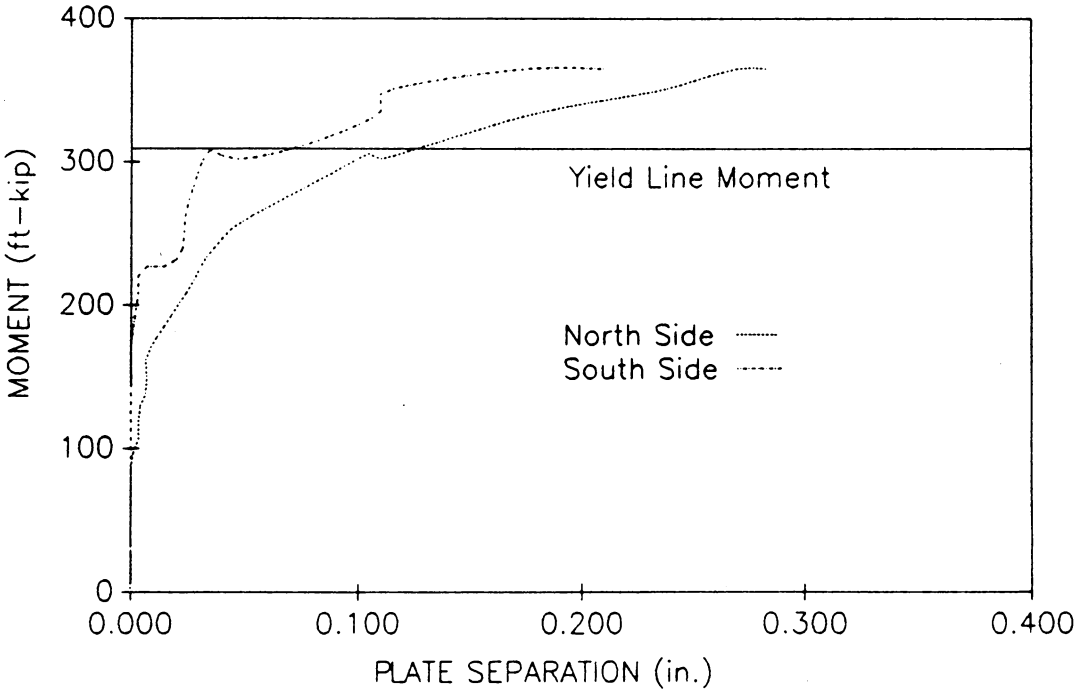

Fig. C.3 Moment versus Plate Separation
Test MRF-1-1/2-28

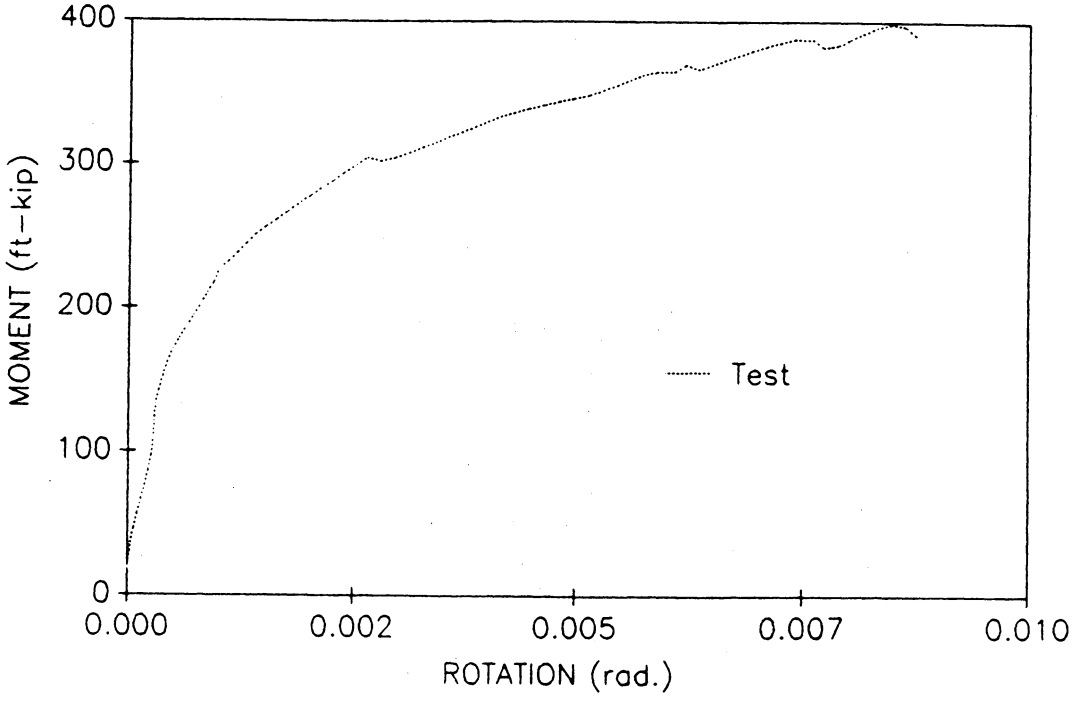

Fig. C.4 Moment versus Rotation
Test MRF-1-1/2-28

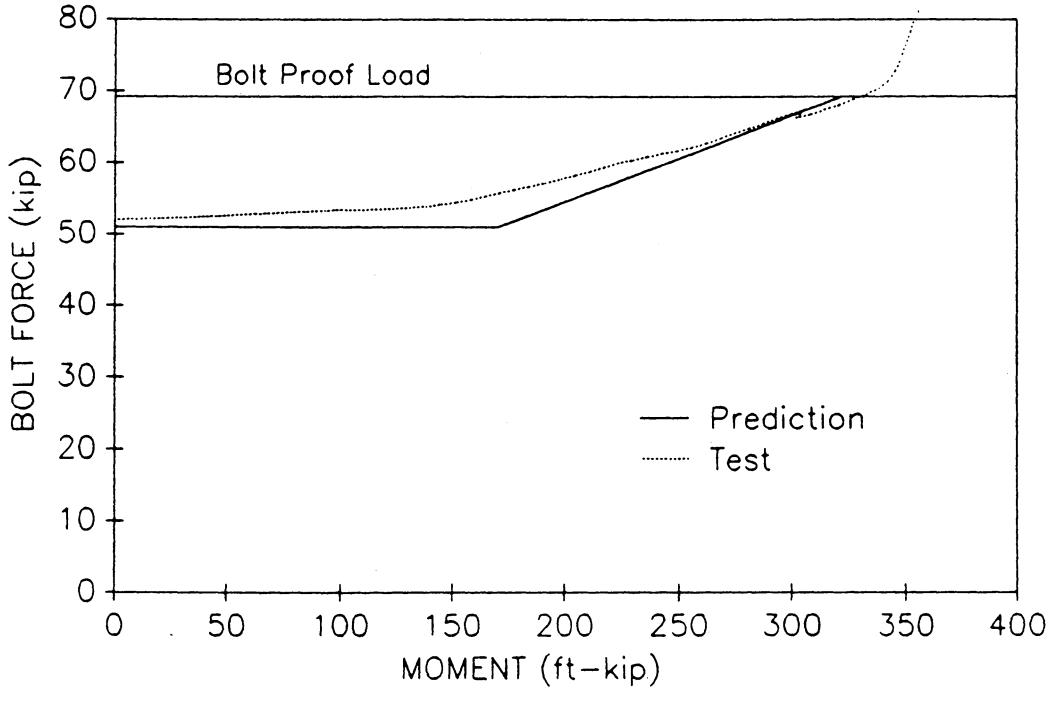

Fig. C.5 Bottom Bolt Force versus Moment
Test MRF-1-1/2-28

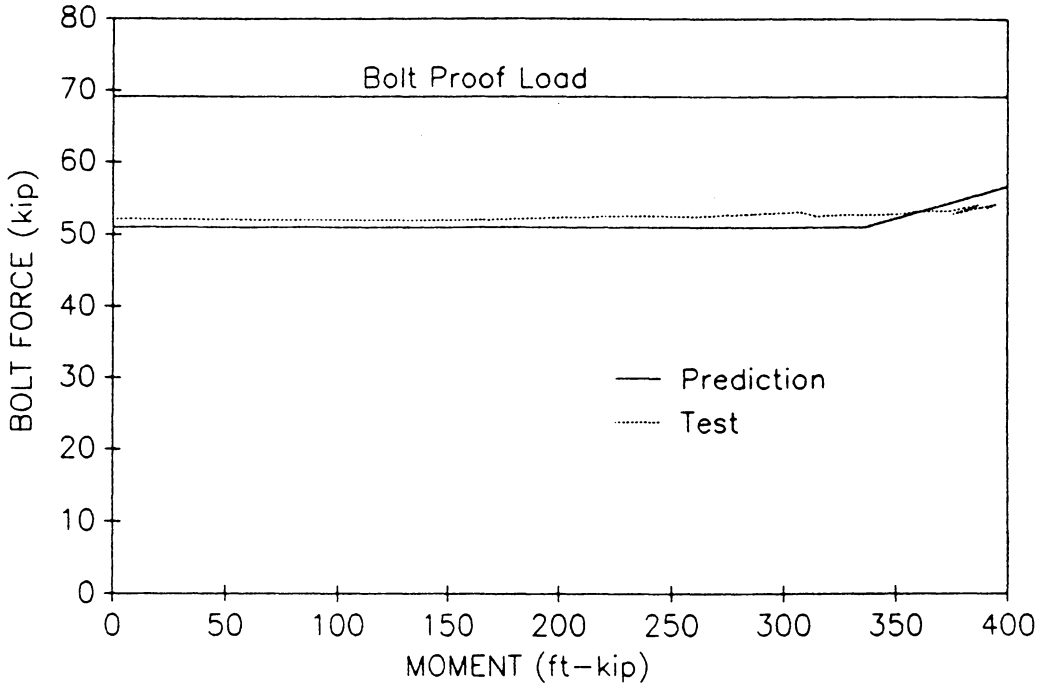

Fig. C.6 Middle Bolt Force versus Moment
Test MRF-1-1/2-28

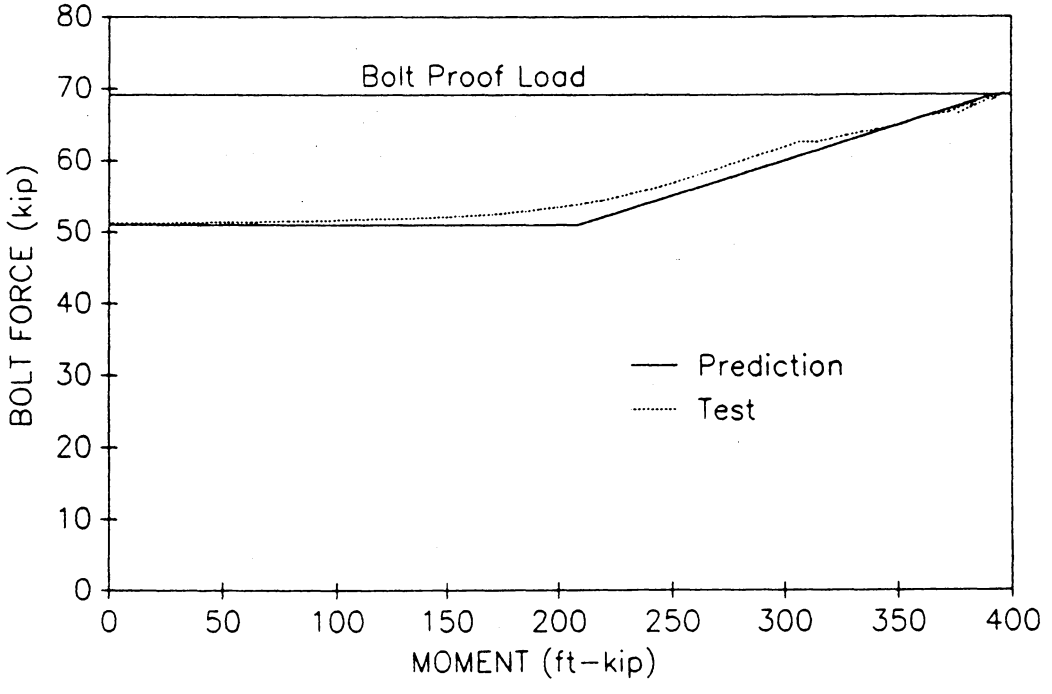

Fig. C.7 Top Bolt Force versus Moment
Test MRF-1-1/2-28

APPENDIX D

MRF-3/4-3/8-36 TEST RESULTS

TEST SYNOPSIS

PROJECT: Varco Pruden Six-Bolt Flush End-plate

TEST: MRF-3/4-3/8-36

TEST DATE: 6/29/89

BEAM DESIGN DATA:

Depth	h	(in.)	36
Flange width	bf	(in.)	6
Web thickness	tw	(in.)	5/16
Flange thickness	tf	(in.)	3/8
Moment of Inertia	I	(in.)	2568

END-PLATE DESIGN DATA:

Plate thickness	tp	(in.)	3/8
Pitch between bolt rows	pb	(in.)	2-1/2
Pitch to bolt from flange	pf	(in.)	2
Gage	g	(in.)	3
Steel yield stress	Fpy	(ksi)	50

BOLT DATA:

Type			A325
Diameter	db	(in.)	3/4
Pretension Force	Tb	(kip)	28

ANALYSIS:

Yield-line moment	Myp	(ft-kip)	210.6
Moment at bolt proof	Myb	(ft-kip)	280.9

TEST:

Moment at bolt failure	(ft-kip)	293.2
Maximum applied moment	(ft-kip)	365
Maximum centerline deflection	(in.)	0.69
Maximum end-plate separation	(in.)	0.20

DISCUSSION:

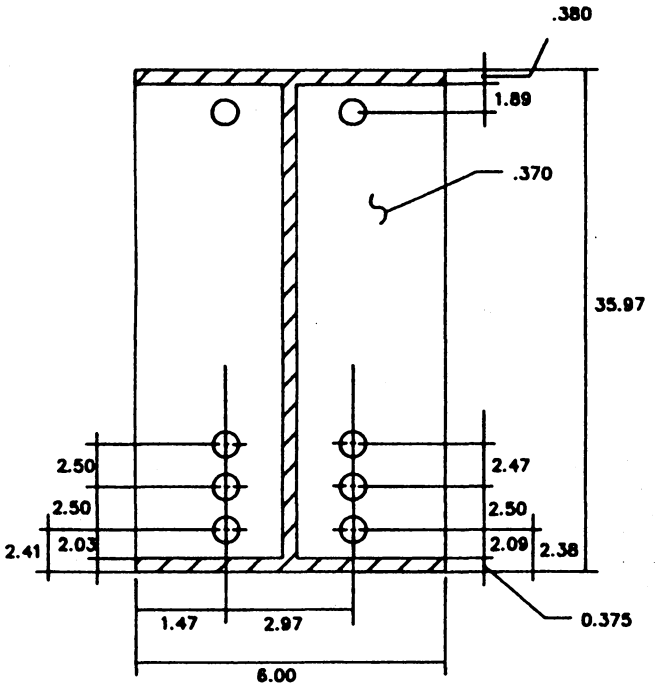

(a) Measured Dimensions End-Plate A

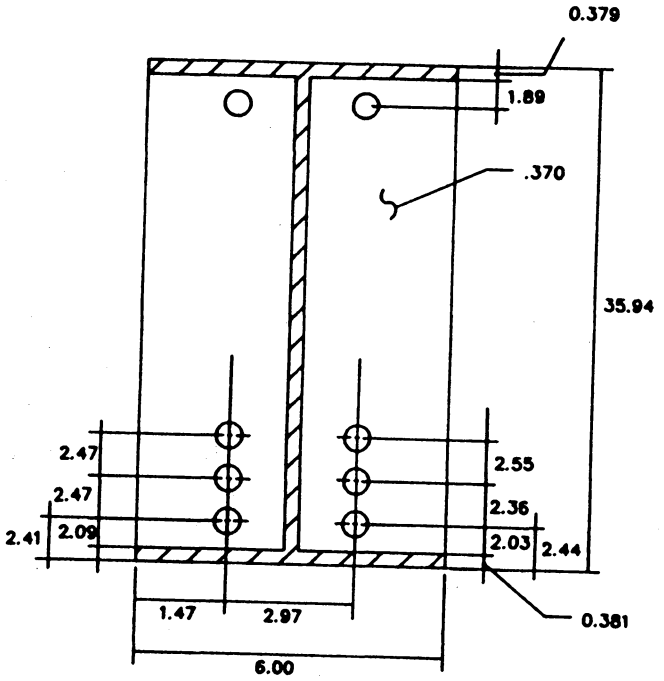

Measured Dimensions End-Plate B

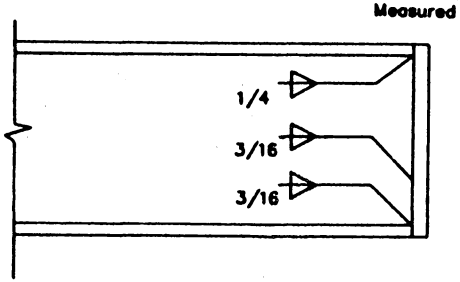

(c) Measured Weld Sizes for End-Plate

Fig. C.1 Measured Dimensions for TEST MRF-3/4-3/8-36

End-Plate Yield Moment

Test MRF-3\4-3\8-36

End-Plate B Controls

Mechanism I

$$u_1 = 1/2((35.97-7.41)(6.0)(2.97)/(35.97-2.41))^{1/2}$$

$$= 1.95 \text{ in.}$$

$$u_2 = 1/2((35.97-7.35)(6.0)(2.97)/(35.97-2.41))^{1/2}$$

$$= 1.95 \text{ in.}$$

$$M_u = 62.7(0.370)^2/2((35.97-2.41)(6.0/2(2.03)$$
$$+2(2.03+2.50+2.50+1.95)/2.97$$
$$+(35.97-7.41)(6.0/2(2.03)+(35.97-2.38)$$
$$(6.0/2(2.09)+2(2.09+2.50+2.47+1.95)/2.97$$
$$+(35.97-7.35)(6.0/2(2.09))/12$$

$$= 210.6 \text{ ft-kips}$$

Mechanism II

$$u = 1/2(6.0(2.97))^{1/2} = 2.11 \text{ in.}$$

$$M_u = 62.7(0.370)^2(2.97+2(2.03)(2.03+2.50+2.50)$$
$$+(35.97-2.41)(6.0/2(2.03$$
$$+2(2.03+2.50+2.50))/2.97+(35.97-7.41)$$
$$(6.0/(2(2.11)+2(2.11)/2.97)$$
$$+2(2.09)(2.09+2.50+2.47)$$
$$+(35.97-2.38)(6.0/2(2.09+2(2.09+2.50+2.47)/2.97$$
$$+(35.97-7.35)(6.0/(2(2.11)+2(2.11)/2.97))$$

$$= 213.8 \text{ ft-kips (controls)}$$

Moment at Bolt Proof Load (Bottom Bolt)

Test MRF-3\4-3\8-36

Plate A controls

$$w' = 6.0/2-(0.750+1/16) = 2.19 \text{ in.}$$

$$F_{11L} = \frac{0.370\text{^}2(62.7)[0.85(6.0/2)+0.8(2.19)]+3.14(0.750)\text{^}385.0/8}{4(2.03)}$$

$$F_{11L} = 6.3 \text{ kips}$$

$$F_{11R} = F_{11L}(2.03)/2.09 = 6.1 \text{ kips}$$

$$Qmax_L = \frac{2.19(0.370)\text{^}2}{4(0.370)}(62.7\text{^}2-3(6.3/((0.370)2.19)1/2$$

$$Qmax_L = 12.4 \text{ kips}$$

$$Qmax_R = \frac{2.19(0.370)\text{^}2}{4(0.370)}(62.7\text{^}2-3(6.1/((0.370)2.19)1/2$$

$$Qmax_R = 12.4 \text{ kips}$$

$$Mu = .0833(36.03-(0.380+0.376)/2)(2(38.4-12.4-12.4))/0.55$$

$$Mu = 280.9 \text{ ft-kips}$$

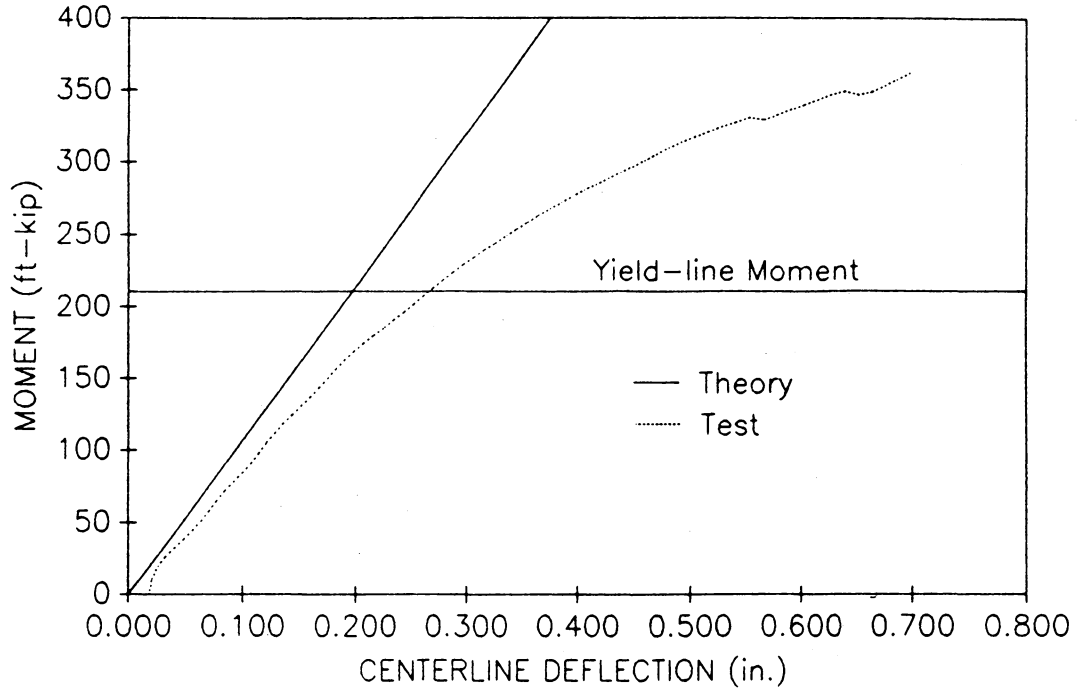

Fig. D.2 Moment versus Centerline Deflection
Test MRF-3/4-3/8-36

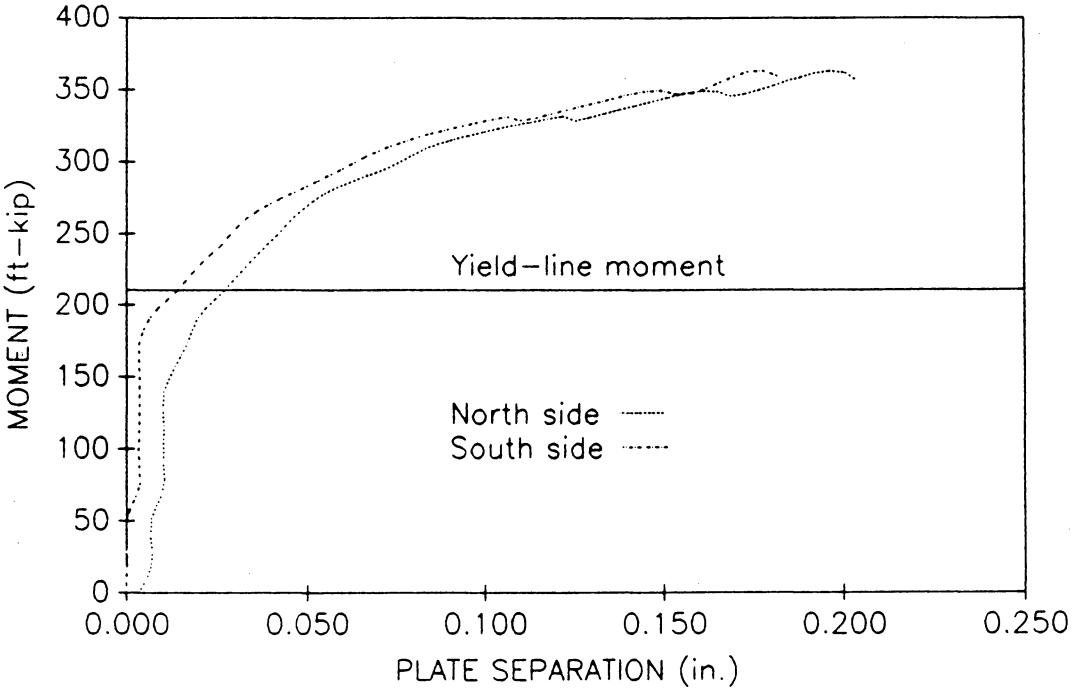

Fig. D.3 Moment versus Plate Separation
Test MRF-3/4-3/8-36

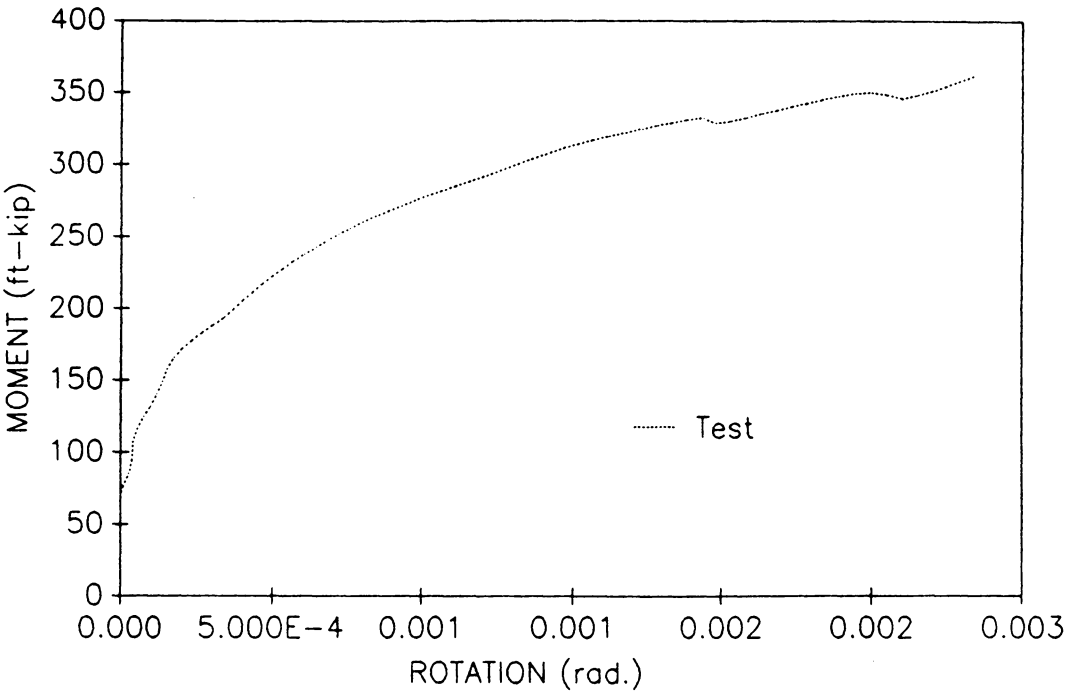

Fig. D.4 Moment versus Rotation
Test MRF-3/4-3/8-36

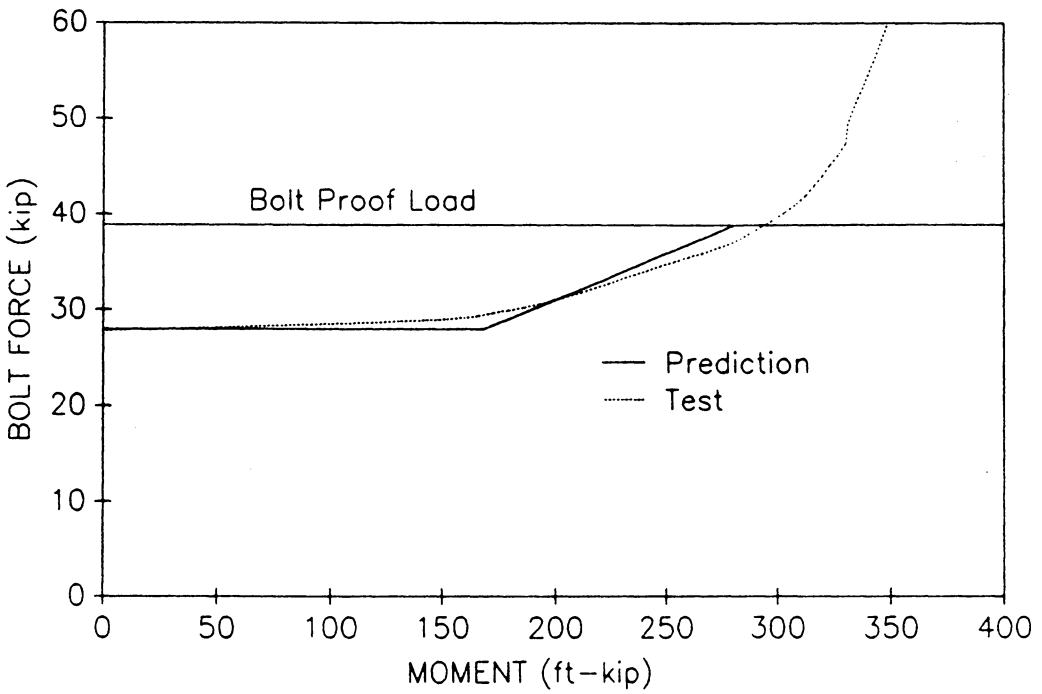

Fig. D.5 Bottom Bolt Force versus Moment
Test MRF-3/4-3/8-36

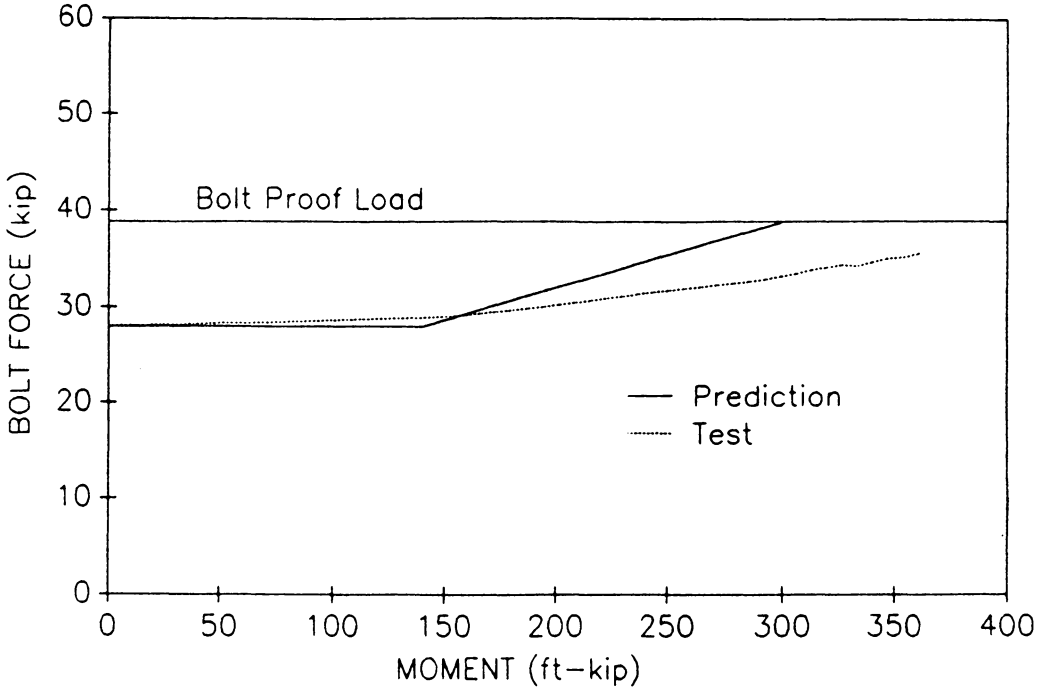

Fig. D.6 Middle Bolt Force versus Moment
Test MRF-3/4-3/8-36

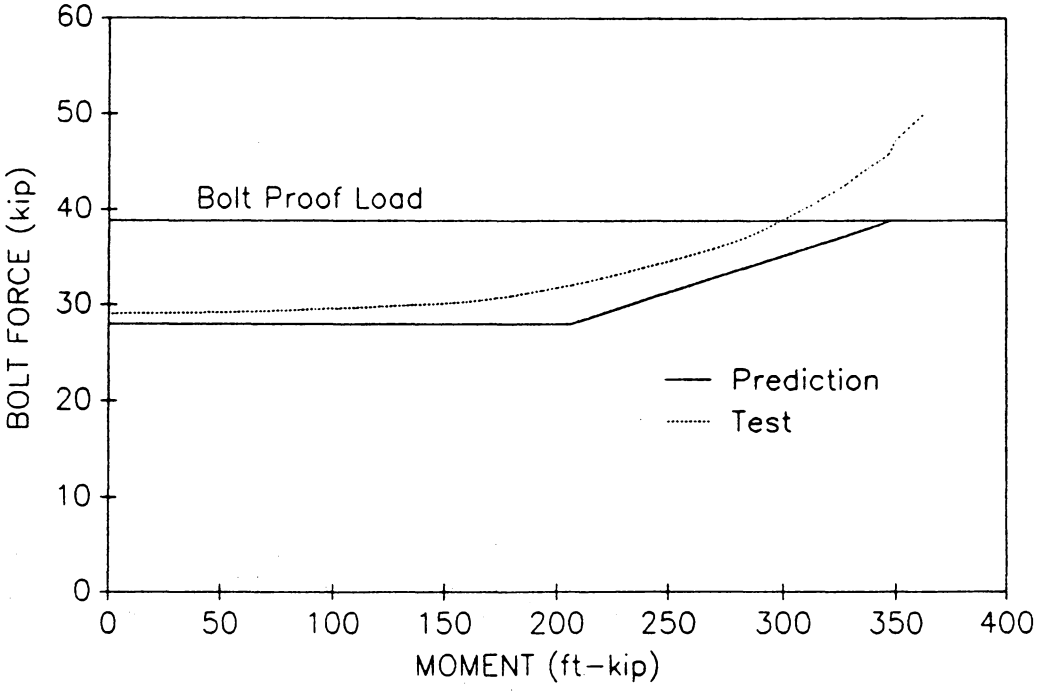

Fig. D.7 Top Bolt Force versus Moment
Test MRF-3/4-3/8-36

APPENDIX E

MRF-7/8-1/2-36 TEST RESULTS

TEST SYNOPSIS

PROJECT: Varco Pruden Six-Bolt Flush End-Plate

TEST: MRF-7/8-1/2-36

TEST DATE: 7/7/89

BEAM DESIGN DATA:

Depth	h	(in.)	36
Flange width	bf	(in.)	6
Web thickness	tw	(in.)	5/16
Flange thickness	tf	(in.)	3/8
Moment of Inertia	I	(in.)	2568

END-PLATE DESIGN DATA:

Plate thickness	tp	(in.)	1/2
Pitch between bolt rows	pb	(in.)	2-1/2
Pitch to bolt from flange	pf	(in.)	1-1/2
Gage	g	(in.)	3-1/2
Steel yield stress	Fpy	(ksi)	50

BOLT DATA:

Type			A325
Diameter	db	(in.)	7/8
Pretension Force	Tb	(kip)	38

ANALYSIS:

Yield-line moment	Myp	(ft-kip)	361.2
Moment at bolt proof	Myb	(ft-kip)	414.1

TEST:

Moment at bolt failure	(ft-kip)	358.8
Maximum applied moment	(ft-kip)	459
Maximum centerline deflection	(in.)	0.81
Maximum end-plate separation	(in.)	0.24

DISCUSSION:

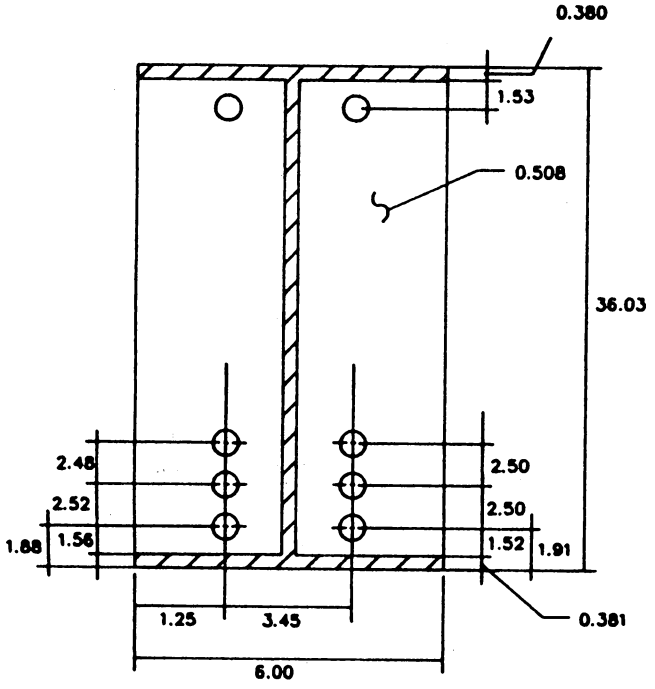

(a) Measured Dimensions End-Plate A

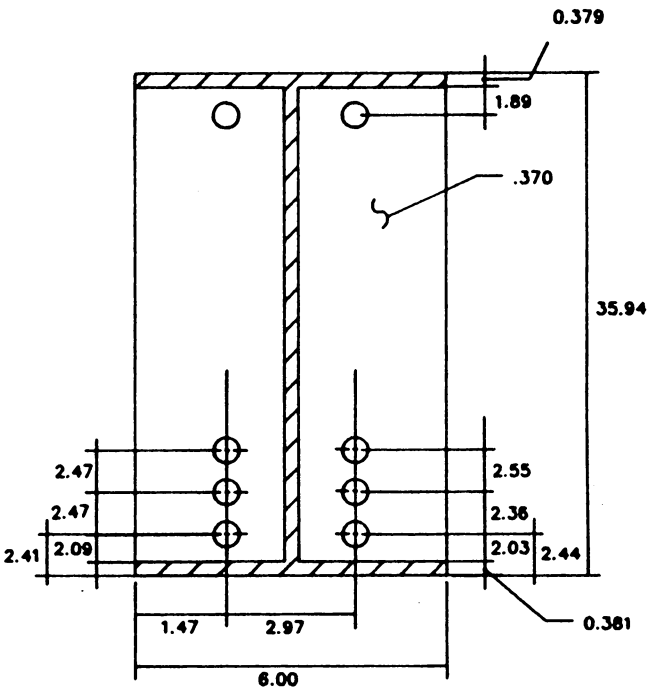

Measured Dimensions End-Plate B

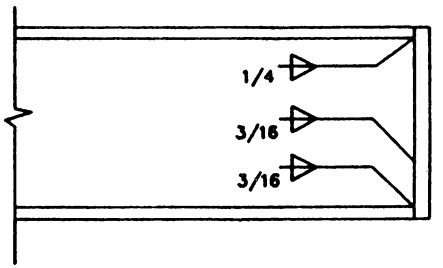

(c) Measured Weld Sizes for End-Plate

Fig. D.1 Measured Dimensions for TEST MRF-7/8-1/2-36

End-Plate Yield Moment

Test MRF-7\8-1\2-36

End-Plate B Controls

Mechanism I

$$u_1 = 1/2((36.03-6.88)(6.00)(3.45)/(36.03-1.88))^{1/2}$$

$$= 2.11 \text{ in.}$$

$$u_2 = 1/2((36.03-6.91)(6.00)(3.45)/(36.03-1.88))^{1/2}$$

$$= 2.11 \text{ in.}$$

$$M_u = 60.4(0.508)^2/2((36.03-1.88)(6.00/2(1.56)$$
$$+2(1.56+2.52+2.48+2.11)/3.45$$
$$+(36.03-6.88)(6.00/2(1.56)+(36.03-1.91)$$
$$(6.00/2(1.52)+2(1.52+2.50+2.50+2.11)/3.45$$
$$+(36.03-6.91)(6.00/2(1.52))/12$$

$$= 361.2 \text{ ft-kips}$$

Mechanism II

$$u = 1/2(6.00(3.45))^{1/2} = 2.28 \text{ in.}$$

$$M_u = 60.4(0.508)^2(3.45+2(1.56)(1.56+2.52+2.48)$$
$$+(36.03-1.88)(6.00/2(1.56$$
$$+2(1.56+2.52+2.48))/3.45+(36.03-6.88)$$
$$(6.00/(2(2.28)+2(2.28)/3.45)$$
$$+2(1.52)(1.52+2.50+2.50)$$
$$+(36.03-1.91)(6.00/2(1.52+2(1.52+2.50+2.50)/3.45$$
$$+(36.03-6.91)(6.00/(2(2.28)+2(2.28)/3.45))$$

$$= 362.8 \text{ ft-kips (controls)}$$

Moment at Bolt Proof Load (Bottom Bolt)

Test MRF-7\8-1\2-36

Plate A controls

$$w' = 6.00/2-(0.875+1/16) = 2.06 \text{ in.}$$

$$F_{11L} = \frac{0.508\text{^}2(60.4)[0.85(6.00/2)+0.8(2.06)]+3.14(0.875)\text{^}385.0/8}{4(1.56)}$$

$$F_{11L} = 14.4 \text{ kips}$$

$$F_{11R} = F_{11L}(1.56)/1.52 = 14.6 \text{ kips}$$

$$Qmax_L = \frac{2.06(0.508)\text{^}2}{4(0.508)}(60.4\text{^}2-3(14.4/((0.508)2.06)1/2$$

$$Qmax_L = 14.6 \text{ kips}$$

$$Qmax_R = \frac{2.06(0.508)\text{^}2}{4(0.508)}(60.4\text{^}2-3(14.6/((0.508)2.06)1/2$$

$$Qmax_R = 14.5 \text{ kips}$$

$$Mu = .0833(36.03-(0.380+0.376)/2)(2(52.9-14.6-14.5))/0.55$$

$$Mu = 414.1 \text{ ft-kips}$$

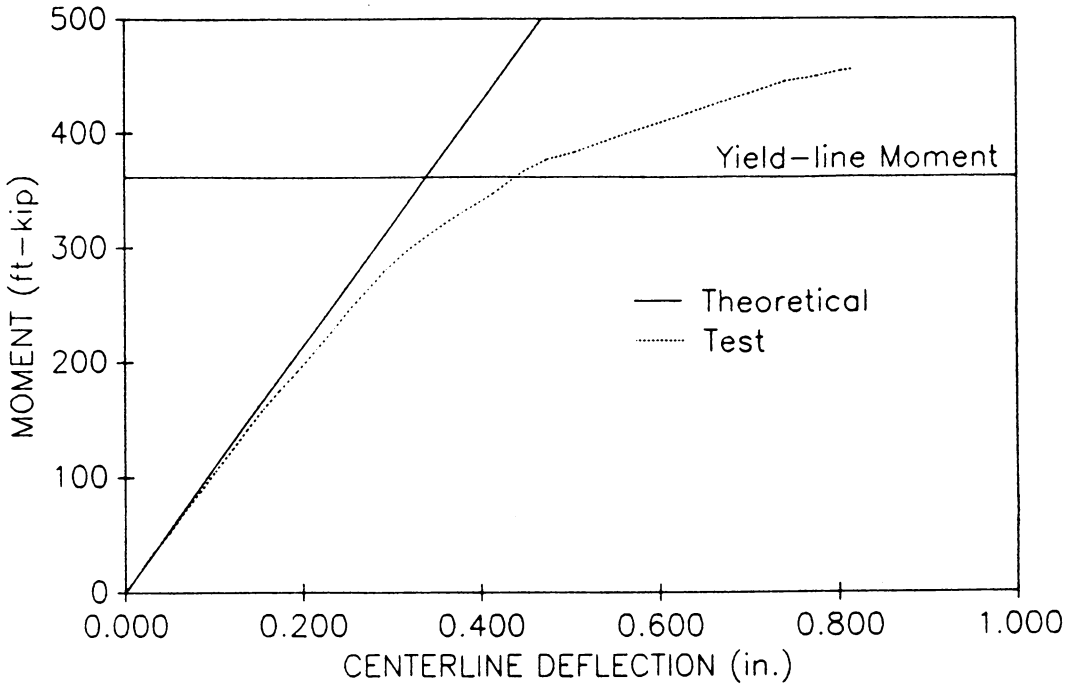

Fig. E.2 Moment versus Centerline Deflection
Test MRF-7/8-1/2-36

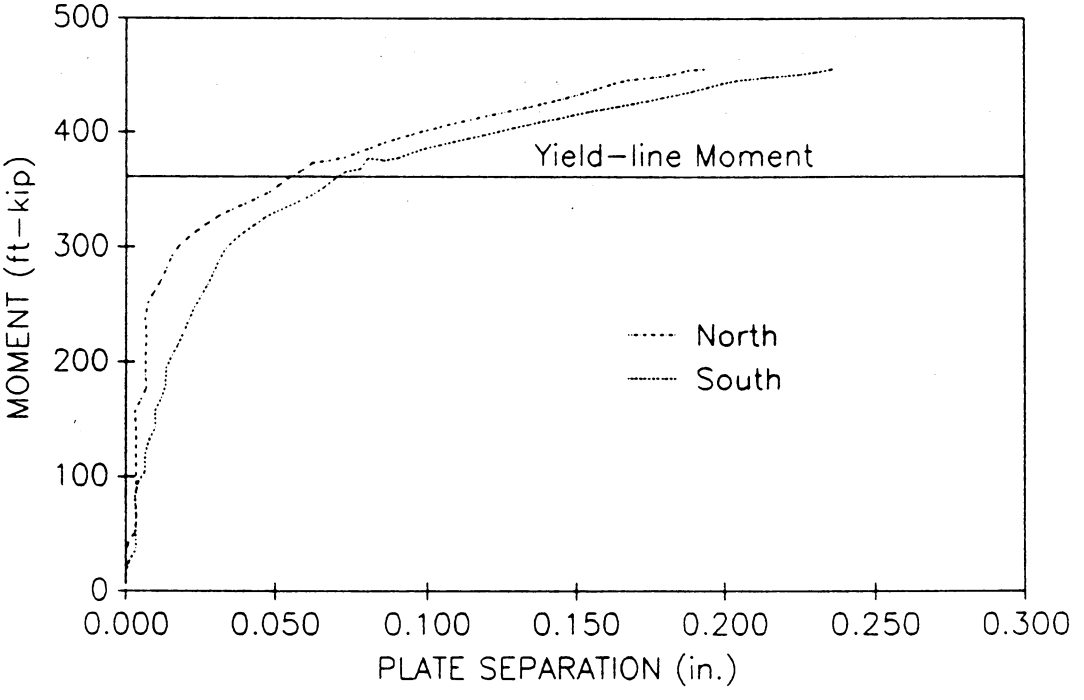

Fig. E.3 Moment versus Plate Separation
Test MRF-7/8-1/2-36

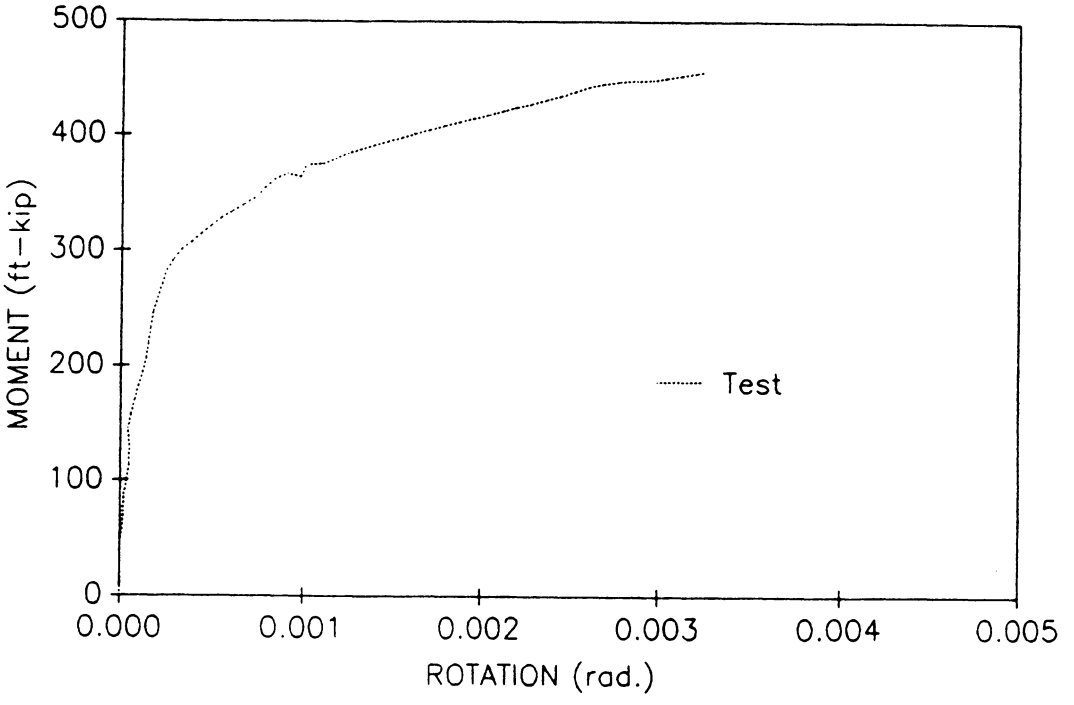

Fig. E.4 Moment versus Rotation
Test MRF-7/8-1/2-36

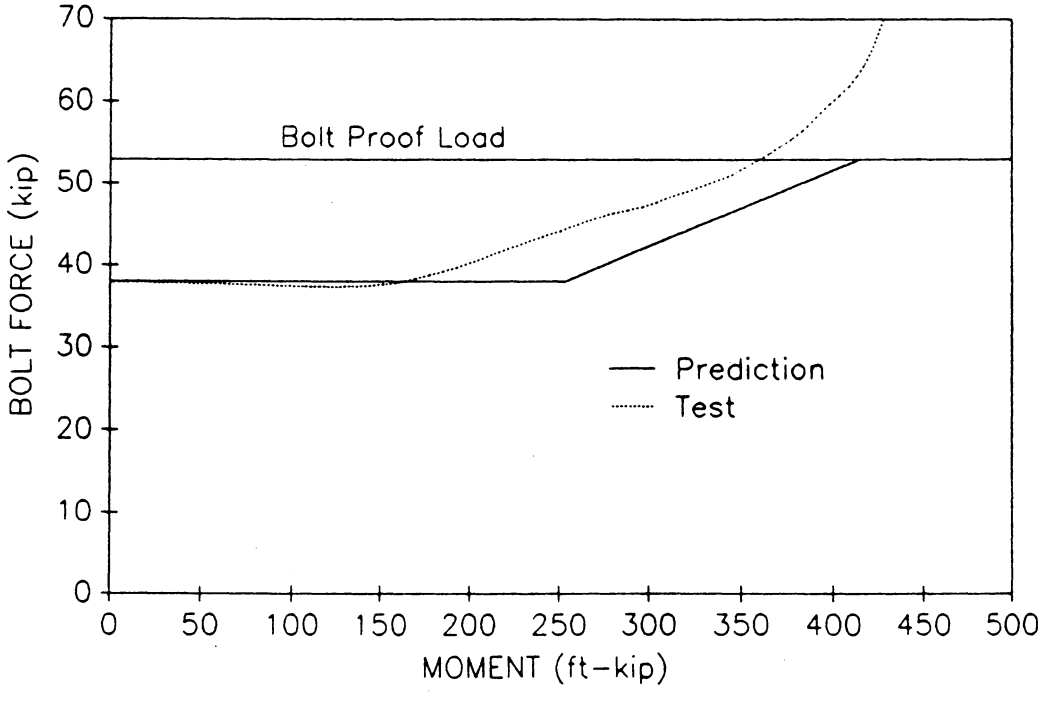

Fig. E.5 Bottom Bolt Force versus Moment
Test MRF-7/8-1/2-36

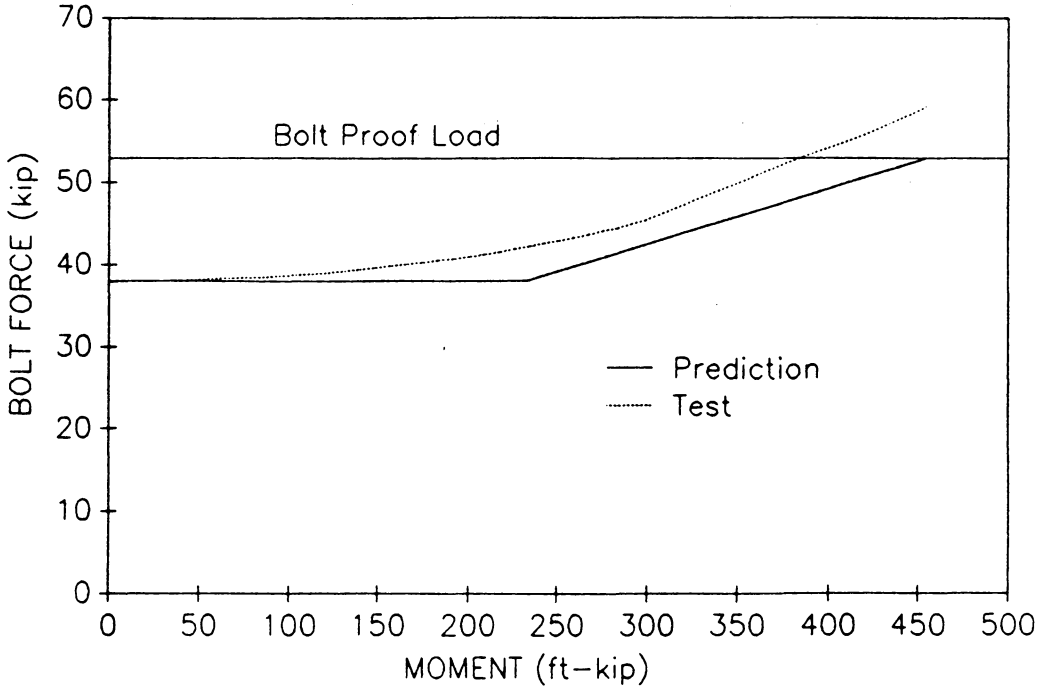

Fig. E.6 Middle Bolt Force versus Moment
Test MRF-7/8-1/2-36

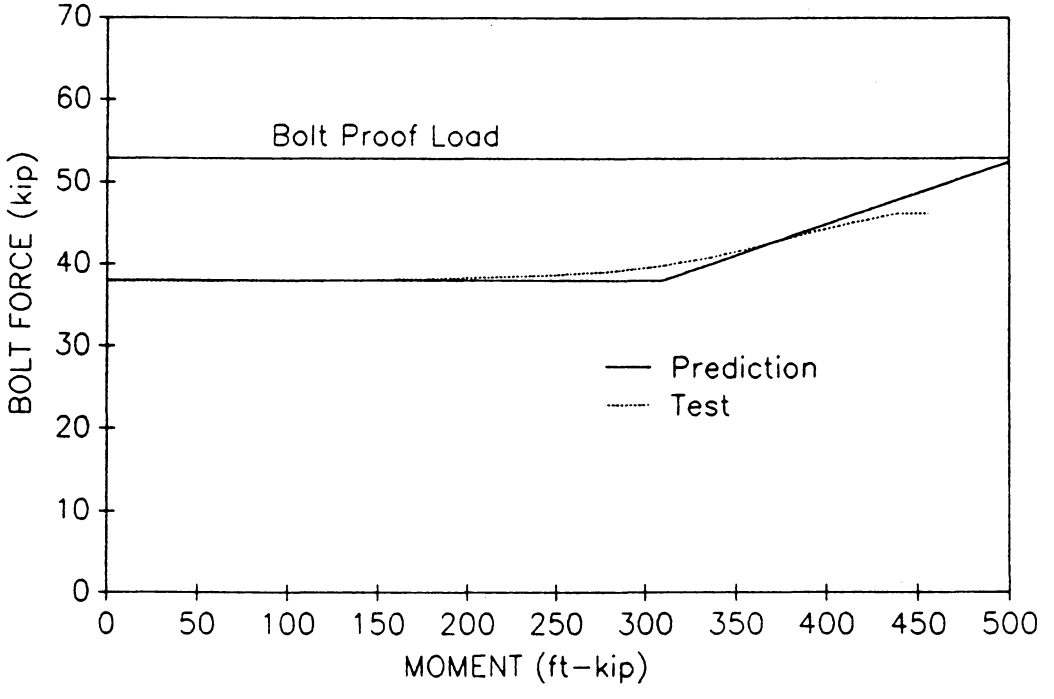

Fig. E.7 Top Bolt Force versus Moment
Test MRF-7/8-1/2-36

APPENDIX F

MRF-7/8-1/2-36B TEST RESULTS

TEST SYNOPSIS

PROJECT: Varco Pruden Six-Bolt Flush End-Plate

TEST: MRF-7/8-1/2-36B

TEST DATE: 7/21/89

BEAM DESIGN DATA:

Depth	h	(in.)	36
Flange width	bf	(in.)	6
Web thickness	tw	(in.)	5/16
Flange thickness	tf	(in.)	3/8
Moment of Inertia	I	(in.)	2568

END-PLATE DESIGN DATA:

Plate thickness	tp	(in.)	1/2
Pitch between bolt rows	pb	(in.)	2-1/2
Pitch to bolt from flange	pf	(in.)	1-1/2
Gage	g	(in.)	3-1/2
Steel yield stress	Fpy	(ksi)	50

BOLT DATA:

Type			A325
Diameter	db	(in.)	7/8
Pretension Force	Tb	(kip)	38

ANALYSIS:

Yield-line moment	Myp	(ft-kip)	357.3
Moment at bolt proof	Myb	(ft-kip)	412.0

TEST:

Moment at bolt failure	(ft-kip)	363.6
Maximum applied moment	(ft-kip)	379
Maximum centerline deflection	(in.)	0.57
Maximum end-plate separation	(in.)	0.13

DISCUSSION: Initially, the end-plates were warped. A loud noise due to a local shear failure between the end-plate and the beam was heard. Test 1 was ended after signficant twisting of the beams was noticed. The specimen was again loaded for a second test, Test 2, until another loud noise occurred because the shear failure increased in size.

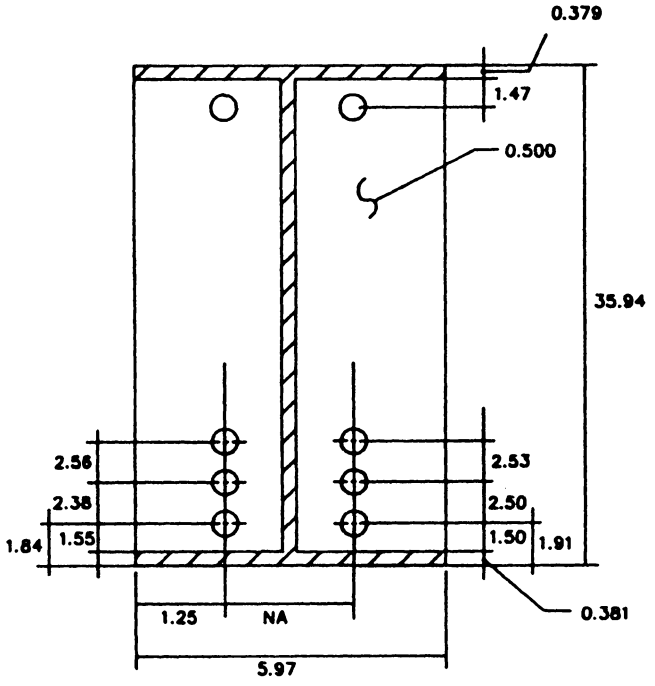

(b) Measured Dimensions End-Plate B

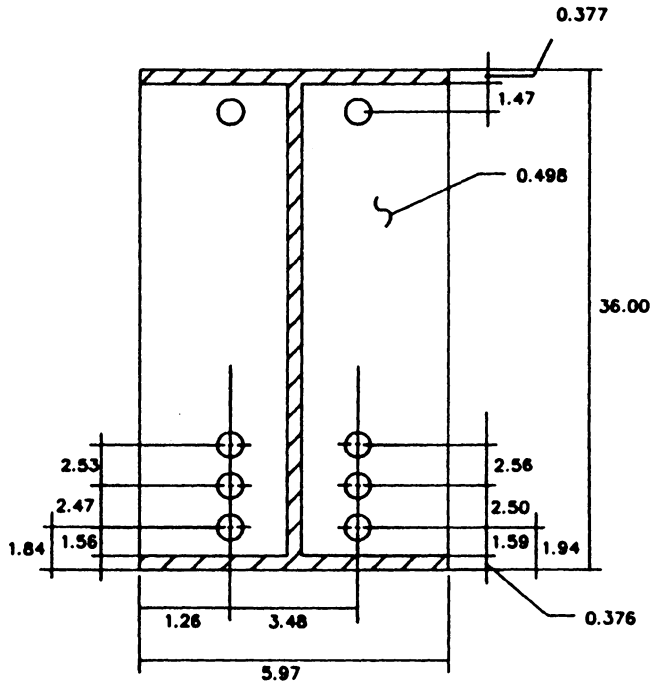

(a) Measured Dimensions End-Plate A

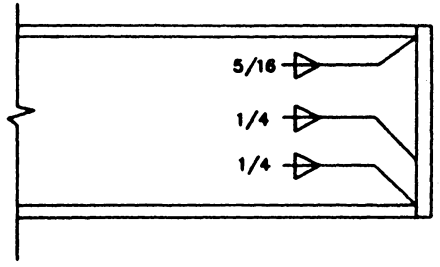

(c) Measured Weld Sizes for End-Plate

Fig. E.1 Measured Dimensions for TEST MRF-7/8-1/2-36B

End-Plate Yield Moment

Test MRF-7\8-1\2-36B

End-Plate A Controls

Mechanism I

$$u_1 = 1/2((36.00-6.84)(5.97)(3.48)/(36.00-1.84))^{1/2}$$

$$= 2.11 \text{ in.}$$

$$u_2 = 1/2((36.00-7.00)(5.97)(3.48)/(36.00-1.84))^{1/2}$$

$$= 2.10 \text{ in.}$$

$$M_U = 62.5(0.498)^2/2((36.00-1.84)(5.97/2(1.56)$$
$$+2(1.56+2.47+2.53+2.11)/3.48$$
$$+(36.00-6.84)(5.97/2(1.56)+(36.00-1.94)$$
$$(5.97/2(1.59)+2(1.59+2.50+2.56+2.10)/3.48$$
$$+(36.00-7.00)(5.97/2(1.59))/12$$

$$= 357.3 \text{ ft-kips (controls)}$$

Mechanism II

$$u = 1/2(5.97(3.48))^{1/2} = 2.28 \text{ in.}$$

$$M_U = 62.5(0.498)^2(3.48+2(1.56)(1.56+2.47+2.53)$$
$$+(36.00-1.84)(5.97/2(1.56$$
$$+2(1.56+2.47+2.53))/3.48+(36.00-6.84)$$
$$(5.97/(2(2.28)+2(2.28)/3.48)$$
$$+2(1.59)(1.59+2.50+2.56)$$
$$+(36.00-1.94)(5.97/2(1.59+2(1.59+2.50+2.56)/3.48$$
$$+(36.00-7.00)(5.97/(2(2.28)+2(2.28)/3.48))$$

$$= 359.1 \text{ ft-kips}$$

Moment at Bolt Proof Load (Bottom Bolt)

Test MRF-7\8-1\2-36B

Plate A controls

$$w' = 5.97/2-(0.875+1/16) = 2.05 \text{ in.}$$

$$F_{11L} = \frac{0.498\text{^}2(62.5)[0.85(5.97/2)+0.8(2.05)]+3.14(0.875)\text{^}385.0/8}{4(1.56)}$$

$$F_{11L} = 14.0 \text{ kips}$$

$$F_{11R} = F_{11L}(1.56)/1.59 = 13.7 \text{ kips}$$

$$Qmax_L = \frac{2.05(0.498)\text{^}2}{4(0.498)}(62.5\text{^}2-3(14.0/((0.498)2.05)1/2$$

$$Qmax_L = 14.7 \text{ kips}$$

$$Qmax_R = \frac{2.05(0.498)\text{^}2}{4(0.498)}(62.5\text{^}2-3(13.7/((0.498)2.05)1/2$$

$$Qmax_R = 14.8 \text{ kips}$$

$$Mu = .0833(36.03-(0.377+0.376)/2)(2(52.9-14.7-14.8))/0.55$$

$$Mu = 412.0 \text{ ft-kips}$$

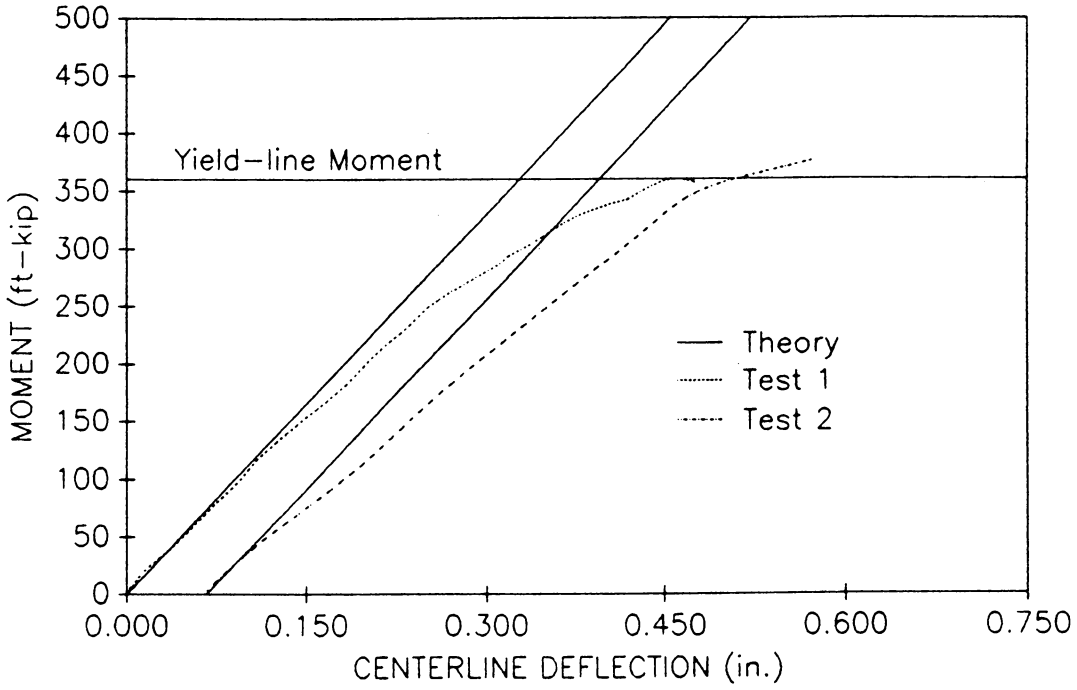

Fig. F.2 Moment versus Centerline Deflection
Test MRF-7/8-1/2-36B

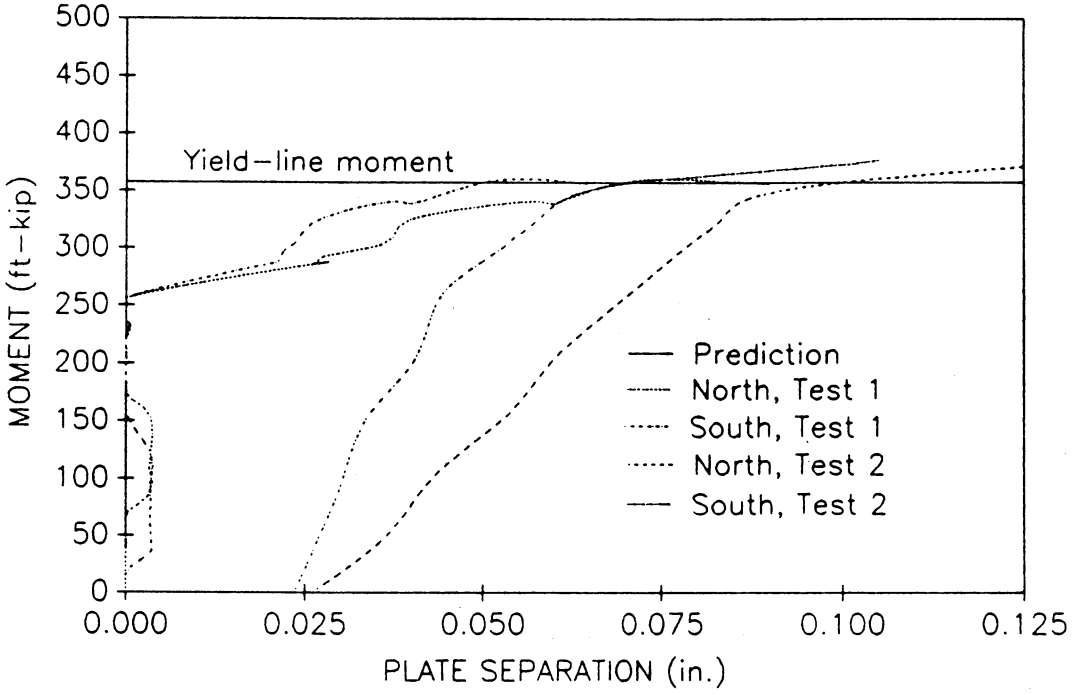

Fig. F.3 Moment versus Centerline Deflection
Test MRF-7/8-1/2-36B

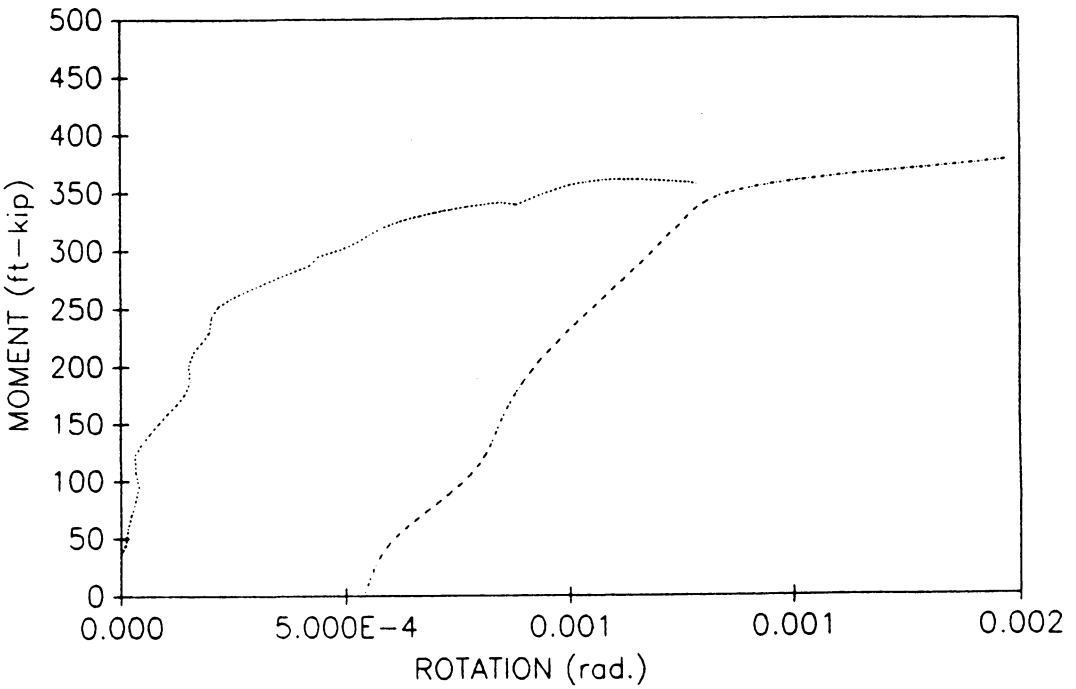

Fig. F.4 Moment versus Rotataion
Test MRF-7/8-1/2-36B

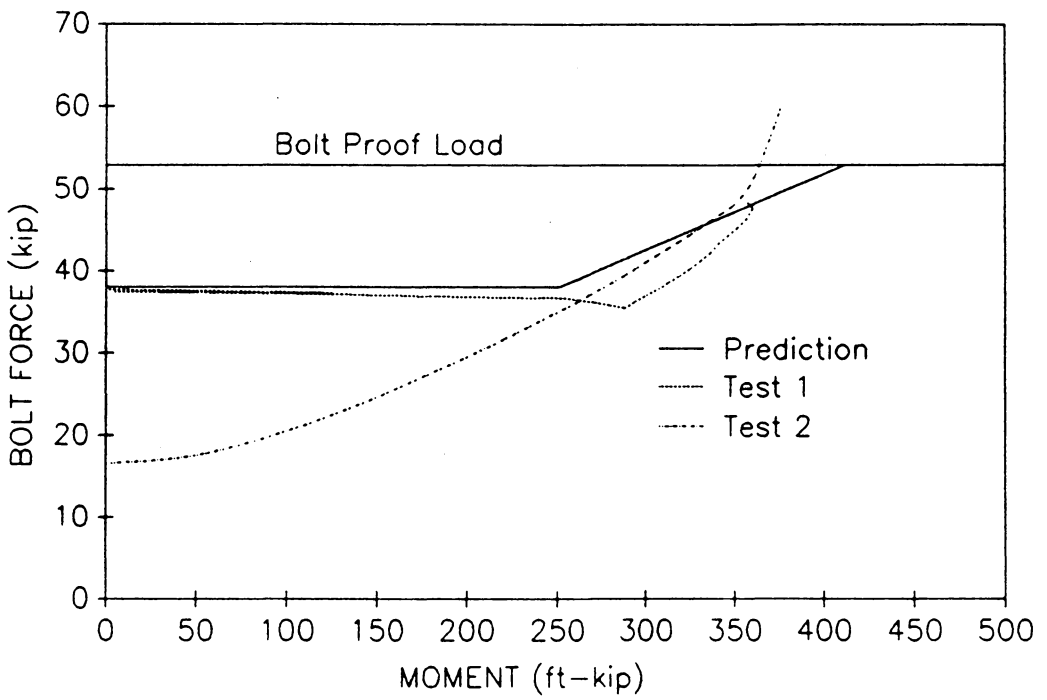

Fig. F.5 Bottom Bolt Force versus Moment
Test MRF-7/8-1/2-36B

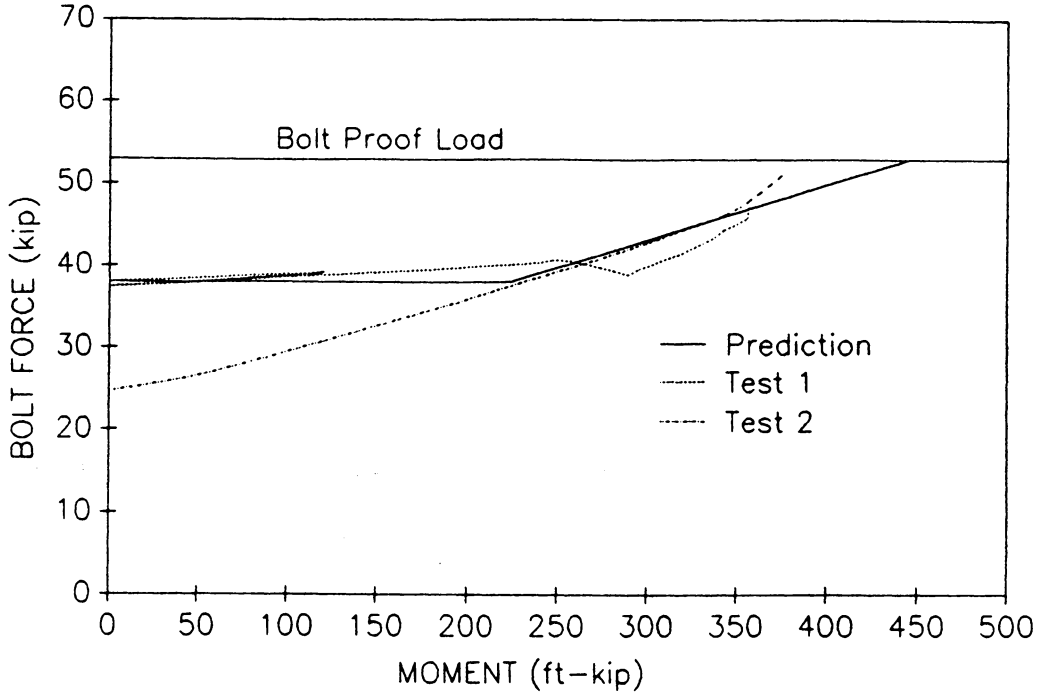

Fig. F.6 Middle Bolt Force versus Moment
Test MRF-7/8-1/2-36B

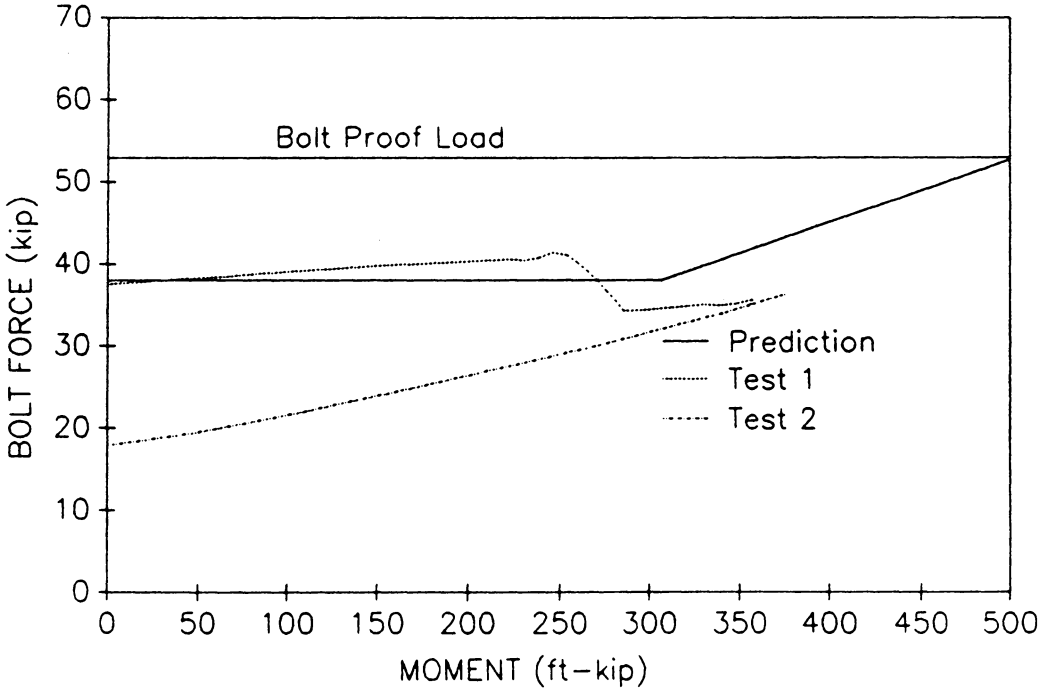

Fig. F.7 Top Bolt Force versus Moment
Test MRF-7/8-1/2-36B

APPENDIX G

COUPON AND TENSILE TEST RESULTS

Table 6.1

End-Plate Tensile Test Results

Test Specimen	Thickness (in)	Width (in)	Yield Stress (ksi)	Ultimate Stress (ksi)
MRF - 7/8 - 3/8 - 28	0.372	0.500	56.45	81.18
MRF - 1 - 1/2 - 28	0.502	0.498	64.00	NA
MRF - 3/4 - 3/8 - 36	0.370	0.500	62.70	94.05
MRF - 7/8 - 1/2 - 36	0.508	0.502	60.38	NA
MRF - 7/8 - 1/2 - 36B	0.499	0.500	62.53	NA

Table 6.2

Bolt Test Results

Test Specimen	Bolt Size (in)	Bolt Length (in)	Sample	Original Area (in^2)	Yield Proof Load (lbs)	Max Load (lbs)	Fracture
MRF - 7/8 - 3/8 - 28	0.875	2.25	1	0.462	39,250	68,500	Threads
	0.875	2.25	2	0.462	39.250	69,500	Threads
MRF - 1 - 1/2 - 28	1.000	2.75	1	0.606	51,500	90,000	Threads
	1.000	2.75	2	0.606	51,500	87,500	Threads
MRF - 3/4 - 3/8 - 36	0.750	2.25	1	0.334	28,400	48,500	Threads
	0.750	2.25	2	0.334	28,400	48,500	Threads
MRF - 7/8 - 1/2 - 36	0.875	2.50	1	0.462	39,250	67,500	Threads
	0.875	2.50	2	0.462	39,250	67,500	Threads
MRF - 7/8 - 1/2 - 36B[1]							

All bolts are ASTM A325. Manufacturer's head I.D. was /△ for all bolts.
Bolt tests performed by Pittsburgh Testing Laboratory using ASTM F-606 test method.

[1]Unused bolts from MRF - 7/8 - 1/2 - 36 test used.

The vita has been removed from the scanned document